National Library of Canada
Canadian Theses Service
Ottawa, Canada
K1A 0N4

Bibliothèque nationale du Canada
Services des thèses canadiennes

CANADIAN THESES

THÈSES CANADIENNES

NOTICE

The quality of this microfiche is heavily dependent upon the quality of the original thesis submitted for microfilming. Every effort has been made to ensure the highest quality of reproduction possible.

If pages are missing, contact the university which granted the degree.

Some pages may have indistinct print especially if the original pages were typed with a poor typewriter ribbon or if the university sent us an inferior photocopy.

Previously copyrighted materials (journal articles, published tests, etc.) are not filmed.

Reproduction in full or in part of this film is governed by the Canadian Copyright Act, R.S.C. 1970, c. C-30. Please read the authorization forms which accompany this thesis.

AVIS

La qualité de cette microfiche dépend grandement de la qualité de la thèse soumise au microfilmage. Nous avons tout fait pour assurer une qualité supérieure de reproduction.

S'il manque des pages, veuillez communiquer avec l'université qui a conféré le grade.

La qualité d'impression de certaines pages peut laisser à désirer, surtout si les pages originales ont été dactylographiées à l'aide d'un ruban usé ou si l'université nous a fait parvenir une photocopie de qualité inférieure.

Les documents qui font déjà l'objet d'un droit d'auteur (articles de revue, examens publiés, etc.) ne sont pas microfilmés.

La reproduction, même partielle, de ce microfilm est soumise à la Loi canadienne sur le droit d'auteur, SRC 1970, c. C-30. Veuillez prendre connaissance des formules d'autorisation qui accompagnent cette thèse.

THIS DISSERTATION
HAS BEEN MICROFILMED
EXACTLY AS RECEIVED

LA THÈSE A ÉTÉ
MICROFILMÉE TELLE QUE
NOUS L'AVONS REÇUE

NL 339 (r. 86/01)

Canada

0-315-24767-3

National Library of Canada
Canadian Theses Division
Ottawa, Canada
K1A 0N4

Bibliothèque nationale du Canada
Division des thèses canadiennes

(27)

PERMISSION TO MICROFILM — AUTORISATION DE MICROFILMER

• Please print or type — Écrire en lettres moulées ou dactylographier

Full Name of Author — Nom complet de l'auteur

CAMERON J. GRAHAM

Date of Birth — Date de naissance	Country of Birth — Lieu de naissance
OCTOBER 9, 1958	CANADA

Permanent Address — Résidence fixe

329 CATHERINE ST.
THUNDER BAY
ONTARIO P7E 1K7

Title of Thesis — Titre de la thèse

DEFLECTION OF REINFORCED CONCRETE SLABS UNDER CONSTRUCTION LOADING.

University — Université

UNIVERSITY OF ALBERTA

Degree for which thesis was presented — Grade pour lequel cette thèse fut présentée

MASTER OF SCIENCE

Year this degree conferred — Année d'obtention de ce grade	Name of Supervisor — Nom du directeur de thèse
1984	A. SCANLON

Permission is hereby granted to the NATIONAL LIBRARY OF CANADA to microfilm this thesis and to lend or sell copies of the film.

The author reserves other publication rights, and neither the thesis nor extensive extracts from it may be printed or otherwise reproduced without the author's written permission.

L'autorisation est, par la présente, accordée à la BIBLIOTHÈQUE NATIONALE DU CANADA de microfilmer cette thèse et de prêter ou de vendre des exemplaires du film.

L'auteur se réserve les autres droits de publication; ni la thèse ni de longs extraits de celle-ci ne doivent être imprimés ou autrement reproduits sans l'autorisation écrite de l'auteur.

Date	Signature
AUG 2, 1984	C Graham

NL-91 (4/77)

THE UNIVERSITY OF ALBERTA

DEFLECTION OF REINFORCED CONCRETE SLABS UNDER CONSTRUCTION LOADING

by

© CAMERON J. GRAHAM

A THESIS

SUBMITTED TO THE FACULTY OF GRADUATE STUDIES AND RESEARCH

IN PARTIAL FULFILMENT OF THE REQUIREMENTS FOR THE DEGREE

OF MASTER OF SCIENCE

DEPARTMENT OF CIVIL ENGINEERING

EDMONTON, ALBERTA

FALL, 1984

THE UNIVERSITY OF ALBERTA

RELEASE FORM

NAME OF AUTHOR CAMERON J. GRAHAM

TITLE OF THESIS DEFLECTION OF REINFORCED CONCRETE SLABS UNDER CONSTRUCTION LOADING

DEGREE FOR WHICH THESIS WAS PRESENTED MASTER OF SCIENCE

YEAR THIS DEGREE GRANTED FALL, 1984

Permission is hereby granted to THE UNIVERSITY OF ALBERTA LIBRARY to reproduce single copies of this thesis and to lend or sell such copies for private, scholarly or scientific research purposes only.

The author reserves other publication rights, and neither the thesis nor extensive extracts from it may be printed or otherwise reproduced without the author's written permission.

(SIGNED) C Graham

PERMANENT ADDRESS:

329 CATHERINE ST.

THUNDER BAY

ONTARIO P7E 1K7

DATED JULY 20 1984

THE UNIVERSITY OF ALBERTA

FACULTY OF GRADUATE STUDIES AND RESEARCH

The undersigned certify that they have read, and recommend to the Faculty of Graduate Studies and Research, for acceptance, a thesis entitled DEFLECTION OF REINFORCED CONCRETE SLABS UNDER CONSTRUCTION LOADING submitted by CAMERON J. GRAHAM in partial fulfilment of the requirements for the degree of MASTER OF SCIENCE.

.....
Supervisor

.....

.....

Date JULY 20, 1984

ABSTRACT

An analytical model to calculate long-time flat plate deflection under early age construction loading is developed. Immediate deflections are calculated using an elastic finite element program, modified to account for the effects of cracking due to applied loads and restrained shrinkage. Individual creep curves that reflect the loading age of concrete are superimposed to obtain total creep deflection. Overall long-time deflection also includes shrinkage warping effects. Prediction by the model of deflections measured for three flat plates is satisfactory. From a model parameter study, the degree of panel restraint and early age loading are identified as important factors when calculating long-time deflection. Based on the proposed model and parameter study, a revised set of long-time deflection multipliers is recommended to account for early age construction loading.

ACKNOWLEDGMENTS

I would like to express my graditude to Dr. A. Scanlon for his guidance, critical review and support towards completion of this thesis.

Funding for this work by the Natural Sciences and Engineering Research Council of Canada, in the form of a Post Graduate Scholarship, is appreciated.

The author acknowledges the contribution of Cameron Matthews for modifications made to the finite element program SAPIV.

The assistance of Tom Casey in several computer-related areas is gratefully appreciated.

Table of Contents

Chapter — Page

List of Tables x

List of Figures xi

List of Symbols xiv

1. INTRODUCTION 1

1.1 General 1

1.2 Problem Statement 2

1.3 Objectives and Scope 2

2. LITERATURE REVIEW 4

2.1 Calculation of Two-Way Slab Deflections 4

2.1.1 Immediate Deflections 4

2.1.2 Long-Time Deflections 7

2.2 Construction Loading 8

2.3 Effects of Cracking 13

2.4 Measured Deflections 17

2.5 Code Requirements for Deflections 21

2.6 Summary 22

3. PROPOSED MODEL FOR SLAB DEFLECTION CALCULATIONS UNDER CONSTRUCTION LOADS 23

3.1 Material Properties 23

3.1.1 Compressive Strength, Modulus of Elasticity, and Modulus of Rupture 23

3.1.2 Creep 25

3.1.3 Shrinkage 27

3.2 Construction Loading 29

3.3 Calculation of Immediate Deflection 31

3.3.1 Iterative Cracking Routine 31

3.3.2 Calculation of Incremental Deflections 34

3.3.3 Finite Element Method 35

3.4 Calculation of Long-Time Deflections 35

3.4.1 Creep Deflections 36

3.4.2 Superposition of Creep Deflection Curves ..37

3.4.3 Shrinkage Warping Deflections 40

3.5 Summary 42

4. MODEL VERIFICATION 56

4.1 Introduction 56

4.2 Heiman's Flat Plate 56

4.2.1 Description of the Structure 56

4.2.2 Material Properties 57

4.2.3 Construction Loads 58

4.2.4 Comparison of Calculated and Measured Deflections 59

4.3 Sbarounis' Flat Plate 61

4.3.1 Description of Structure 61

4.3.2 Material Properties 61

4.3.3 Construction Loads 61

4.3.4 Comparison of Calculated and Measured Deflections 63

4.4 Taylor's Flat Plate 65

4.4.1 Description of Structure 65

4.4.2 Material Properties 66

4.4.3 Construction Loads 66

4.4.4 Comparison of Calculated and Measured Deflections 67

4.5 Discussion 70

4.6 Summary 71

5. PARAMETER STUDY 85

5.1 Outline of Study 85

5.1.1 Slab Details 85

5.2 Parameters Considered 86

5.2.1 Modulus of Rupture 88

5.2.2 Degree of Creep Recovery 90

5.2.3 Span-to-Depth Ratio 91

5.2.4 Number of Shored Levels 92

5.2.5 Number of Reshored Levels 94

5.2.6 Construction Cycle Time 95

5.2.7 Effective Depth to Top Reinforcement 97

5.3 Summary 99

6. SIMPLIFIED METHOD FOR DEFLECTION CALCULATIONS UNDER CONSTRUCTION LOADS 116

6.1 Introduction 116

6.2 Calculation of Maximum Construction Load 116

6.3 Calculation of Immediate Deflection 118

6.4 Calculation of Long-Time Deflection 120

6.4.1 Immediate Deflection due to Sustained Loads 120

6.4.2 Derivation of Long-Time Multipliers 121

6.4.2.1 Basis for Multipliers 121

6.4.2.2 One-Year and Ultimate Multipliers 122

6.4.3 Recommended Multipliers 124

6.5 Simplified Deflection Calculation Examples 126

6.6 Summary 127

7. SUMMARY, CONCLUSIONS, RECOMMENDATIONS 134

7.1 Summary 134

7.2 Conclusions 135

7.3 Recommendations 139

REFERENCES 141

APPENDIX A - CALCULATION OF CONSTRUCTION LOAD RATIOS AND LOADS 149

APPENDIX B - PROGRAM LISTING AND DATA FOR ITERATIVE CRACKING ROUTINE 156

APPENDIX C - PROGRAM LISTING AND INPUT DATA FOR SUPERPOSITION OF CREEP CURVES AND CALCULATION OF TOTAL LONG-TIME DEFLECTION 169

APPENDIX D - ANALYSIS OF HEIMAN'S FLAT PLATE 179

APPENDIX E - ANALYSIS OF SBAROUNIS' FLAT PLATE 185

APPENDIX F - ANALYSIS OF TAYLOR'S FLAT PLATE 192

APPENDIX G - DERIVATION OF LONG-TIME MULTIPLIERS 198

List of Tables

Table		Page
3.1	Assumed Effective Modulus of Rupture Values	44
5.1	Slab Designs for Parameter Study	100
5.2	Parameter Study Summary	101
5.3	Construction Load Histories for 165 mm Slab	103
5.4	Construction Load Ratios for Various Supporting Assemblies	104
5.5	Effect of Reshored Levels on Ultimate Deflections	104
6.1	Average Total One-Year and Ultimate Multipliers	128
6.2	Recommended One-Year and Ultimate Multipliers	129
6.3	Comparison of Recommended Design Multipliers	130
6.4	Multiplier Examples	131
D.1	Heiman's Flat Plate - Construction Load Stage Data	182
E.1	Sbarounis' Flat Plate - Construction Load Stage Data	189
G.1	One-Year and Ultimate Multipliers	200

List of Figures

Figure		Page
3.1	Creep Compliance Curves	45
3.2	Basic Shoring Operations	46
3.3	Maximum Absolute and Converged Construction Load Ratios for Two Levels of Shores (2+0)	47
3.4	Typical Construction Load Sequence	48
3.5	Iterative Cracking Routine	49
3.6	Moment-Curvature Relationship Showing Progressive Reduction in Stiffness	50
3.7	Calculation of Incremental Deflection	51
3.8	Boundary Conditions for a Typical Interior Quarter Panel	52
3.9	Creep Curves	53
3.10	Superposition of Creep Curves	54
3.11	Effect of Variable Creep Recovery on Strain-Time History	55
4.1	Heiman's Flat Plate	72
4.2	Heiman's Flat Plate - Construction Sequence	73
4.3	Heiman's Flat Plate - Construction Load Sequence	74
4.4	Heiman's Flat Plate - Long-Time Deflections ($f = 4\sqrt{f'_c}$ psi)	75
4.5	Heiman's Flat Plate - Long-Time Deflections ($f = 6\sqrt{f'_c}$ psi)	76
4.6	Heiman's Flat Plate - Long-Time Deflections ($f = 7.5\sqrt{f'_c}$ psi)	77
4.7	Sbarounis' Flat Plate - Construction Load Sequence	78
4.8	Sbarounis' Flat Plate - Long-Time Deflections (Full Creep Recovery)	79
4.9	Sbarounis' Flat Plate - Long-Time Deflections (One-Half Creep Recovery)	80

Figure		Page
4.10	Sbarounis' Flat Plate - Long-Time Deflections (Zero Creep Recovery)	81
4.11	Sbarounis' Flat Plate - Comparison of One-Year Deflections	82
4.12	Taylor's Flat Plate	83
4.13	Taylor's Flat Plate - Long-Time Deflections	84
5.1	Parameter Study - Plan of Reinforcement	105
5.2	Parameter Study - Modulus of Rupture	106
5.3	Parameter Study - Cracking Distribution ($f_r = 0.60\sqrt{f'_c}$ MPa)	107
5.4	Parameter Study - Cracking Distribution ($f_r = 0.32\sqrt{f'_c}$ MPa)	108
5.5	Parameter Study - Degree of Creep Recovery	109
5.6	Parameter Study - Span-to-Depth-Ratio	110
5.7	Parameter Study - Number of Shored Levels	111
5.8	Parameter Study - Construction Cycle Time	112
5.9	Parameter Study - Load Sequences for Construction Cycle Time Comparison	113
5.10	Parameter Study - Effective Depth to Top Reinforcement	114
5.11	Parameter Study - Yield Locations With Reduced Effective Depth to Top Reinforcement	115
6.1	Load-Deflection Curves Showing Secant Unloading	132
6.2	Calculation of Total Multiplier	133
A.1	Calculation of Load Ratios (3+0)	152
A.2	Calculation of Load Ratios (2+1)	153
A.3	Load Ratio History (3+0)	154
A.4	Load Ratio History (2+1)	154
A.5	Construction Load History (3+0)	155

Figure		Page
A.6	Construction Load History (2+1)	155
B.1	Finite Element Grid for Slab Series LH100	161
D.1	Heiman's Flat Plate - Reinforcement Areas (in^2/in)	183
D.2	Heiman's Flat Plate - Finite Element Grid	184
E.1	Sbarounis' Flat Plate - Reinforcement Areas (in^2/in)	190
E.2	Sbarounis' Flat Plate - Finite Element Grid	191
F.1	Taylor's Flat Plate - Reinforcement Areas (in^2/in)	196
F.2	Taylor's Flat Plate - Finite Element Grid	197

LIST OF SYMBOLS

A_s = tensile steel area

A'_s = compressive steel area

c, c_1, c_2 = constants

$C(t,t_o)$ = creep coefficient at time t for load applied at time t_o

C_u = ultimate creep coefficient

d = effective depth to reinforcement

D = flexural plate rigidity

$E_c(t)$ = time-dependent modulus of elasticity

$E_c(t_o)$ = modulus of elasticity at time of load application, t_o

f'_c = compressive concrete strength

$f'_c(t)$ = time-dependent compressive concrete strength

$f'_c(28)$ = 28-day compressive concrete strength

f_r = modulus of rupture

$f_r(t)$ = time-dependent modulus of rupture

f_y = steel yield strength

G = shear modulus

h = slab or plate thickness

I_{cr} = cracked moment of inertia

I_e = effective moment of inertia

I_g = gross moment of inertia

k = construction load ratio

k_{max} = maximum converged construction dead load ratio

k_r = factor to account for compression reinforcement and neutral axis shifts

K = construction cycle number

K_w = coefficient, depending on member end conditions, for use in shrinkage warping deflection calculations

L = span

M = bending moment

M_a = maximum bending moment at the stage for which deflection is being computed

M_{cr} = cracking moment

M_{max} = maximum bending moment

n = time between casting of top floor in supporting assembly and removal of the lowest level of shores/reshores

N = total number of levels in the supporting assembly

t = time since casting

t' = any time < t

t_o = time of load application

t_m = length of moist-curing period

t_{max} = time of maximum construction load application

$(t-t_o)$ = time since load application

$(t-t_m)$ = time since moist-curing period

T = construction cycle time

w = construction load or transverse load

w_c = mass density of concrete

w_{dmax} = maximum converged construction dead load

w_ℓ = construction live load

w_{max} = maximum construction load

w_s = slab self weight

$w_{s\ell}$ = sustained load

y_t = distance from centroidal axis of gross section, neglecting reinforcement, to extreme fibre in tension

α = degree of cracking

γ = shear strain

$\delta(t,t_o)$ = creep per unit stress (specific creep or compliance)

Δ = deflection

Δ_{cp} = long-time creep deflection

Δ_{cr} = additional immediate deflection due to cracking

Δ_e = immediate elastic deflection

Δ_i = incremental immediate deflection

Δ_{icp} = total immediate-plus-creep deflection

Δ_{max} = immediate deflection due to the maximum construction load applied as a single increment

Δ_o = total immediate deflection (including Δ_{cr})

Δ_{scp} = superimposed creep deflection

Δ_{sh} = long-time shrinkage deflection

Δ_{shc} = shrinkage deflection of column strip

Δ_{shm} = shrinkage deflection of middle strip

$\Delta_{s\ell}$ = immediate deflection due to sustained load accounting for the effects of construction loading at early age

Δ_t = total long-time deflection

Δ_{360} = total deflection 360 days after casting

Δ_{1080} = total deflection 1080 days after casting

ϵ = normal strain

$\epsilon_{sh}(t)$ = shrinkage strain at time, t, for moist-curing period, t_m

ϵ_{shu} = ultimate shrinkage strain

θ = rotation

λ = additional long-time multiplier

λ_c = creep component multiplier

λ_{ic} = immediate-plus-creep component multiplier

λ_{sh} = shrinkage component multiplier

λ_t = total multiplier

λ'_t = revised total multiplier

ν = Poisson's ratio

ρ = tensile reinforcement percentage

ρ' = compressive reinforcement percentage

σ = normal strain

τ = shear strain

ϕ_{sh} = shrinkage curvature

$\phi(t,t_o)$ = total elastic strain-plus-creep deformation under a unit stress

1. INTRODUCTION

1.1 General

Recent trends in the design and construction of concrete structures have led to reduced member dimensions. For two-way construction, a reduction in slab thickness for a given span has two effects. Additional reinforcement is needed to maintain the necessary strength requirements. Secondly, more attention must be directed to ensure that serviceability limits related to the control of cracking and deflections are met.

The need to predict long-time deflections of two-way slabs, with reasonable accuracy, is illustrated by problems created by excessive deflections. Cracked partitions and finishes, jammed doors and windows, aesthetically unacceptable floor slopes, and ponding of water on roofs may all result from large slab deformatioms.

Present procedures contained in the CSA A23.3 M77 (1) and ACI 318-83 (2) Codes outline minimum thicknesses of two-way construction for which deflections need not be computed. In most instances, these requirements appear to produce satisfactory designs in terms of serviceability. For thicknesses below the minimum, the calculation of long-time deflection is based on 28-day concrete properties and the sustained service load.

However, more critical loading situations can occur, which may adversely influence deflections for slabs

otherwise meeting the minimum thickness standards. Taylor and Heiman (3) have noted that loading of slabs during construction through shoring procedures is a source of increased deflection. This loading often occurs at early age and may produce extensive cracking and loss of slab stiffness.

1.2 Problem Statement

Slabs constructed through shoring procedures in multistory structures are subjected to loads that may exceed the total design service load. Application of these loads often occurs before the slab has reached the specified design strength. The combination of early age loading and reduced concrete material properties may lead to increased cracking and loss of slab stiffness. As a direct result, immediate, as well as long-time deflections will increase. Prediction of increased long-time deflections considering this behaviour is required.

1.3 Objectives and Scope

The main objectives of the study may be summarized as follows:

1. To study the effects of early age construction loading on two-way slab deflections.
2. To assess the effect of cracking due to restraint stresses from shrinkage.
3. To identify and evaluate significant factors regarding

deflections associated with the construction of multistory structures.

4. To develop a simplified deflection calculation method accounting for loading at early age.

The scope of the work undertaken in this study consisted of the following:

1. A review the existing deflection calculation methods for two-way slabs.
2. Development of a model, based on a finite element analysis, to calculate flat plate deflections under construction loading including the following:
   i) early age concrete properties
   ii) the effects of cracking due to loads and restraint
   iii) long-time creep and shrinkage deflections
3. Verification of the proposed model using existing flat plate deflection studies.
4. Identification of the most important factors affecting the model through a parameter study, and use of the results to generate revised ultimate deflection multipliers for a simplified deflection calculation method.

2. LITERATURE REVIEW

2.1 Calculation of Two-Way Slab Deflections

Calculation of two-way slab deflections is complicated by the three-dimensional nature of the problem, degree of cracking in the slab and time-dependent concrete properties. The problem can be simplified by considering immediate and long-time deflections separately. The following gives a review of available deflection calculation methods for each case.

2.1.1 Immediate Deflections

Both classical and numerical methods are available to calculate immediate deflections of a flat plate subjected to a uniformly distributed load.

Classical elastic plate theory is based on thin isotropic plates and small deformations. Deflection at a point (x,y) is found by solving the Plate Equation:

$$\frac{\partial^4 \Delta}{\partial x^4} + \frac{2\partial^4 \Delta}{\partial x^2 \partial y^2} + \frac{\partial^4 \Delta}{\partial y^4} = \frac{w}{D} \qquad (2\text{-}1)$$

where: Δ = deflection at point (x,y)

w = transverse load

D = flexural plate rigidity

$$= \frac{E_c h^3}{12(1 - \nu^2)}$$

h = plate thickness

ν = Poisson's ratio

E_c = modulus of elasticity

Timoshenko and Woinowsky-Krieger (4) have catalogued such solutions for numerous isolated plate cases. However for two-way continuous floor systems, individual cases must be combined using indeterminate structure solution techniques. Alternatively, approximate solutions are also given in Reference 4 where plate moments are calculated using coefficients tabulated according to panel aspect ratios and support conditions. Coefficients are also developed for calculating centrepanel deflections for typical interior flat plate panels supported on columns.

The equivalent frame method is a standard method of two-way slab design in both the CSA A23.3 M77 (1) and ACI 318-83 (2) Codes. The slab system is approximated by continuous frames centred along column lines in both directions. Peabody (5) initially outlined this method in 1948 for continuous elastic frame analysis.

A method to calculate deflections based on an equivalent frame approach is described by Vanderbilt, Sozen and Siess (6). A continuous slab system is broken into beam and plate elements bounded by lines of contraflexure. Deflection at the midpanel point consists of the centreline

deflection of a long beam element plus the deflection of the beam edge with respect to the centreline plus the additional deflection of the plate element.

A more direct application of an equivalent frame procedure was proposed by Nilson and Walters (7). This method computes deflections for orthogonal middle and column strips separately, then uses superposition to obtain final midpanel deflections. Kripanarayanan and Branson (8) extended the method to include the effects of cracking. In calculating deflections, the equivalent frame stiffness is modified by using a weighted average of effective inertia terms calculated at the positive and negative moment locations.

More recently Rangan (9) proposed calculating the midpanel deflection of a flat plate as the sum of the midspan deflections of the column-beam strip (in the long direction) and middle-beam strip (in the short direction). Each strip is considered as a separate beam carrying a uniformly distributed load and applied end moments. Scanlon and Murray (10) proposed a similar procedure, but used an equivalent uniform strip load and actual beam end moments in the deflection calculation.

The finite element method provides a more general approach to plate analysis than the equivalent frame methods described above. A state-of-the-art report by ACI Committee

435 (11) lists several finite element programs currently available. The majority of finite element programs apply only to linear elastic analyses. However Jofriet (12), Jofriet and McNeice (13), Scanlon (14), and Scanlon and Murray (10) considered the inelastic range by modifying element stiffness matrices to account for flexural concrete cracking. The effects of cracking on two-way slab deflections is discussed in Section 2.3.

2.1.2 Long-Time Deflections

The main components of long-time deflection of concrete members are creep and shrinkage. It has become standard Code procedure to use a simplified multiplier approach to calculate additional creep and shrinkage deflection based on a calculated initial elastic deflection. This multiplier approach was derived on the basis of tests carried out by Washa and Fluck (15,16), and Yu and Winter (17) on cracked beams subjected to sustained loading. The basic additional creep and shrinkage multiplier adopted by the ACI Code (2) for one-way action is:

$$\lambda = [2 - 1.2A'_s/A_s] > 0.6 \qquad (2\text{-}2)$$

where: λ = additional long-time deflection multiplier

A_s = tensile steel area

A'_s = compressive steel area

This multiplier can also be used for two-way systems. Flat slabs seldom contain significant amounts of compressive steel, so the instantaneous elastic deflections are usually doubled to obtain the additional long-time deflection due to creep and shrinkage.

Alternatively, creep and shrinkage deflections may be calculated separately using the procedures developed by Branson (18) and outlined by ACI Committee 209 in Reference 19. A more detailed description of the method and equations used is given in Section 3.4. This procedure, although requiring a greater input of parameters, is still suitable for design office use.

Time-dependent effects have been incorporated directly into a finite element analysis of slab deflections by Scanlon (14). This approach is useful in developing proper serviceability requirements and simplified deflection calculation methods. For practical use, ACI Committee 435 (11) recommends an initial elastic finite element analysis to calculate instantaneous deflection, including effects of cracking, together with a multiplier approach to calculate additional long-time deflection.

2.2 Construction Loading

Calculation of ultimate deflection is dependent on the loading history of the structure. Flat plate construction in multistory buildings results in a particular sequence of loads that greatly influences long-time deflection. These

loads may differ in magnitude and time of application compared with total service loads applied at twenty-eight days.

In the construction of multistory flat slab structures fresh slabs are usually supported by several previously cast slabs through a series of forms, shores, and reshores, collectively known as the supporting assembly. Shoring usually consists of a system of vertical posts and horizontal longitudinal and transverse members that provide uniform support for the formwork and freshly cast slab to lower levels. Reshores, similar to shores but with no associated formwork, are substituted for shores to free formwork for use on subsequent levels. Initially reshores carry negligible load. Analytical methods have been developed to estimate loads transferred to slabs in the supporting assembly.

Nielsen (20) gave a detailed analysis of the distribution of load between a system of connected shores and floor slabs. The method considered both the deformation characteristics of the slabs and shores. Construction loads carried by the slabs and shores were expressed in terms of load ratios defined as:

$$k = \frac{\text{load carried by slab}}{\text{slab+formwork weight}} \qquad (2\text{-}3)$$

where: k = construction load ratio

The maximum load ratio obtained by Nielsen on a slab assuming three levels of shores was 2.56.

Grundy and Kabaila (21) developed a simplified method to calculate the distribution of load between floor slabs during construction, based on the following assumptions:

i) shores are infinitely rigid in comparison with the slabs in vertical displacement

ii) shores are spaced close enough to treat the reactions as a distributed load

iii) a load applied to the system is distributed between the slabs in proportion to their relative flexural stiffnesses

The maximum load ratio for a slab occurs when the slab reaches the bottom of the supporting assembly.

Although the absolute maximum load ratio occurs when the shores connecting the supporting assembly with the ground level are removed, the ratio converges for upper floor levels. For the same structure considered by Nielsen, Grundy and Kabaila obtained an absolute maximum load ratio of 2.36, while the converged value for upper floor levels was 2.00. Altering the number of shored levels has little effect on the maximum load ratio value. However by decreasing the number of shored levels, the age of the slab at which the maximum ratio occurs also decreases, producing a more critical condition.

Grundy and Kabaila carried out analyses assuming both constant and varying flexural stiffnesses for the supporting

assembly slabs. Modifying the slab stiffnesses to account for their different ages (and subsequent different E_c values) did not change appreciably the maximum load ratios.

In addition to variations in E_c due to concrete age, cracking of slabs that occurs during construction affects the distribution of load between slabs in the supporting assembly. Sbarounis (22) reports that incorporating the effects of cracking into the load distribution factors for the supporting slabs reduces the previously calculated maximum load ratios by approximately 10 percent.

Blakey and Beresford (23) recommended a step sequence of construction in a system of floors and shores to control the construction loads imposed on each component. With this method, a fresh slab is given more time to develop adequate strength before the application of construction load from the casting of a new slab.

Taylor (24) suggested a technique of stripping formwork to reduce the loads imposed on a slab during construction. By slackening and tightening adjustable shores before each new slab is cast, the loads distributed to the shores and slabs are reduced considerably. With this method all shores at one level must be slackened simultaneously, thus requiring greater supervision and inspection. Taylor reports that the maximum load ratio is reduced from the 2.36 obtained by Grundy and Kabaila to a value 1.44.

Several studies have been carried out to confirm theoretical construction load values. Agarwal and

Gardner (25) measured form and reshore loads for two high-rise buildings under construction. Good agreement was found between field-measured construction loads and those predicted by the simplified theory of Grundy and Kabaila. Lasisi and Ng (26) reported a mean maximum measured load ratio some 4 percent greater than the corresponding theoretical value for a fifteen-story flat slab office building.

Although the previously defined load ratios reflect the slab-plus-formwork dead weights, a construction live load is also present. Hurd (27) suggests a minimum construction live load of 2.4 kPa (50 psf) for designing forms. Grundy and Kabaila's approach does not consider any construction live load in computing expected loads distributed to slabs and shores. The previously outlined study by Lasisi and Ng (26) presented a method to include the live load effect. For a typical flat plate structure assuming a supporting assembly of two shore levels plus one reshore level, a construction live load of 2.4 kPa removed after the casting day and constant E_c for the connected slabs, the absolute maximum load ratio increases 9 percent over that predicted by Grundy and Kabaila. Both Agarwal and Gardner (25) and Sbarounis (22) account for the construction live load effect by increasing the maximum load carried by the lowest slab in the supporting assembly. Sbarounis recommends additional loads, due to a 50 psf live load, of 55/N and 35/N psf for uncracked and cracked slabs respectively. Here N represents

the total number of levels in the supporting assembly.

2.3 Effects of Cracking

Deflection of reinforced concrete slabs is influenced greatly by the degree and distribution of cracking. Cracking may occur in slab members due to restraint of shrinkage as well as flexure resulting from applied loads.

Flexural cracking takes place when loading develops bending moments that exceed the cracking moment of the concrete. The cracking moment is a direct function of the concrete tensile strength. Variations in ambient temperature, relative humidity, and wind conditions can significantly alter the normal curing procedure for concrete and thus early age concrete properties, including strength. Shrinkage resulting from poor curing conditions and that due to warping of the section can both increase the degree of cracking. Restraints in a slab system provided by column supports, adjacent panels, and reinforcement may also reduce the effective tensile capacity of the concrete, and increase cracking.

The effects of cracking result in a reduced overall slab panel flexural stiffness. Although most cracking in flat plates occurs around panel supports, extensive cracking may also develop in the midpanel regions. When a particular location in a panel cracks, moments are redistributed to adjacent uncracked regions. This redistribution of moments promotes further cracking in these adjacent locations.

Reduced slab stiffness increases both initial and long-time panel deflections.

The effect of cracking can be accounted for by reducing the flexural rigidity in cracked regions. Branson (28) developed an empirical relationship to calculate an effective moment of inertia for a concrete section subjected to a moment greater than the cracking moment. The expression, based on tests on simple and continuous rectangular beams (28,15,16) and simple T-beams (17), is given by:

$$I_e = \left(\frac{M_{cr}}{M_a}\right)^3 I_g + \left[1 - \left(\frac{M_{cr}}{M_a}\right)^3\right] I_{cr} \qquad (2\text{-}4)$$

where: I_e = effective moment of inertia

I_g = gross moment of inertia

I_{cr} = fully cracked moment of inertia

M_{cr} = cracking moment

$= \frac{f_r I_g}{y_t}$

f_r = modulus of rupture

y_t = distance from centroidal axis of gross section, neglecting reinforcement, to extreme fibre in tension

M_a = maximum moment at the stage for which deflection is being computed

It should be noted that Equation 2-4 is recommended for calculating effective moment of inertia for simple beams or between inflection points of continuous beams. The same equation to the fourth power is recommended for effective moment of inertia at a section. However, solutions using the two power variations differ by only 3 percent (18).

Equation 2-4 has also been adopted for use in deflection calculations for partially cracked two-way slabs. Using an equivalent frame procedure for calculating deflections, Branson (18) recommended the following distributions of strip stiffnesses for typical cases:

i) for slabs without beams
   - for dead load deflections use I_g for all strips.
   - for dead plus live load deflections use I_g for the middle strips in both directions and I_e for the column strips in both directions.

ii) for slabs with beams
   - for dead load deflections use I_g for all strips.
   - for dead plus live load deflections use I_g for the column strips in both directions and I_e for the middle strips in both directions.

For both column and middle strips where there are positive and negative moment regions, a weighted strip I_e is

calculated using 70 percent positive and 15 percent of each negative value.

Both Heiman (29) and Rangan (9) have reported that use of Equation 2-4, as recommended in both CSA A23.3 M77 and ACI 318-83 Codes, to account for slab cracking gives less than conservative results. Use of this formula would typically predict slight cracking in column strips and little or no cracking in middle strips. This does not completely agree with actual crack patterns in flat plates and slabs where more extensive cracking often occurs (29,30,31).

Attempts have been made to more accurately assess the intensity and distribution of cracking in slabs to aid in deflection prediction. Heiman (29) calculated much smaller deflections than those actually measured on four separate slabs using the ACI effective moment of inertia procedure, but obtained better results when greater degrees of cracking were assumed. Rangan (9) proposed, under long-term loading, the use of fully cracked moment of inertia for column strips and an average of fully cracked and uncracked moments of inertia for middle strips. These assumptions gave good agreement with slab deflections measured by Heiman, but may not necessarily apply to all cracked slabs. Scanlon and Murray (10) have suggested a more general method to account for the effects of cracking, including those due to restraint.

Accurate prediction of slab deflections is dependent on the assessment of cracking within the slab. Although significant amounts of cracking may occur due to shrinkage and restraint, loading of the slab causing moments to exceed the cracking moment is a major source of cracking. Significant loading at early age, that may occur during construction, can induce such moments into the slab. The problem is further complicated by the reduced tensile strength of concrete at early age.

2.4 Measured Deflections

Documentation of field-measured two-way slab deflections is not extensive. Most recorded data relate to flat slabs and plates constructed in Australia. Although construction materials and procedures may differ from those in North America, these studies still indicate the extent of two-way slab deflection problems.

Blakey (32) in 1961 reported on an experimental lightweight concrete flat plate. After a period of 200 days, the ratio of deflection to the initial dead load deflection was seven for the centre of an interior panel. In a separate investigation, Blakey (33) described deflections for an experimental 3.5 in thick lightweight concrete flat plate, spanning three bays of 9 ft in one direction and three bays of 12 ft in the other, with cantilevers of 4.5 ft in the long direction. In eight months, loaded only by self weight, the deflections at the centre of the interior panel

increased by twelve times over the initial elastic deflection. Of this measured deflection, 20 percent was attributed to differential column settlements, 40 percent to further cracking causing reduced stiffness and to local bond slip, and 40 percent to creep. It was noted that the slab was constructed of expanded shale concrete, underwent fluctuations in temperature and relative humidity, and was exposed to direct sunlight during the construction and observation periods.

Branson (18) reported on deflection measurements taken for a normal weight two-way slab system of nine panels, each 6 by 6 ft, and relatively deep beams. The slab was loaded by sand bags at 30 days for a period of 500 days. It was found that the ultimate ratio of time-dependent to initial deflection was approximately five.

In 1970 Taylor (30) described long-time deflections for a reinforced concrete flat plate constructed in North Sydney, Australia. The longer span-to-depth ratio was 31.0. Ratios of initial (three-day) deflection measurements to those taken 2.5 years later indicate increases of 6.5 to 10 for deflections at the centre of four interior panels. It was thought a partial reason for the large multipliers was the high creep and shrinkage characteristics of the concrete used. Comparison with calculted long-time deflections indicated best results were obtained when creep and shrinkage deflections were considered separately using Branson's procedure (18), thus allowing for cracking in the

slab.

The deflections of flexural members in four different Australian buildings were reported by Heiman in 1974 (29). These slab systems consisted of:

i) a flat plate roof in two-story commercial building (L/h=31)

ii) a flat slab in a three-story unenclosed car park (L/h=36)

iii) a flat plate in a four-story motel and car park (L/h=31)

iv) a tapered beam and slab construction in a fifty-story circular high-rise (L/h=21 for beams)

Deflection measurements were recorded for periods ranging from 2.5 to 8 years.

The first two systems had negligible construction loads as the slabs were propped directly to the ground below or supported no upper level slabs. For system (i) the long-time to initial deflection ratio was 8.7, while for system (ii) the ratio ranged from 5.1 to 6.3. Shrinkage deflections were thought to be a major factor in both these structures.

The latter two systems were subjected to heavy construction loads from the subsequent slabs cast above. In addition, the props bearing directly onto the ground in system (iii) settled during construction causing additional slab loading and deformation. Heiman noted the extensive cracking and loss of of stiffness associated with the construction loading at early age.

Long-time deflections were calculated for all four buildings using the methods of the ACI Code and those of Branson. With the former method, calculated deflections ranged from 34 to 67 percent below those measured, while using the latter method the range was 13 percent below to 17 percent above. The second range was dependent on the assumed degree of cracking in the slabs.

Jenkins (34) reported on deflections taken on the fourth floor of a five-story flat plate structure constructed in Australia. The ratio of one-year dead load deflection to the initial (ten-day) deflection was approximately four. The slab supported heavy construction loads from the above floor slab and storage of bricks for partition construction.

More recently, Sbarounis (35) summarized deflections for a multistory flat plate structure constructed in the United States. The longer span-to-depth ratio was 36.4. Measurements were taken over 175 bays on 13 alternating floors. In 90 percent of the cases, the measured one-year deflections exceeded one inch. Long-time deflections were calculated assuming a total one-year multiplier of 4.2 (36) and were in good agreement with average measured one-year deflections.

The majority of reported two-way slab deflections pertains to construction outside North America. Total long-time multipliers from measured deflections usually exceed the present accepted Code multiplier of three.

Abnormally high multipliers may be attributed to high creep and shrinkage characteristics of certain concretes, plus extreme environmental conditions during construction. Slabs subjected to heavy construction loading at early age experience increased cracking and reduced stiffness. The resulting larger initial deflections can influence the overall long-time deformations.

2.5 Code Requirements for Deflections

Present Code limitations for deflection of two-way slabs are based on minimum thickness requirements. Both CSA A23.3 M77 and ACI 318-83 Codes provide similar minimum thickness equations that consider spans, panel shape, effect of edge panels, size of supporting columns, presence of edge beams and/or drop panels, and grade of reinforcement. For slabs without beams, the controlling minimum thickness relation is a function of only clear span and reinforcement grade.

If a slab meets the minimum thickness requirements, then deflections need not be computed. For smaller slab thicknesses, computed deflections must not exceed specified limits. These limits pertain to immediate live load deflection and long-time deflection occurring after the attachment of non-structural elements due to all sustained loads, plus immediate deflection due to any additional live load. The additional long-time deflection is computed as a multiple of the immediate elastic deflection (usually two

for slab systems).

There are no separate provisions accounting for the effects of construction loads at early age. Increased cracking will cause larger immediate deflections. Any underestimation of immediate deflection will be magnified when a multiplier approach is used to calculate additional long-time deflection. In addition, maximum construction loads may be higher than the total service loads that are used to check the serviceability limits specified in the Code. Both these factors may lead to unsatisfactory deflections in slabs otherwise meeting Code requirements.

2.6 Summary

A review of the available literature on calculation methods for two-way slab deflection was presented. These included classical elastic plate theory, equivalent frame, and finite element methods. Additional factors affecting deflections, such as construction loading and cracking, were discussed. Examples of documented slab deflections were reviewed and present Code requirements governing deflections outlined.

3. PROPOSED MODEL FOR SLAB DEFLECTION CALCULATIONS UNDER CONSTRUCTION LOADS

3.1 Material Properties

3.1.1 Compressive Strength, Modulus of Elasticity, and Modulus of Rupture

Time-dependent properties of concrete are required to estimate deflections during the construction period and service life of the structure. Ideally the most accurate information regarding these properties is obtained from tests on specimens undergoing similar curing conditions to the concrete used in the structure under investigation. In lieu of this information, expressions given by ACI Committee 209 (19) for modulus of elasticity and tensile strength at early age give reasonable predictions, and are used in this model. These properties are functions of the time-dependent compressive strength.

Assuming moist-cured concrete (normal or lightweight) using Type I cement, the following equations are recommended by ACI Committee 209:

$$f'_c(t) = \frac{t}{4 + 0.85t} f'_c(28) \qquad (3\text{-}1)$$

$$f_r(t) = 0.013 \sqrt{w_c} \sqrt{f'_c(t)} \qquad (3\text{-}2)$$

$$E_c(t) = 0.043 \, w_c^{3/2} \sqrt{f'_c(t)} \qquad (3\text{-}3)$$

where: $f'_c(28)$ = 28-day compressive concrete strength (MPa)

$f'_c(t)$ = time-dependent compressive strength (MPa)

$f_r(t)$ = time-dependent rupture modulus (MPa)

$E_c(t)$ = time-dependent modulus of elasticity (MPa)

w_c = mass density of concrete (kg/m^3)

t = time since casting (days)

The constants in Equations 3-1, 3-2, and 3-3 are based on standard conditions as specified by ACI Committee 209.

Some consideration must be given to the modulus of rupture. Vanderbilt, Sozen and Siess (6) report a reduction in the modulus of rupture for reinforced concrete due to restraint stresses. When shrinkage occurs, presence of the reinforcement induces additional stress in the concrete and causes cracking. For a series of five test slabs, reduced effective modulus values ranging from 44 to 75 percent of the measured value were used for calculation of cracking moments. These values are summarized in Table 3.1. Reduction of the nominal Code modulus of $0.60\sqrt{f'_c}$ MPa by the same range would result in effective modulus of rupture values between $0.26\sqrt{f'_c}$ and $0.45\sqrt{f'_c}$ MPa.

Scanlon and Murray (10) also indicate that restraint stresses due to shrinkage may result in a lower effective

modulus of rupture. The limiting Code value of $0.60\sqrt{f'_c}$ MPa was obtained from tests on small unreinforced concrete specimens where shrinkage was not a major factor. However most concrete slab systems are restrained against shrinkage to some degree. The tensile stresses induced by this restraint are only partially relieved by creep effects.

Scanlon and Murray also found that with reinforcement percentages approaching minimum requirements, the moment-curvature relationship for a section in the service load range is more sensitive to the effective modulus of rupture. They suggest a restraint stress of approximately $0.20\sqrt{f'_c}$ to $0.32\sqrt{f'_c}$ MPa, resulting in effective modulus values of $0.40\sqrt{f'_c}$ to $0.28\sqrt{f'_c}$ MPa.

Both these studies indicate overall slab stiffness may be greatly reduced due to restraint.

3.1.2 Creep

Creep characteristics of concrete are required for long-time deformation calculations. The basic creep property of concrete is given by a creep coefficient. For this model, the creep coefficient expression given by ACI Committee 209 (19) is used.

The ACI creep coefficient is derived as the ratio of creep strain at any age t, after application of the load at time t_o, to the elastic strain at the age of application of load t_o. Thus:

$$C(t,t_o) = \delta(t,t_o)\, E_c(t_o) \qquad (3\text{-}4)$$

where: $C(t,t_o)$ = creep coefficient at time t for load applied at time t_o

$\delta(t,t_o)$ = creep per unit stress (specific creep or compliance) (1/MPa)

$E_c(t_o)$ = modulus of elasticity at time of load application (MPa)

The expression for the time-dependent creep coefficient given by ACI Committee 209 is:

$$C(t,t_o) = \frac{(t - t_o)^{0.6} C_u}{10 + (t - t_o)} \qquad (3\text{-}5)$$

where: $(t-t_o)$ = time since load application (days)

C_u = ultimate creep coefficient

An average ultimate creep coefficient of 2.35 is recommended by ACI Committee 209. Correction factors may be applied to this value allowing for non-standard age at loading, relative humidity, member thickness, concrete slump, percent fine aggregates, air content, and curing conditions.

The total elastic strain-plus-creep deformation under a unit stress, or total compliance, is given by:

$$\phi(t,t_o) = \frac{1}{E_c(t_o)} [1 + C(t,t_o)] \qquad (3\text{-}6)$$

where: $\phi(t,t_o)$ = total elastic strain-plus-creep deformation under a unit stress (1/MPa)

A typical series of compliance functions is shown in Figure 3.1 for increasing loading ages.

Most studies on creep and the resulting models refer to creep in compression. The characteristics of tensile creep are important to estimate shrinkage cracking and evaluate the validity of certain mechanisms and models (ie. creep under variable stress history). Neville, Dilger and Brooks (37) summarize several studies comparing creep in compression and tension. They report no general agreement on the tensile creep behaviour of concrete. Possible reasons include the difficulty in testing in true axial tension, the difficulty in accurate measurement of low strain levels associated with tensile creep tests, and concurrent drying shrinkage effects of test specimens several orders of magnitude greater than the creep effects. For this model, tensile and compressive creep characteristics are assumed to be equal.

3.1.3 Shrinkage

The second component associated with long-time deformation calculations is shrinkage. Concrete shrinkage is

not dependent on the load level, but is due to changes in the moisture content and physio-chemical changes (ie. cement hydration) of the concrete. However shrinkage may lead to increased cracking, reduced section stiffness, and thus load redistribution.

Shrinkage characteristics of a concrete are given by a shrinkage strain. Again the ACI Committee 209 (19) shrinkage strain expression is used for the model. For moist-cured concrete the shrinkage strain at any time t, measured from the end of the moist-curing period t_m, is given by:

$$\epsilon_{sh}(t) = \frac{(t - t_m)}{35 + (t - t_m)} \epsilon_{shu} \qquad (3\text{-}7)$$

where: $\epsilon_{sh}(t)$ = shrinkage strain at time t for moist-curing period t_m (mm/mm)

ϵ_{shu} = ultimate shrinkage strain (mm/mm)

$(t-t_m)$ = time since moist-curing period (days)

An average ultimate shrinkage strain of 780×10^{-6} mm/mm is suggested by ACI Committee 209. As with the ultimate creep coefficient, correction factors may be applied for non-standard length of moist-curing period, relative humidity, member thickness, concrete slump, percent fine aggregates, cement content, and air content.

3.2 Construction Loading

The calculation of construction loads for use in the model is based on the theory proposed by Grundy and Kabaila (21). Estimation of these loads requires a general understanding of the construction process involved.

Loads are introduced to the slabs in the supporting assembly during the construction period by a repeated sequence of operations. Initially shores and forms are erected on the top floor level and a new slab is cast. Secondly, forms and shores at the lowest level are stripped and moved to the new top floor level. Alternatively if a series of reshores is used, the second step involves removing the lowest level of reshores, then stripping the lowest level of forms and corresponding shores, and immediately reshoring this slab. These operations are summarized in Figure 3.2 for supporting assemblies consisting of three levels of shores, and two levels of shores plus one level of reshores.

At each load stage a slab in the supporting assembly will carry a certain multiple of the slab-plus-formwork deadweight, previously defined in Section 2.2 as a load ratio. The magnitudes of the load ratios are dependent on the number of shore and reshore levels in the supporting assembly. The absolute maximum load ratio for a slab occurs when the shores connecting that slab in the supporting assembly with the ground are removed. Although slight variations in the maximum load ratio occur for lower level

slabs, the ratio converges to a single maximum value for upper level slabs. This is shown in Figure 3.3 for the case of two levels of shores. In general, the maximum converged load ratio for a slab occurs when the slab reaches the bottom of the supporting assembly. The resulting stepped construction load sequence is illustrated in Figure 3.4.

In calculating actual load ratios for different support assemblies, constant stiffness is assumed for all slabs in the supporting assembly. Unless accurate information concerning the weight of forms, shores, and reshores is available, these may be taken as 10 percent of the slab self weight (21,26). The effect of a minimum 2.4 kPa construction live load applied to the supporting assembly is approximated by increasing the maximum load on a slab by 2.64/N kPa (22), where N represents the total number of levels in the supporting assembly. This additional load is applied at the beginning of the maximum construction load increment, as shown in Figure 3.4.

The relevant construction loads may be summarized as follows:

i) load at any stage

$$w = (\text{load ratio})(1.1)(\text{slab self weight}) \quad (\text{kPa}) \qquad (3\text{-}8)$$

ii) maximum construction load (including live load)

$$w_{max} = (\text{max. load ratio})(1.1)(\text{slab self weight}) + 2.64/N \quad (\text{kPa}) \qquad (3\text{-}9)$$

Appendix A gives typical calculations of construction load ratios and loads using the above assumptions for two

different support assemblies.

The converged set of construction load ratios is not dependent on the construction cycle time. The effect of reduced construction cycle times is to subject the slab to its maximum load at an earlier age. This same situation occurs as the number of shored levels in the supporting assembly is decreased.

3.3 Calculation of Immediate Deflection

Several methods for calculating immediate two-way slab deflections have been outlined in Section 2.1.1. Calculation of immediate deflection in the proposed model uses a finite element technique. Although most finite element programs are based on linear elastic material properties, the procedure outlined by Scanlon and Murray (10) is used to incorporate the effects of cracking into the finite element analysis.

3.3.1 Iterative Cracking Routine

The general methodology of the iterative cracking routine used is shown schematically in Figure 3.5. Initially moments and deflections are calculated using the material properties corresponding to the concrete age at the particular construction load stage and degree of cracking (if any) up to that stage. Once the applied load is sufficient to cause the cracking moment to be exceeded, the slab becomes precracked for all subsequent load stages. Moments are calculated using orthotropic stress-strain

relations for a plane stress condition, which are given by:

$$\begin{Bmatrix} \sigma_x \\ \sigma_y \\ \tau_{xy} \end{Bmatrix} = \begin{bmatrix} \frac{E_{cx}}{1 - \nu_x \nu_y} & \frac{\nu_x E_{cx}}{1 - \nu_x \nu_y} & 0 \\ \frac{\nu_y E_{cx}}{1 - \nu_x \nu_y} & \frac{E_{cy}}{1 - \nu_x \nu_y} & 0 \\ 0 & 0 & G_{xy} \end{bmatrix} \begin{Bmatrix} \varepsilon_x \\ \varepsilon_y \\ \gamma_{xy} \end{Bmatrix} \qquad (3\text{-}10)$$

where: σ_x, σ_y = normal stresses in x and y directions

τ_{xy} = shear stress

ϵ_x, ϵ_y = normal strains in x and y directions

γ_{xy} = shear strain

ν_x, ν_y = Poisson's ratio in x and y directions

G_{xy} = shear modulus

E_{cx}, E_{cy} = modulus of elasticity in x and y directions

For linear elastic isotropic materials:

$$E_{cx} = E_{cy} = E_c(t) \qquad (3\text{-}11)$$

$$\nu_x = \nu_y = \nu \qquad (3\text{-}12)$$

$$G_{xy} = G = \frac{E_c(t)}{2(1 + \nu)} \qquad (3\text{-}13)$$

In the model, Poisson's ratio for concrete is taken as 0.15.

Flexural stiffness of each element is reduced in both directions using the previously defined effective moment of inertia Equation 2-4 to the third power. The degree of cracking, or reduced stiffness in each direction is given by:

$$\alpha_x = \frac{I_{ex}}{I_{gx}} \qquad \alpha_y = \frac{I_{ey}}{I_{gy}} \tag{3-14}$$

where: α_x, α_y = degree of cracking in x and y directions
I_{ex}, I_{ey} = effective moment of inertia for an element
I_{gx}, I_{gy} = gross moment of inertia for an element

In calculating the effective moment of inertia, the effect of restraint stresses may be accounted for by reducing the modulus of rupture value in the cracking moment calculation given in Equation 2-4. Material properties are reduced by the same ratio:

$$\begin{aligned} E_{cx} &= \alpha_x E_c(t) & \nu_x &= \alpha_x \nu \\ E_{cy} &= \alpha_y E_c(t) & \nu_y &= \alpha_y \nu \end{aligned} \tag{3-15}$$

For simplicity, as recommended by Scanlon and Murray (10), the shear modulus is not reduced after cracking.

The finite element analysis is repeated using these reduced material properties to calculate new elastic

constants, and subsequent iterations are made until no further cracking occurs. A complete program listing and sample input for the iterative cracking routine is given in Appendix B.

3.3.2 Calculation of Incremental Deflections

The typical construction load sequence (Figure 3.4) for a flat plate is broken into individual load stages. At a given time, the slab is subjected to a particular total load, depending on the supporting assembly used. The finite element analysis, including the iterative cracking routine, calculates a final set of element deflections for the slab at each load stage.

With this procedure, the degree of cracking, and thus reduction in slab stiffness, is assessed for each load stage. Figure 3.6 shows a moment-curvature relationship for a typical slab element. The element stiffness is given by $E_c I_g$ until the cracking moment, M_{cr}, is attained. Beyond this point, cracking reduces the stiffness to $E_c I_e$, depending on the moment level. Analyzing the slab at each construction load stage allows a stepped approximation along the moment-curvature diagram, rather than a single approximation of the slab stiffness at the maximum service moment level. Incremental immediate deflection between applied successive load levels is obtained by subtracting the deflection from the previous total load level. Incremental deflections for a typical construction load

sequence are shown in Figure 3.7. These incremental deflections are used in calculating long-time deflections.

3.3.3 Finite Element Method

For this study, the finite element program SAPIV (38) is used. The program was modified to incorporate the iterative cracking routine described in Section 3.3.1. Analysis of the slabs uses four-noded quadrilateral plate bending elements, with each node having three translational and three rotational degrees of freedom.

In most cases, the analysis of interior panels of a slab system allows the use of symmetry, and quarter panel sections are considered. Figure 3.8 shows the boundary conditions used for a typical interior quarter panel.

3.4 Calculation of Long-Time Deflections

The two components of long-time deflection considered in the model are creep and shrinkage warping. Rather than a direct multiplier approach, creep and shrinkage deflections are calculated separately using procedures given by Branson (18) and adopted by ACI Committee 209 (19). These deflections, together with the incremental immediate deflections, are combined using superposition to obtain total long-time deflections.

3.4.1 Creep Deflections

Long-time creep deflections are calculated using the ACI Committee 209 expression:

$$\Delta_{cp} = k_r C(t,t_o)\Delta_e \qquad (3\text{-}16)$$

where: Δ_{cp} = long-time creep deflection

$C(t,t_o)$ = time-dependent creep coefficient as defined by Equation 3-5

k_r = factor to account for compression reinforcement and neutral axis shifts = 0.85

Δ_e = immediate elastic deflection

This definition includes both basic creep, or creep occurring under conditions of no moisture movement; and drying creep, the additional creep caused by drying.

Equation 3-16 is used to calculate a series of time-dependent creep deflection curves based on incremental immediate deflections, Δ_i, at each load stage. Figure 3.9 shows the typical set of creep deflection curves generated for the construction loading sequence and incremental deflections of Figure 3.7. Note that a negative incremental deflection produces a corresponding negative creep deflection curve.

3.4.2 Superposition of Creep Deflection Curves

The preceeding set of creep deflection curves, representing the entire construction load history, are combined to obtain the total instantaneous-plus-creep deflection. McHenry (39) proposed the theory of reversibility of creep, using the principle of superposition, to combine a series of elastic-plus-creep strain curves, including those due to positive and negative stress increments. More specifically, strains produced at a time t by a stress increment at age $t' < t$ are independent of strains produced at an earlier or later time.

For a typical construction load history, each stress increment is considered to produce a deformation component continuing for an infinite time. A stress decrement, or removal of load, is taken as an increment with a negative sign. The resulting creep strains are equal and opposite to those of a corresponding positive increment applied at the same time. Although derived in terms of creep strain or compliance, the superposition method is equally applicable to actual creep deflections. Figure 3.10 illustrates the principle of superposition for the creep deflection curves given previously in Figure 3.9. Note that the negative stress increment produces an initial decrease in total deflections, but that total deflections may then increase again due to the time-dependent deflection components of positive stress increment creep curves.

The validity of the principle of superposition has certain limitations. Bazant (40) has suggested conditions under which superposition agrees well with experimental data:

i) the stress magnitudes are 40 to 50 percent of the concrete strength (ie. approximately within the service stress range).

ii) the strains do not decrease in magnitude, but the stresses can.

iii) the specimen undergoes no significant drying during creep.

iv) there is no large increase of stress magnitude late after initial loading.

Bazant suggests the fourth condition introduces less error than the first three, and may be neglected in most analyses. The second condition is an important consideration in the linearity of creep curves since it deals with creep recovery after unloading has taken place.

When unloading occurs, recovery of strain is twofold. First, an immediate recovery equivalent to the elastic strain corresponding to the stress removed and modulus of elasticity at time of load removal occurs. A second gradual recovery of strain, or creep recovery, also occurs. As stated earlier, this creep recovery is assumed equal to creep under negative load in the superposition method. Both Bazant (40) and Branson (18) have noted that creep recovery is overestimated using the superposition principle. Neville,

Dilger and Brooks (37) also present experimental data indicating some degree of irrecoverable creep under decreasing load. They report a small general bias for the principle of superposition to overestimate deformations under increasing load and underestimate deformations under decreasing load. Also the effects of creep recovery are more pronounced when complete unloading occurs.

Some consideration of creep recovery is included in the model. Varying degrees of irrecoverable creep due to decreasing load are obtained by modifying the superposition procedure. Figure 3.11 illustrates the modified superposition principle for a constant stress level applied at time t_1 and removed at time t_2. Thus for negative stress increments, only a certain portion of the time-dependent creep strain is recovered. Bazant (40) suggests that up to twice the actual recovery is predicted by superposition, while CEB-FIP (41) indicates that recovery is approximately two-thirds of full creep recovery when full unloading occurs. Investigations herein using the model assume creep recoveries ranging from full to one-half the quantity predicted by superposition.

The basis for creep recovery in the principle of superposition is to represent removal of load by applying a negative compressive stress in a direction opposite to that of recovery. Alternatively, the removal of load could be represented by the addition of a tensile stress in the same direction as recovery. Neville, Dilger and Brooks (37)

report on tests comparing the two methods. They conclude no overall improvement in the prediction of creep recovery by the principle of superposition when the removal of load is represented by a load applied in the same direction as recovery.

Appendix C contains a listing of the program used to superimpose individual creep deflection curves and a sample input of data. The program requires only the incremental immediate deflections for each load step from the finite element analysis, and allows for variable creep recovery.

3.4.3 Shrinkage Warping Deflections

Long-time shrinkage deflection for a uniform beam is given by ACI Committee 209 as:

$$\Delta_{sh} = K_w \phi_{sh} L^2 \qquad (3\text{-}17)$$

where: Δ_{sh} = long-time shrinkage deflection

L = span

K_w = coefficient depending on end conditions

= 11/128 (one end continuous)

= 1/16 (both ends continuous)

ϕ_{sh} = shrinkage curvature

$$= \frac{0.7\varepsilon_{sh}(t)\rho^{1/3}}{h} \quad \text{(singly reinforced section)}$$

$$= \frac{0.7\varepsilon_{sh}(t)}{h} (\rho - \rho^{1/3}) \left[\frac{\rho - \rho'}{\rho}\right]^{1/2}$$

(doubly reinforced section)

h = slab thickness

ρ = tensile reinforcement percentage

ρ' = compressive reinforcement percentage

$\epsilon_{sh}(t)$ = time-dependent shrinkage strain as defined in Equation 3-7

This equation represents the shrinkage warping deflection due to the volumetric shrinkage of the concrete being resisted by the reinforcing steel. The shrinkage curvature is greatest for members with nonsymmetric reinforcement, and is generally of the same sign as that due to transverse loads. Thus shrinkage warping will increase the deflection due to transverse load.

Equation 3-17 may be adopted to find total shrinkage deflections in two-way slabs by using an equivalent frame procedure. The panel is broken into a column-beam strip (in long direction), and an orthoganal middle-beam strip (in short direction) (9). The equation is applied to find the midpoint shrinkage deflection of each strip. These deflections are added to obtain the total midpanel shrinkage deflection.

For column-beam strips, the span length is taken as the clear span distance between columns in flat plates or flat slabs. For middle-beam strips, the span is taken as the clear span distance between columns in flat plates, and the clear span distance between column capitals in flat slabs.

Total long-time deflection is obtained by adding the time-dependent shrinkage deflection to the superimposed instantaneous plus creep deflections:

$$\Delta_t = \Delta_{shc} + \Delta_{shm} + \Delta_{scp} \qquad (3\text{-}18)$$

where: Δ_t = total long-time deflection

Δ_{shc} = shrinkage deflection of column strip (Equation 3-17)

Δ_{shm} = shrinkage deflection of middle strip (Equation 3-17)

Δ_{scp} = superimposed creep deflection (Figure 3.10)

The program given in Appendix C also calculates the shrinkage deflection for the column and middle strips, and resulting total long-time deflection.

3.5 Summary

A model to calculate two-way slab deflections under construction loads was developed. Included in the model were ACI Committee 209 expressions for early age concrete properties, a stepped construction load sequence, and an iterative routine to include the effects of cracking. Immediate deflections were calculated using the finite element program SAPIV. Long-time deflections due to creep and shrinkage warping were calculated separately. The

principle of superposition was used to combine the long-time deflection components.

Table 3.1 Assumed Effective Modulus of Rupture Values

STRUCTURE	f'_c (psi)	f_r MEASURED (psi)	c_1 ($c_1\sqrt{f'_c}$)	f_r EFFECTIVE (ASSUMED) (psi)	c_2 ($c_2\sqrt{f'_c}$)	c_2/c_1
FLAT PLATE	2510	700	14.0	310	6.2	0.44
FLAT SLAB	2760	600	11.4	360	6.9	0.60
FLAT SLAB (WWF REINF.)	3760	800	13.0	600	9.8	0.75
TWO-WAY SLAB (DEEP BEAMS)	2830	590	11.1	400	7.5	0.68
TWO-WAY SLAB (SHALLOW BEAMS)	3550	940	15.8	550	9.2	0.59

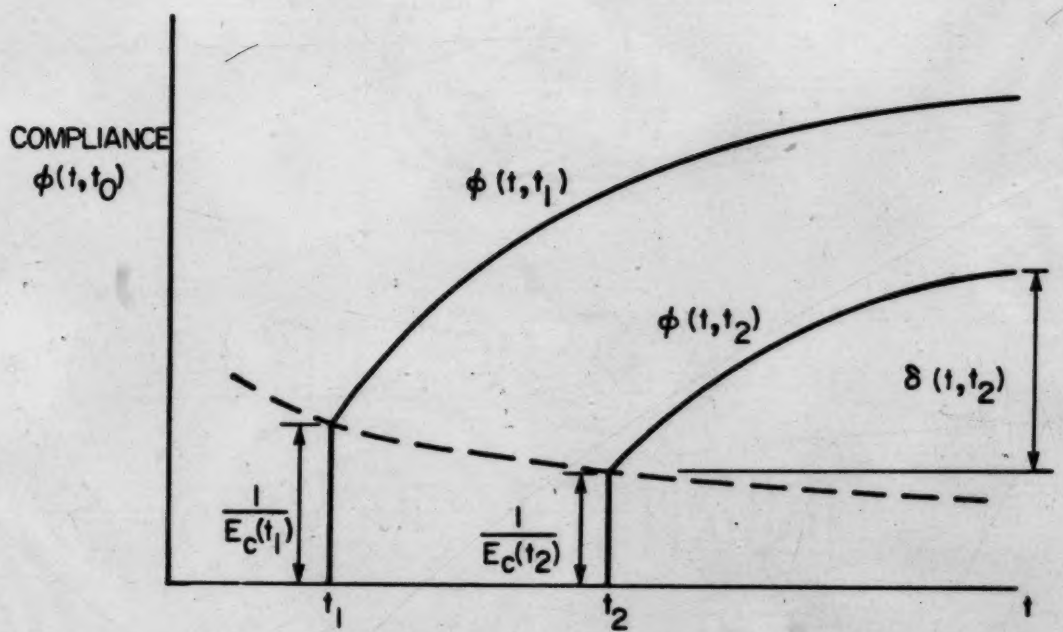

Figure 3.1 Creep Compliance Curves

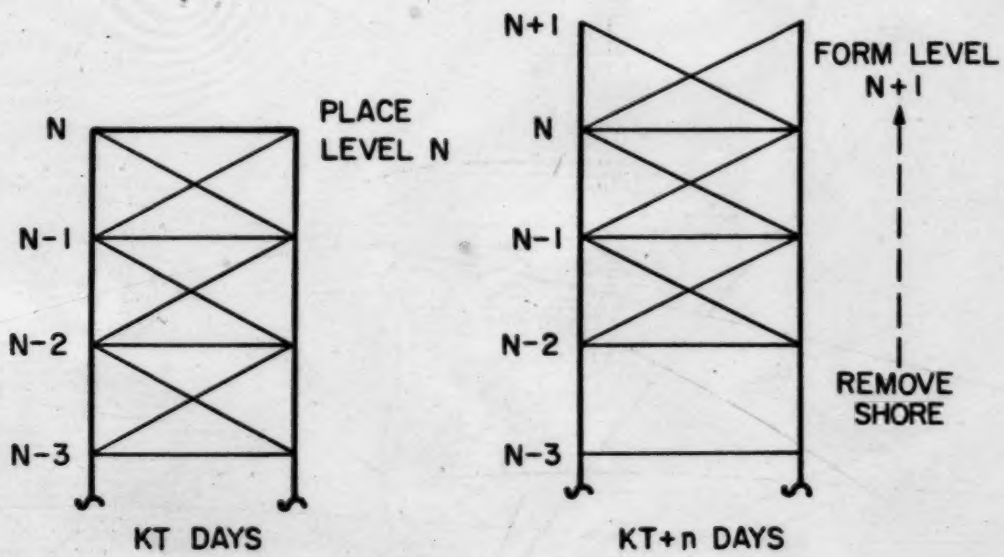

a) Three Levels of Shores (3+0)

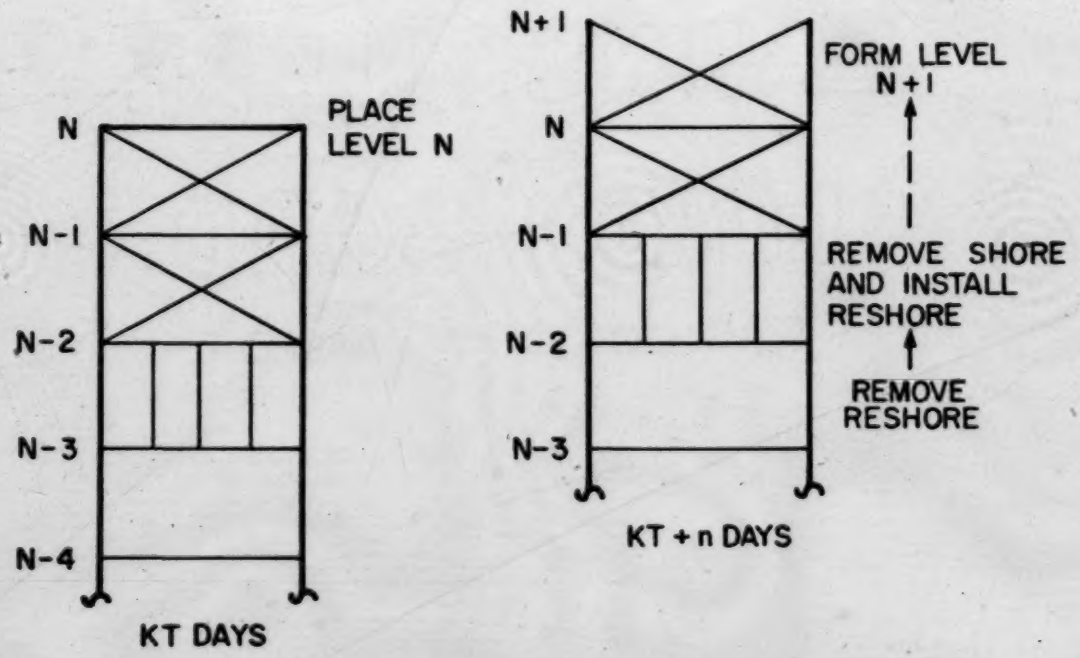

b) Two Levels of Shores, One Level of Reshores (2+1)

Figure 3.2 Basic Shoring Operations

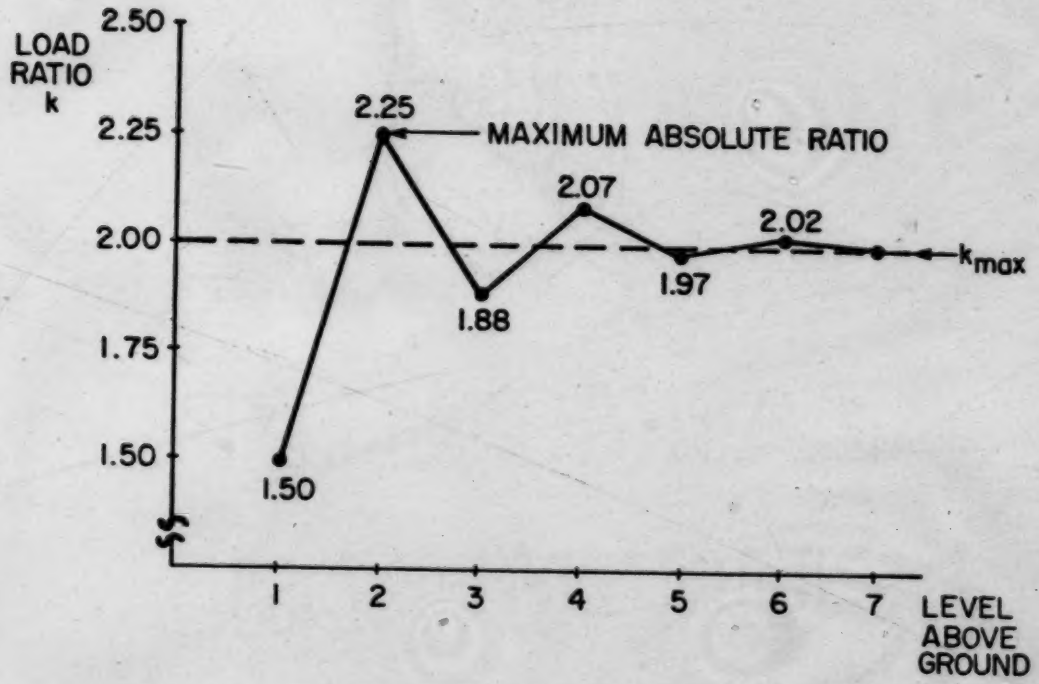

Figure 3.3 Maximum Absolute and Converged Construction Load Ratios for Two Levels of Shores (2+0)

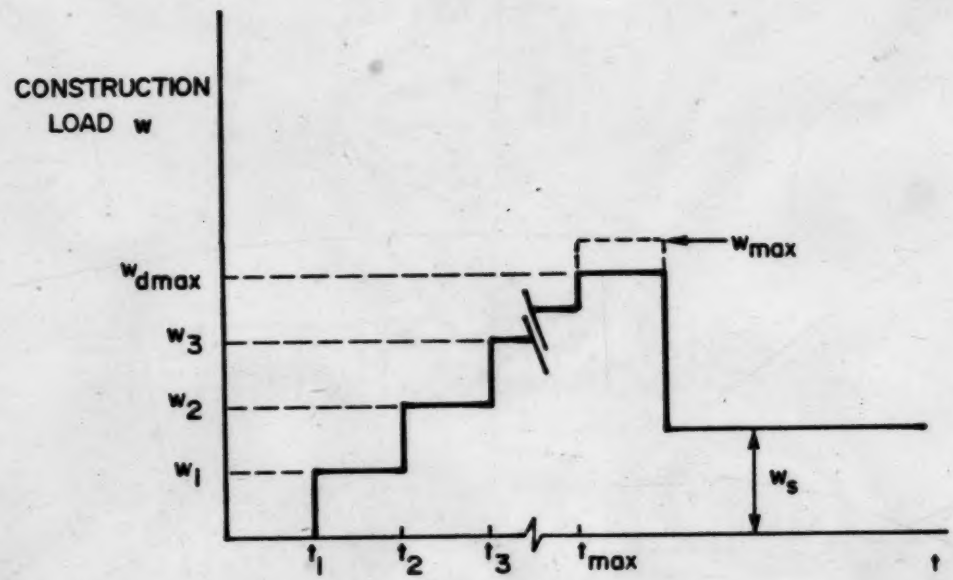

Figure 3.4 Typical Construction Load Sequence

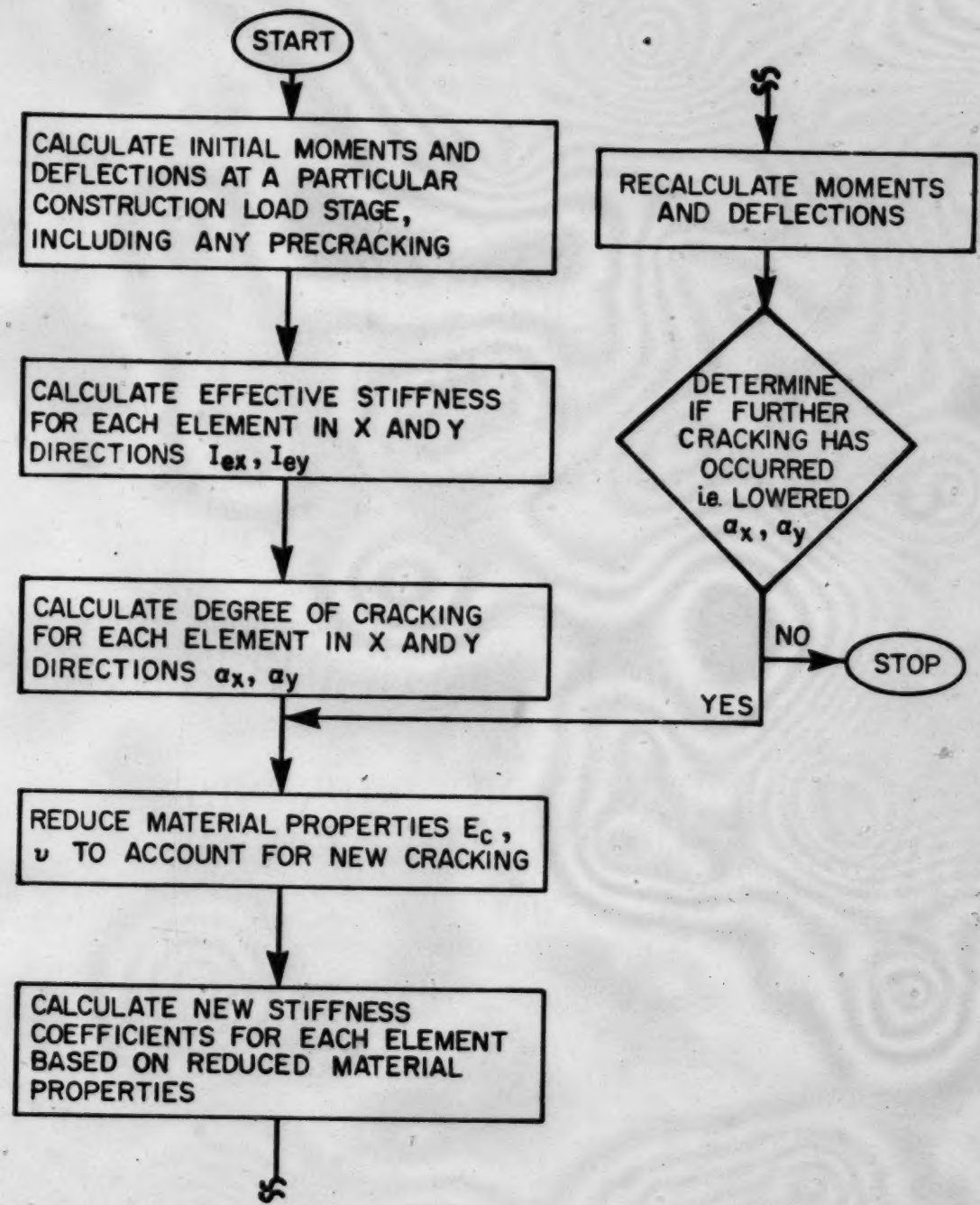
START
CALCULATE INITIAL MOMENTS AND DEFLECTIONS AT A PARTICULAR CONSTRUCTION LOAD STAGE, INCLUDING ANY PRECRACKING
CALCULATE EFFECTIVE STIFFNESS FOR EACH ELEMENT IN X AND Y DIRECTIONS I_{ex}, I_{ey}
CALCULATE DEGREE OF CRACKING FOR EACH ELEMENT IN X AND Y DIRECTIONS α_x, α_y
REDUCE MATERIAL PROPERTIES E_c, υ TO ACCOUNT FOR NEW CRACKING
CALCULATE NEW STIFFNESS COEFFICIENTS FOR EACH ELEMENT BASED ON REDUCED MATERIAL PROPERTIES
RECALCULATE MOMENTS AND DEFLECTIONS
DETERMINE IF FURTHER CRACKING HAS OCCURRED i.e. LOWERED α_x, α_y
NO
STOP
YES

Figure 3.5 Iterative Cracking Routine

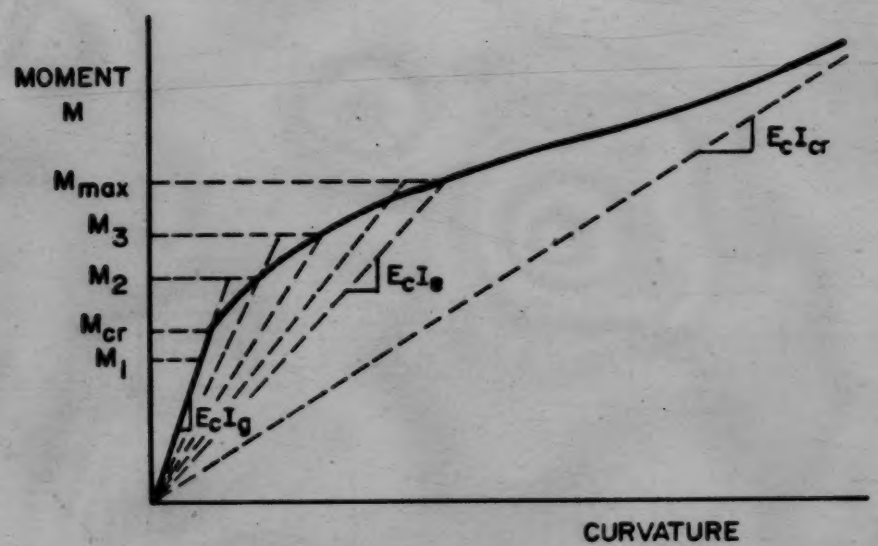

Figure 3.6 Moment-Curvature Relationship Showing Progressive Reduction in Stiffness

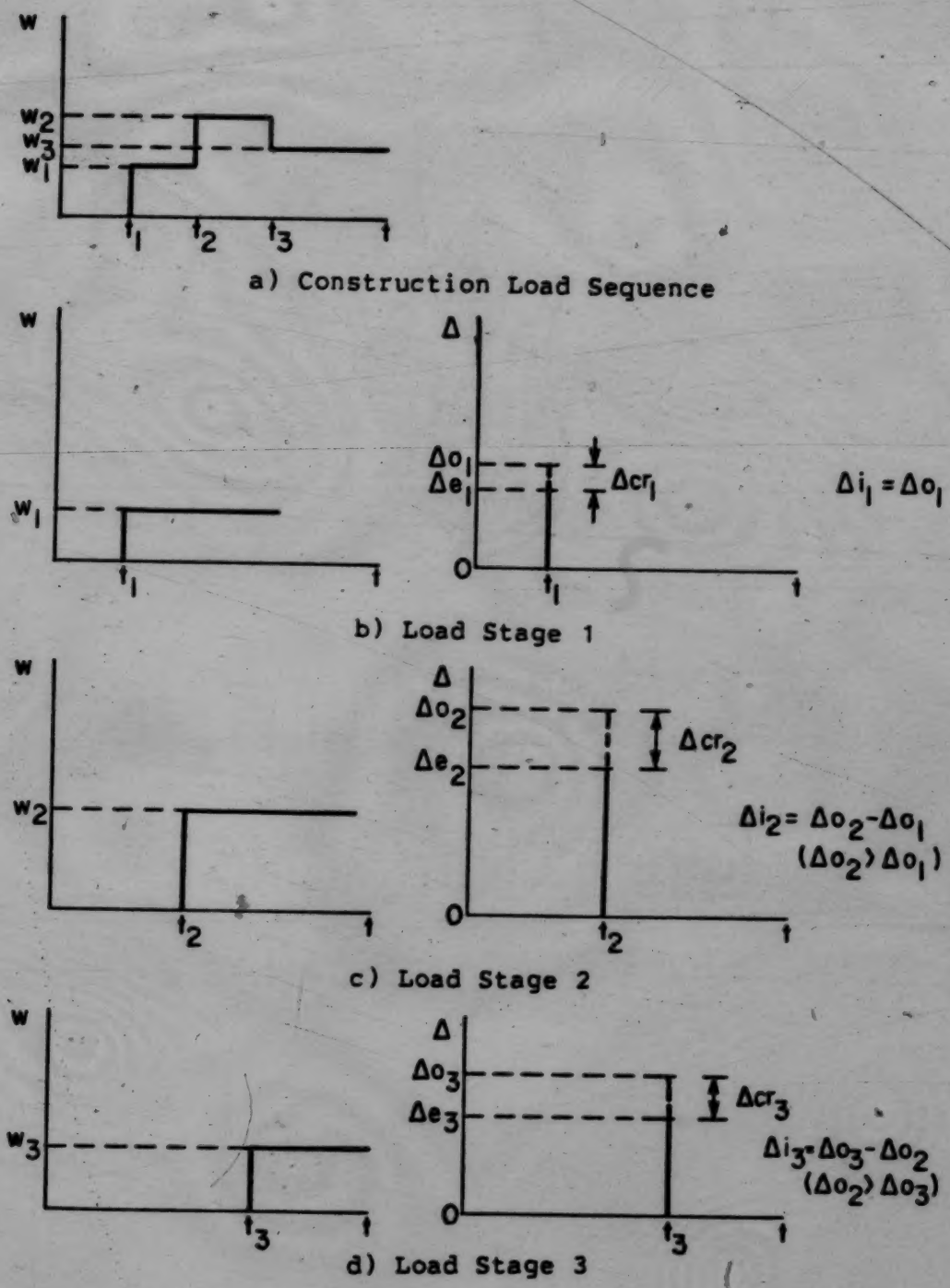

Figure 3.7 Calculation of Incremental Deflection

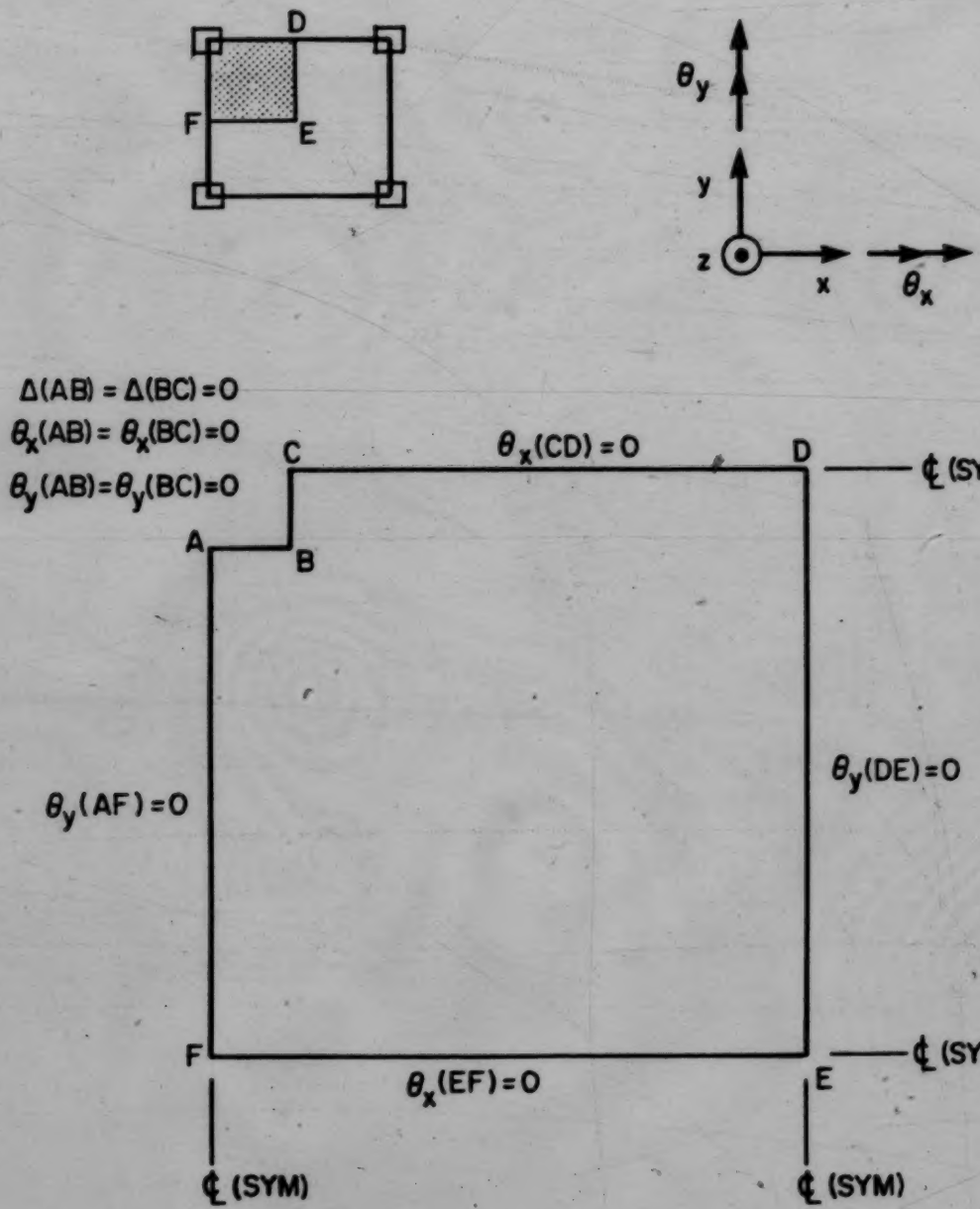

Figure 3.8 Boundary Conditions for a Typical Interior Quarter Panel

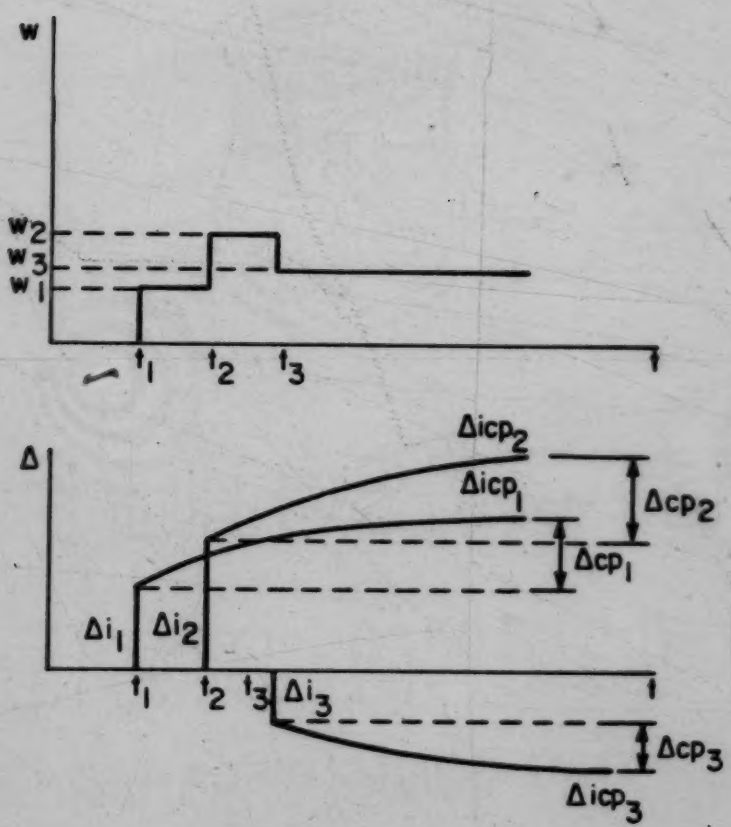

Figure 3.9 Creep Curves

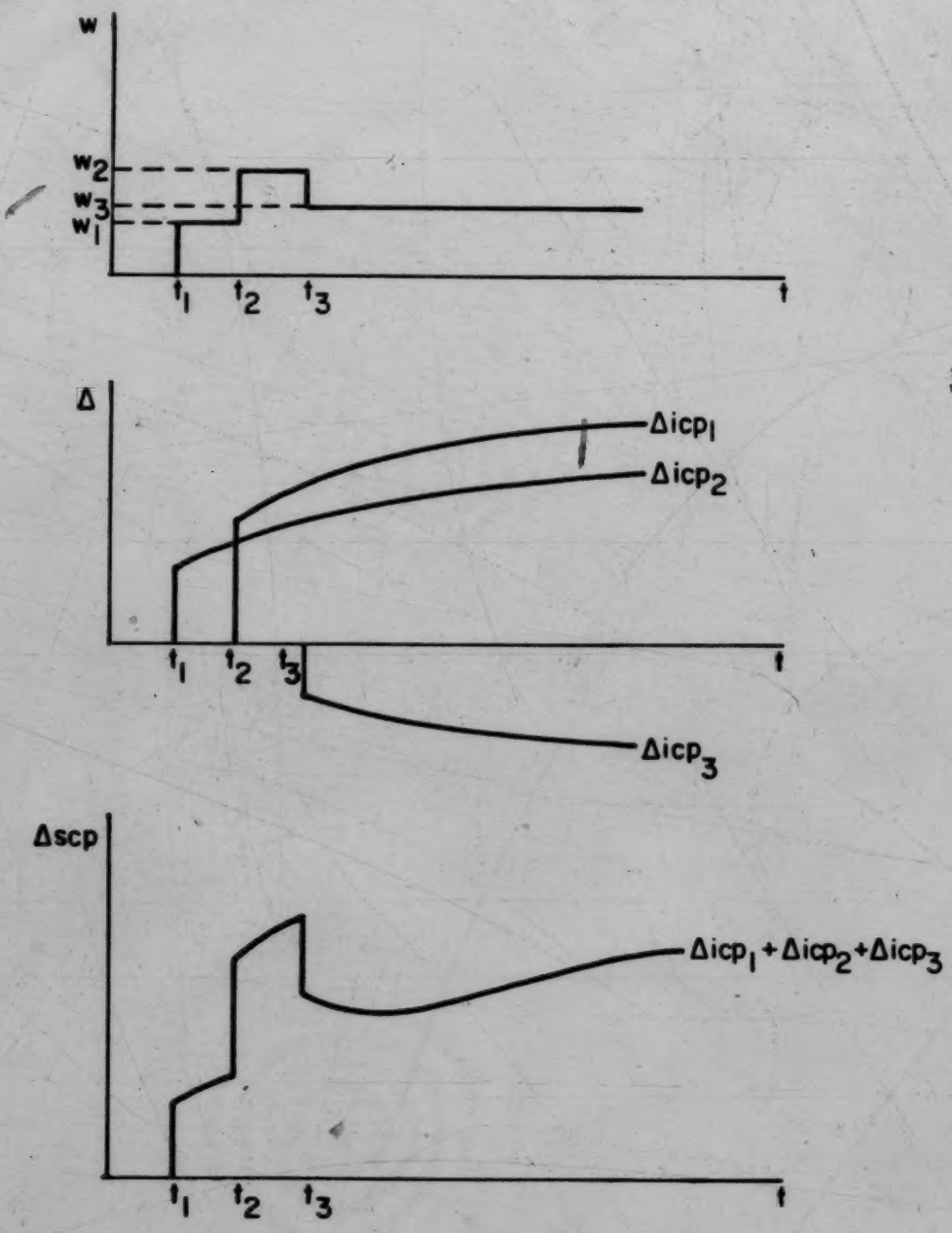

Figure 3.10 Superposition of Creep Curves

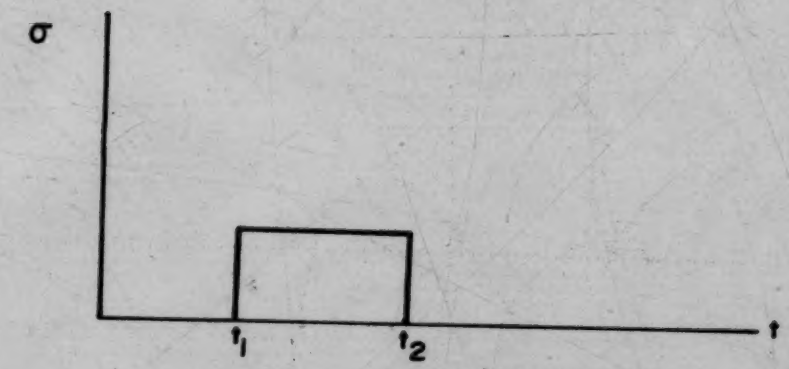

a) Stress Increment

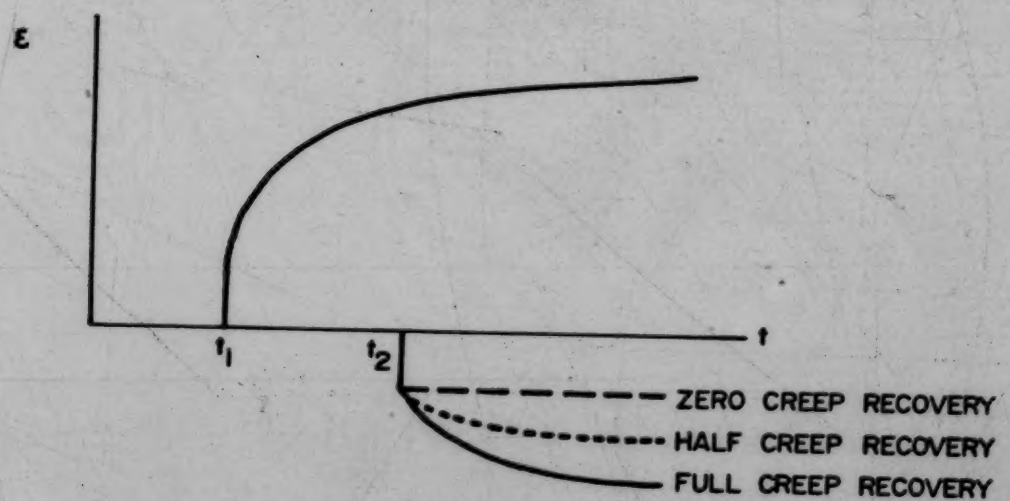

b) Specific Elastic-Plus-Creep Strains

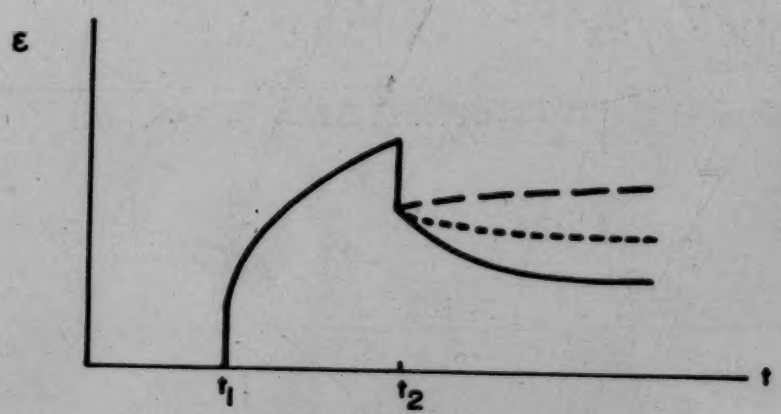

c) Superimposed Strains

Figure 3.11 Effect of Variable Creep Recovery on Strain-Time History

4. MODEL VERIFICATION

4.1 Introduction

Available data on field-measured deflections is not extensive. Section 2.4 summarized cases where excessive deflections have been measured. The proposed model applies to slabs subjected to general early age loading, but focuses on the loading sequence due to multistory construction.

Three slab systems are analyzed using the proposed deflection calculation procedure. One represents a true multistory construction, and the other two involve general early age loading. Together these slabs represent a range of span, thickness, and construction load histories. Calculated and measured deflections are compared.

4.2 Heiman's Flat Plate

4.2.1 Description of the Structure

The flat plate is located on level one of an enclosed car park in a motel building constructed in Sydney, Australia (29,31). Typical interior bays are 24 ft 9 in by 23 ft 9 in with three spans in one direction and five in the other direction. The slab thickness is 9.5 in, giving a longer span-to-depth ratio of 31.0.

The structure was designed as an elastic frame using a slab dead weight of 115 psf and car park live load of 60 psf. Reinforcement is typical of flat plate construction. A

complete description and data for analysis is included in Appendix D.

Figure 4.1 shows the floor plan and panel investigated. Duct openings adjacent to the interior columns were considered offset by the additional reinforcement placed, and were not included in the analysis.

Deflections were measured at the middle of three interior panels starting at 17 days after the slab was cast, continuing for a period of approximately 1300 days.

4.2.2 Material Properties

Material properties for this slab are discussed extensively in Reference (29). The design concrete strength was 3000 psi, and the average compressive strength of 28-day cores taken from the floor was 3300 psi. Additional concrete specimens were tested yielding a 28-day modulus of elasticity of approximately 3.2×10^6 psi and shrinkage strain at one year of 620×10^{-6} mm/mm. The creep coefficient corresponding to a two-year loading period was measured as 1.3.

For modelling purposes, time-dependent compressive strength, modulus of rupture, and modulus of elasticity were calculated based on the design concrete strength of 3000 psi. Calculated 28-day modulus of elasticity (3.3×10^6 psi) is in good agreement with the measured value (3.2×10^6 psi). The ultimate creep coefficient using ACI Committee 209 procedures is 1.56. When adjusted for a loading period of

589 days, the coeffient becomes 1.28, which is in general agreement with that reported. Shrinkage strains are taken as those measured.

4.2.3 Construction Loads

The slab under investigation was supported by props bearing directly onto the ground below which consisted partly of weathered shale and clay, and partly of compacted fill. The floor above was poured fourteen days after the test slab was cast. Most of the props below the test slab were removed twenty-one days after casting, with the remainder removed one day later. The floor above was partly stripped twenty-eight days after placement of the test slab, with all props removed eight days later. This sequence of operations is shown in Figure 4.2.

Large settlement of the props during construction caused heavy loads to be carried by the test slab at early age. The ratio of load transferred to the ground and that carried by the test slab is not known. Measured deflections for the slab prior to the removal of props bearing on the ground indicate a large portion of the load was carried by the test slab. For this investigation it was assumed 67 percent of the slab-plus-formwork weight was carried by the slab seven days after casting. Heiman reported an estimated maximum construction load of 170 psf carried by the test slab when the floor above was poured. At age twenty-one days, the test slab was assumed to be carrying only its self

weight. The full construction load sequence used for analysis is shown in Figure 4.3.

4.2.4 Comparison of Calculated and Measured Deflections

Deflections calculated by the model for modulus of rupture values $4\sqrt{f'_c}$, $6\sqrt{f'_c}$, and $7.5\sqrt{f'_c}$ psi and those measured are shown in Figures 4.4, 4.5, and 4.6 respectively. Using an effective modulus of rupture equal to $6\sqrt{f'_c}$ psi gives a lower bound to the measured deflections. Calculated deflections at 1300 days (0.67 in full creep recovery; 0.72 in half creep recovery) are below the measured range of 0.85 to 0.94 in. Reducing the modulus of rupture to $4\sqrt{f'_c}$ psi more closely predicts initial and long-time deflections (0.87 in full creep recovery; 0.94 in half creep recovery), but gives greater than measured deflections for the period between 50 and 300 days since casting. Note that by using the standard modulus of rupture value $7.5\sqrt{f'_c}$ psi for this slab, ultimate deflections are well below those measured (0.64 in full creep recovery; 0.68 in half creep recovery).

In all cases it appears the shape of the predicted long-time deflection curve is not consistent with the gradual increase shown by the measured deflections. This could result from the concrete used in the test slab having different time-dependent properties than those used in generating the ACI creep and shrinkage expressions. Also the actual loading sequence may differ from that assumed.

Shrinkage deflections calculated for the slab are a major portion of the total long-time deflection. A curing compound was applied to the slab the morning after casting. A 21-day moist curing period was assumed corresponding to the removal of forms from the test slab.

For this slab, the degree of creep recovery has little effect. Long-time deflections assuming half versus full creep recovery increase less than 10 percent.

Heiman reports extensive cracking for this slab on the upper surface around the columns and on the bottom surface in the midpanel regions. The cracking was first noticed two months after the slab was placed, but probably commenced soon after casting, and increased with time as a result of shrinkage. The reduced modulus of rupture values were used to account for this cracking due to shrinkage. With a modulus equal to $6\sqrt{f'_c}$ psi in the model, the middle strip remained virtually uncracked, and the column strip stiffness reduced to between 40 and 90 percent of the gross value. Using $4\sqrt{f'_c}$ psi for the rupture modulus produced approximately 50 percent cracking in the midpanel region, and 60 to 70 percent cracking around the columns. This condition more accurately represents the actual cracking observed.

4.3 Sbarounis' Flat Plate

4.3.1 Description of Structure

Deflections were measured on several levels of a multistory flat plate structure (35). Typical interior centre-to-centre spans were 22 ft, with a clear span of 20.9 ft. The specified slab thickness was 7.25 in, giving a span-to-depth ratio of 36.4. Measurements of actual slab thickness produced an average value close to the specified value.

In addition to the slab weight, specified design loads included a 40 psf live load and a 20 psf partition allowance. Appendix E contains a complete description and data for analysis of the slab.

4.3.2 Material Properties

The slab was cast from lightweight concrete having a specified 28-day compressive strength of 4000 psi. Creep and shrinkage properties of the concrete were given as the standard ACI Committee 209 values of 2.35 for the ultimate creep coefficient, and 800 x 10^{-6} in/in for the ultimate shrinkage strain.

4.3.3 Construction Loads

The supporting assembly used in construction consisted of three levels of forms and shores, with five to seven levels of reshores. A two floor per week schedule was

maintained.

Sbarounis reported the stripping procedure used during construction significantly affected the supporting assembly. On most levels, stripping occurred over large areas or over complete floors prior to reshoring. In addition, reshoring was not closely spaced and did not line up floor to floor. Stripping of the lowest level of forms in large areas will cause the stripped slab to carry construction loads attributable to a three-level supporting assembly. Thus it was felt the effective supporting assembly consisted of three shored levels instead of eight total shored and reshored levels.

The maximum construction load estimated by Sbarounis was 157 psf. This compares with an ultimate design load of 190 psf and total service load of 127 psf. The actual construction load sequence used for the model analysis based on a three-level support assembly is shown in Figure 4.7. It was assumed a new slab was cast every four days, and forms stripped and slabs reshored two days after casting. Materials for construction of partitions, ceiling, and building exterior were stored on the respective floors approximately two months after casting. These were reported as being equal to a 20 psf load applied sixty days after casting.

4.3.4 Comparison of Calculated and Measured Deflections

Deflection measurements were taken over 175 bays on 13 floors. The net measured one-year midpanel deflections ranged from 0.53 in to 2.16 in, with an average of 1.35 in, a standard deviation of 0.29 in and coefficient of variation of 21.2 percent. In 90 percent of the cases, the measured deflections exceeded one inch.

A typical interior quarter panel section was analyzed using the proposed model. To determine the sensitivity of calculated deflections to degree of cracking and amount of creep recovery, analyses were made for modulus of rupture values in the range 2 to $7.5\sqrt{f'_c}$ psi, and for zero, one-half, and full creep recovery under decreasing load. The resulting calculated long-time deflection curves are given in Figures 4.8, 4.9, and 4.10.

Assuming full creep recovery, the average measured deflection corresponds to a calculated deflection based on a modulus of rupture close to $4\sqrt{f'_c}$ psi. For one-half creep recovery the average measured deflection corresponds to a modulus of rupture near $6\sqrt{f'_c}$ psi. For zero creep recovery the average measured deflection is between the deflection calculated based $7.5\sqrt{f'_c}$ psi and an uncracked slab.

For the range of modulus of rupture and degree of creep recovery considered, all calculated deflections are within the range of measured deflections except for the case when modulus of rupture equals $2\sqrt{f'_c}$ psi and zero creep recovery. Figure 4.11 illustrates the effect of assumed modulus of

rupture on calculated one-year deflections.

From this analysis it appears the assumed degree of creep recovery has a significant effect on the calculated deflections, due to the large unloading increment during the construction load history. As noted in Section 3.4.2, the superposition method used to determine long-time deflections tends to overestimate creep recovery under decreasing load (full creep recovery case). A value somewhere between one-half and full recovery is a more realistic choice. For an interior panel, adjacent panels would provide restraint against shrinkage. Thus an effective modulus of rupture below the standard $7.5\sqrt{f'_c}$ psi value is reasonable. With one-half creep recovery and a modulus of rupture between $4\sqrt{f'_c}$ and $6\sqrt{f'_c}$ psi, a range of deflections close to those measured is predicted for this slab.

Calculated deflections based on service dead-plus-live load applied instantaneously at twenty-eight days, followed by a sustained load of dead load plus 20 psf superimposed dead load are also shown in Figures 4.8, 4.9, and 4.10. Modulus of rupture was assumed equal to $7.5\sqrt{f'_c}$ psi. This load sequence produces significantly less deflection at one year than that including the construction loads. Applying the current Code multiplier of three to the instantaneous deflection due to sustained loads produces a total long-time deflection of 0.63 in. This is well below the actual average measured deflection.

Sbarounis also calculates a one-year deflection value of 1.25 in for this slab. The method used for this calculation of long-time deflection, taking account of construction loading, is based on an equivalent frame procedure and standard ACI Committee 209 creep and shrinkage provisions (36). The analysis produces a one-year deflection close to the average measured value, but fails to predict the wide range of deflections measured.

4.4 Taylor's Flat Plate

4.4.1 Description of Structure

A flat plate roof was added to an existing two-story reinforced concrete building located in North Sydney, Australia. Initial and long-time deflections for the slab were documented and reported by Taylor (42). The typical interior column grid was 20 ft 10 in by 16 ft 8 in, with 14 in square interior columns. Slab thickness was 8 in, giving a longer span-to-depth ratio for an interior panel of 31.0. Figure 4.12 shows the plan of the slab and the test panel investigated.

The slab was designed for future use as a floor slab. Specified design loads included the slab self weight of 100 psi, finishes of 10 psi, and superimposed live load of 75 psi. Layout of reinforcement and data for analysis of the test slab is included in Appendix F.

4.4.2 Material Properties

The slab was constructed using normal weight concrete with a specified 28-day compressive strength of 3000 psi. Specified yield strength of the reinforcement was 50000 psi.

Additional material properties for age at loading of the slab were reported by Taylor. Modulus of elasticity was given as 3.55×10^6 psi. The modulus of rupture was given as 600 psi, and assumed reduced by Taylor to a value of 350 psi due to shrinkage stresses. For the model study, rupture modulus values were taken as $4\sqrt{f'_c}$ and $2\sqrt{f'_c}$ psi (218 and 109 psi respectively) to more closely predict initial deflection measurements.

Creep and shrinkage properties of the concrete were not measured. It was thought the concrete used did exhibit higher than average creep and shrinkage characteristics. The ultimate creep coefficient was taken as 1.95 (according to ACI Committee 209 recommendations), corresponding to a creep coefficient of 1.65 at 864 days after the slab was cast. The shrinkage strain was taken as 800×10^{-6} in/in at 864 days after casting, as given by Taylor. Curing of the test slab was reported good, with impervious building paper applied the day after casting. Shrinkage was assumed to begin fourteen days after casting, when the slab was stripped.

4.4.3 Construction Loads

The test slab was supported by shores to the floor slab below for a period of fourteen days. At the time of

stripping, the slab was not subjected to any additional superimposed load and carried only its self weight. An additional load of 4 psf was allowed for metal deck and roof insulation. Thus the equivalent construction load sequence consisted of a single 104 psf sustained load applied at fourteen days after casting. Although this load history is less severe than typical construction loads applied in multistory buildings, it represents loading at early age for which excessive long-time deflections were measured.

4.4.4 Comparison of Calculated and Measured Deflections

Deflection measurements were recorded at the midpoint of an interior panel for a period of 850 days after removal of shores. Initial deflection readings were taken three days after stripping of the slab. Taylor noted that these deflections would also include the creep deflection of the first floor slab during the period it supported the test slab. This increment of long-time creep deflection was assumed to be negligible. Figure 4.13 shows the measured deflections for the centre of an interior panel.

After a period of 2.5 years, measurements indicated an additional deflection of approximately 5.5 times the initial deflection three days after the removal of shores. This far exceeds the current additional deflection multiplier of two.

Deflections were calculated using the proposed model for the same interior panel. Use of a symmetrical three-span frame in the analysis included the effects of the adjacent

external panel. The resulting total deflections assuming modulus of rupture values equal to $4\sqrt{f'_c}$ and $2\sqrt{f'_c}$ psi, and shrinkage deflections are shown in Figure 4.13. With a rupture modulus equal to $4\sqrt{f'_c}$ psi, the initial measured deflection is closely matched, but deflections after 2.5 years are underestimated. Reduction to $2\sqrt{f'_c}$ psi gives long-time deflections close to those measured. In both cases, the shape of the predicted long-time deflection curve is different from that measured. Actual deflections for the test slab increase gradually, while those predicted increase rapidly at first, then level off to a constant value. This is similar to the deflection behaviour described for the slab in Section 4.2.4.

Taylor suggests the extent of initial flexural cracking may have greatly influenced deflections for this slab. Upon removal of shores, most of the slab would have been subject to relatively small flexural compressive stress. With a load producing few initial cracks, sustained loading may cause the formation of a high proportion of new cracks when stresses exceed service levels. This situation could occur as a result of the peak negative moments at an interior column. Thus when little initial cracking occurs, a higher ratio of final long-time to initial deflection may be expected. In addition, Taylor notes the concrete used in the construction had relatively high shrinkage warping characteristics. This is illustrated by the large component of shrinkage deflection in Figure 4.13. Large shrinkage

warping deflections will cause further cracking and increased loss of slab stiffness.

It appears that when using ACI Committee 209 procedures to predict long-time deflections, the initial deflection used in a multiplier method must accurately reflect the cracking characteristics and material properties of the concrete. Calculations for this slab by Taylor gave a prediction of only 43 percent of the measured long-time deflection when an initial elastic deflection, based on a mostly uncracked section, was used with the standard multiplier of three. Good results were obtained considering the interior panel made up of a column strip, cantilever element, and simply supported plate (6), with the column strip fully cracked and the remaining components 50 percent cracked. Rather than a multiplier, creep and shrinkage deflections were calculated separately using the procedure of Branson (18). Computed initial deflection exceeded that measured due to the extent of cracking assumed, but provided a more realistic evaluation of the long-time condition of the slab.

For this slab, excessive construction loads were not present. Referring to Figure 4.13, although a rupture modulus of $4\sqrt{f'_c}$ psi matched the initial deflection, relatively little cracking resulted in an underestimation of long-time deflection. With $2\sqrt{f'_c}$ psi, the more extensive cracking predicted with the single load application gave an initial deflection that, used with ACI Committee 209

procedures, reflected the measured long-time deflections.

4.5 Discussion

The slab systems considered in this chapter illustrate several important features of the proposed model. In all cases it appears the assumed value of the modulus of rupture has a significant effect on the calculated deflections. Use of the standard Code value often underestimated the degree of cracking. A reduced effective modulus of rupture more closely predicted the extensive cracking of Heiman's Flat Plate. For loading at early age, a reduced modulus will greatly increase the incremental deflection and the corresponding creep deflection.

Accuracy of the deflections calculated by the model will depend on the assumed loading history and time-dependent concrete properties. If the support assembly and construction cycle time are reasonably known, as with Sbarounis' Flat Plate, the construction load sequence can be closely estimated. This was also the case for Taylor's Flat Plate, where excessive constructions loads were not present, and the loading history consisted of only self weight. However, as with Heiman's Flat Plate, the loading sequence is not always known and must be estimated from the construction procedure used. The maximum load level and time of application appear to be important parameters.

Use of ACI Committee 209 expressions for early age properties, and creep and shrinkage characteristics will not

apply equally to all concretes. These expressions give representative average values, and may require adjustment depending on the situation. Actual field-measured concrete properties for the slab being investigated allow verification of the properties calculated by the model.

The proposed model is capable of predicting a range of deflection for a given slab, instead of a single ultimate value. The importance of this is illustrated by the range of measured deflections reported by Sbarounis. In addition to the modulus of rupture, the degree of creep recovery under unloading can be altered. A comparison of Heiman's and Sbarounis' Flat Plates indicates variable creep recovery is important only when significant unloading occurs. This is usually the case when a multistory supporting assembly is used during construction.

4.6 Summary

The proposed model was used to calculate deflections for three previously documented flat plates. Comparison of calculated and measured deflections were satisfactory in two cases. For the third slab, ultimate deflections were matched when a small effective modulus of rupture was considered. These analyses indicated calculated deflections were dependent on the construction load history, early age concrete properties, effectve modulus of rupture, and degree of creep recovery.

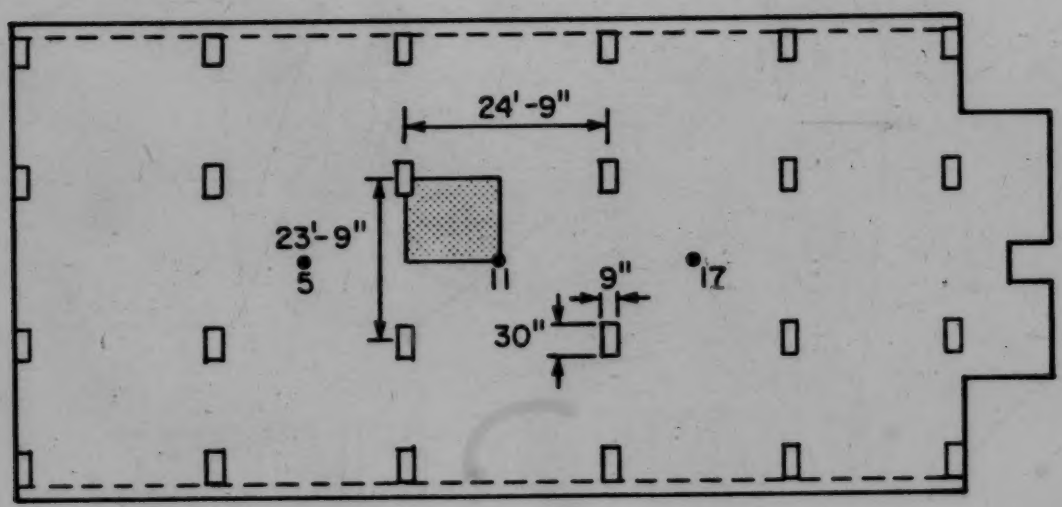

- TYPICAL INTERIOR QUARTER PANEL ANALYZED

5, 11, 17 - DEFLECTION MEASUREMENT POINTS

Figure 4.1 Heiman's Flat Plate

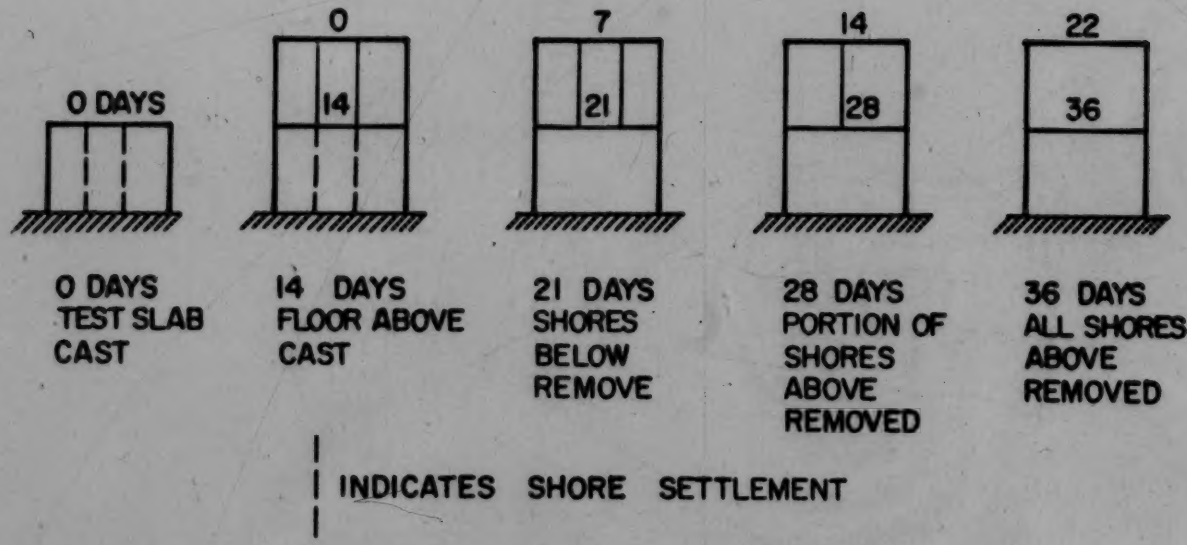

Figure 4.2 Heiman's Flat Plate - Construction Sequence

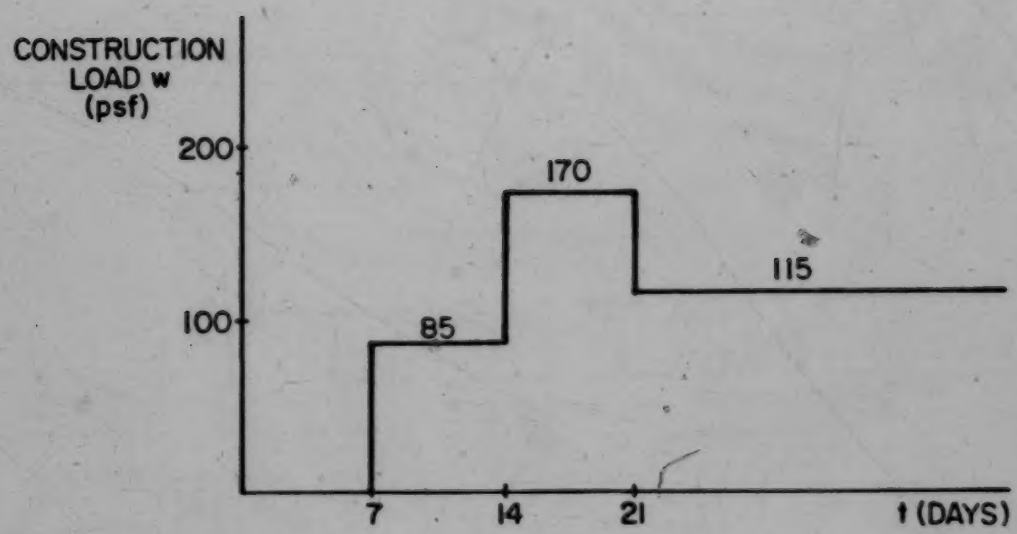

Figure 4.3 Heiman's Flat Plate - Construction Load Sequence

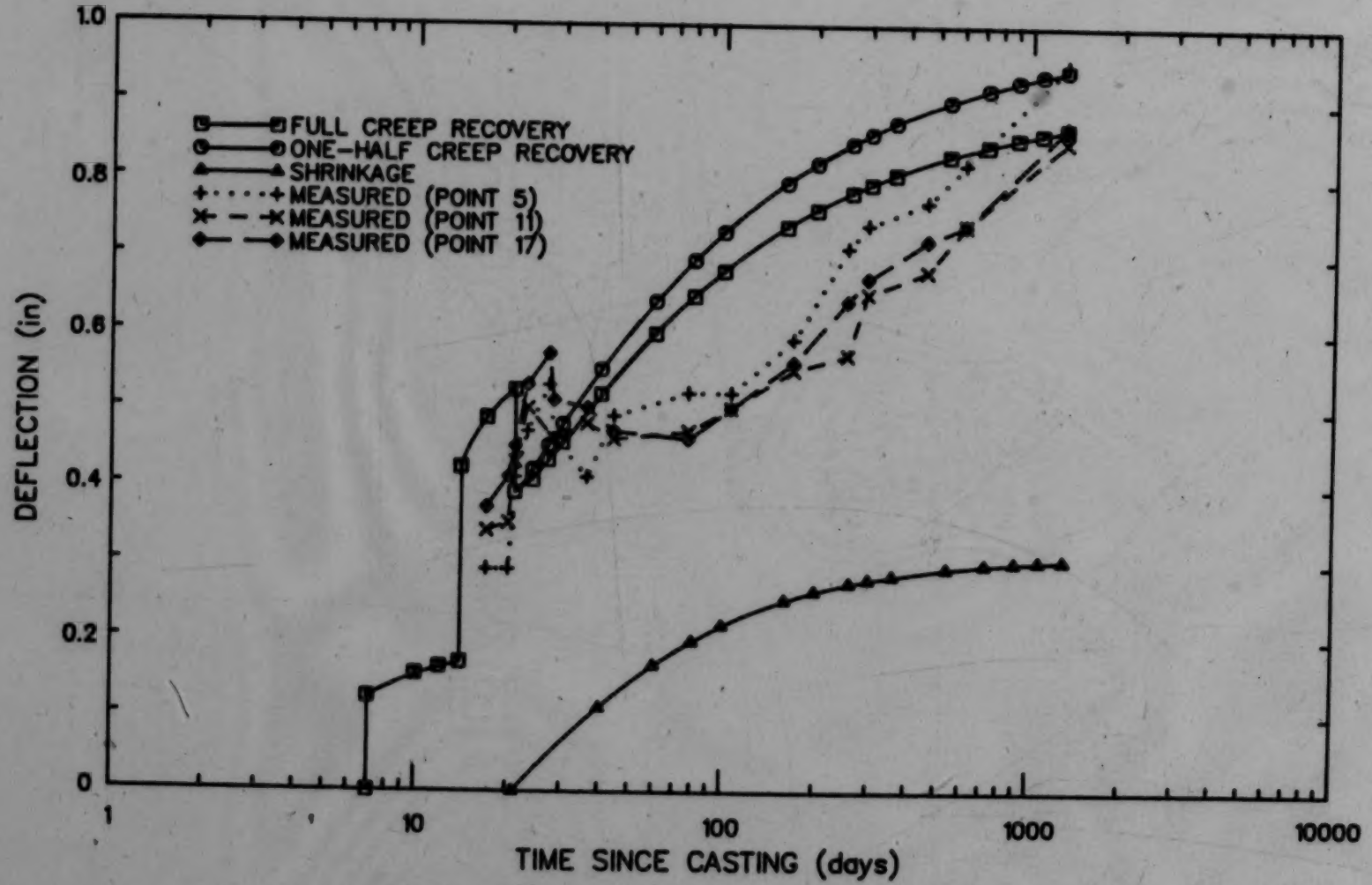

Figure 4.4 Heiman's Flat Plate - Long-Time Deflections
($f_r = 4\sqrt{f'_c}$ psi)

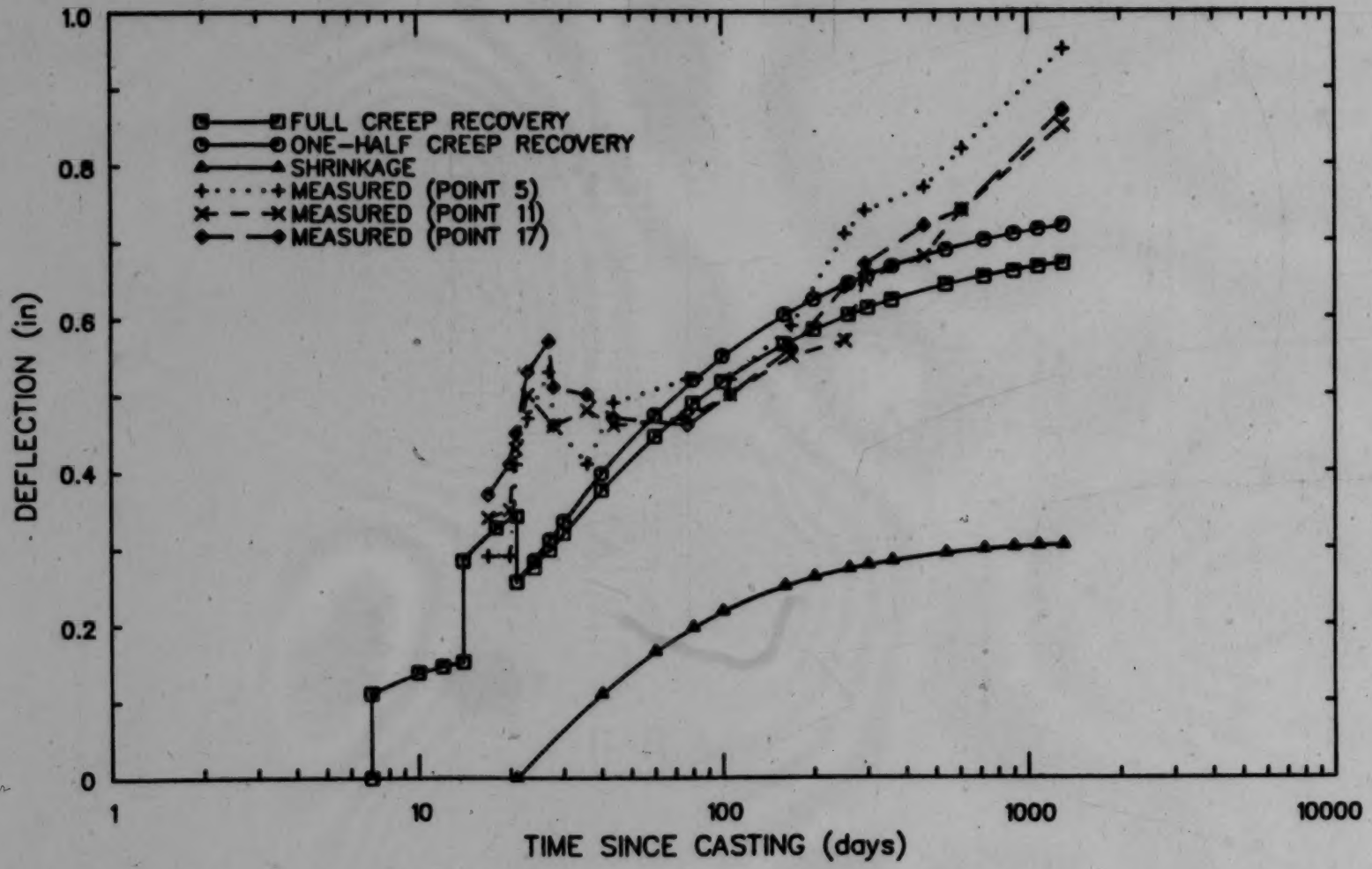

Figure 4.5 Heiman's Flat Plate - Long-Time Deflections
($f_r = 6\sqrt{f'_c}$ psi)

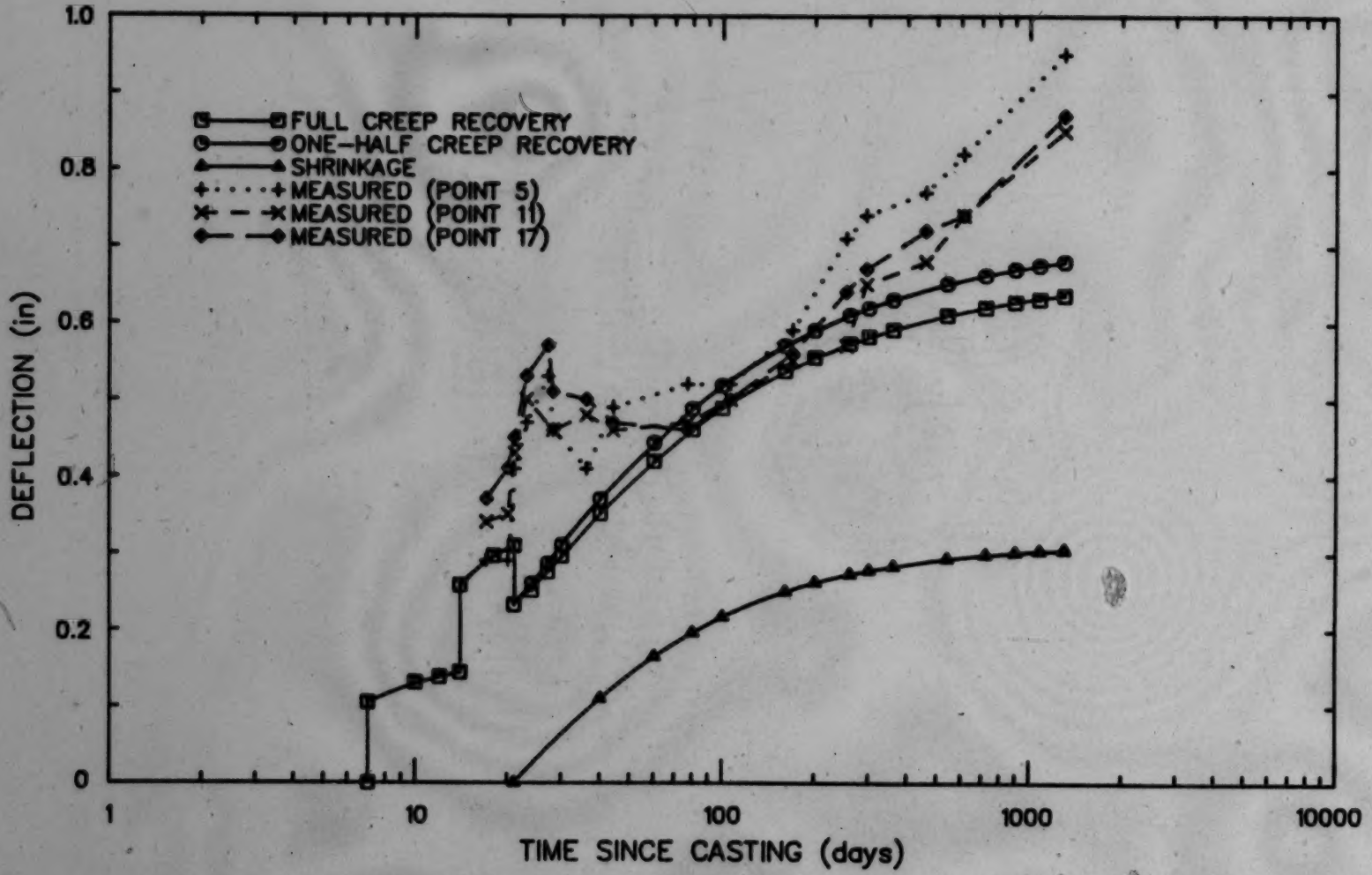

Figure 4.6 Heiman's Flat Plate - Long-Time Deflections
($f_r = 7.5\sqrt{f'_c}$ psi)

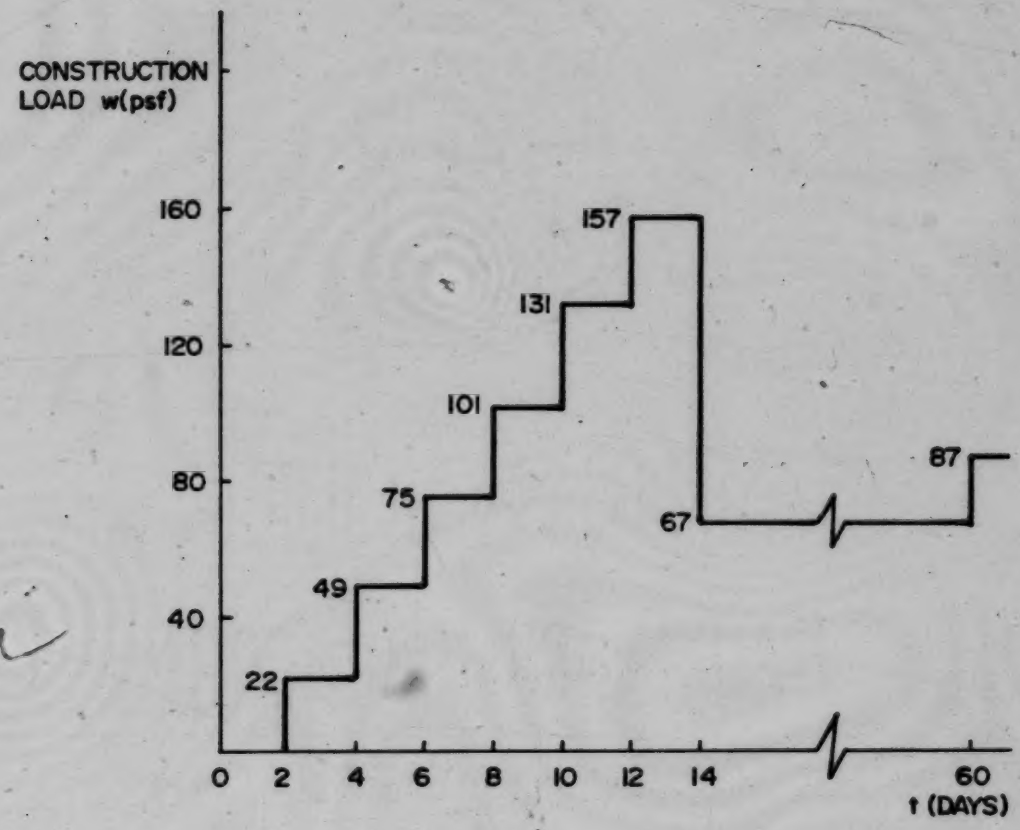

Figure 4.7 Sbarounis' Flat Plate - Construction Load Sequence

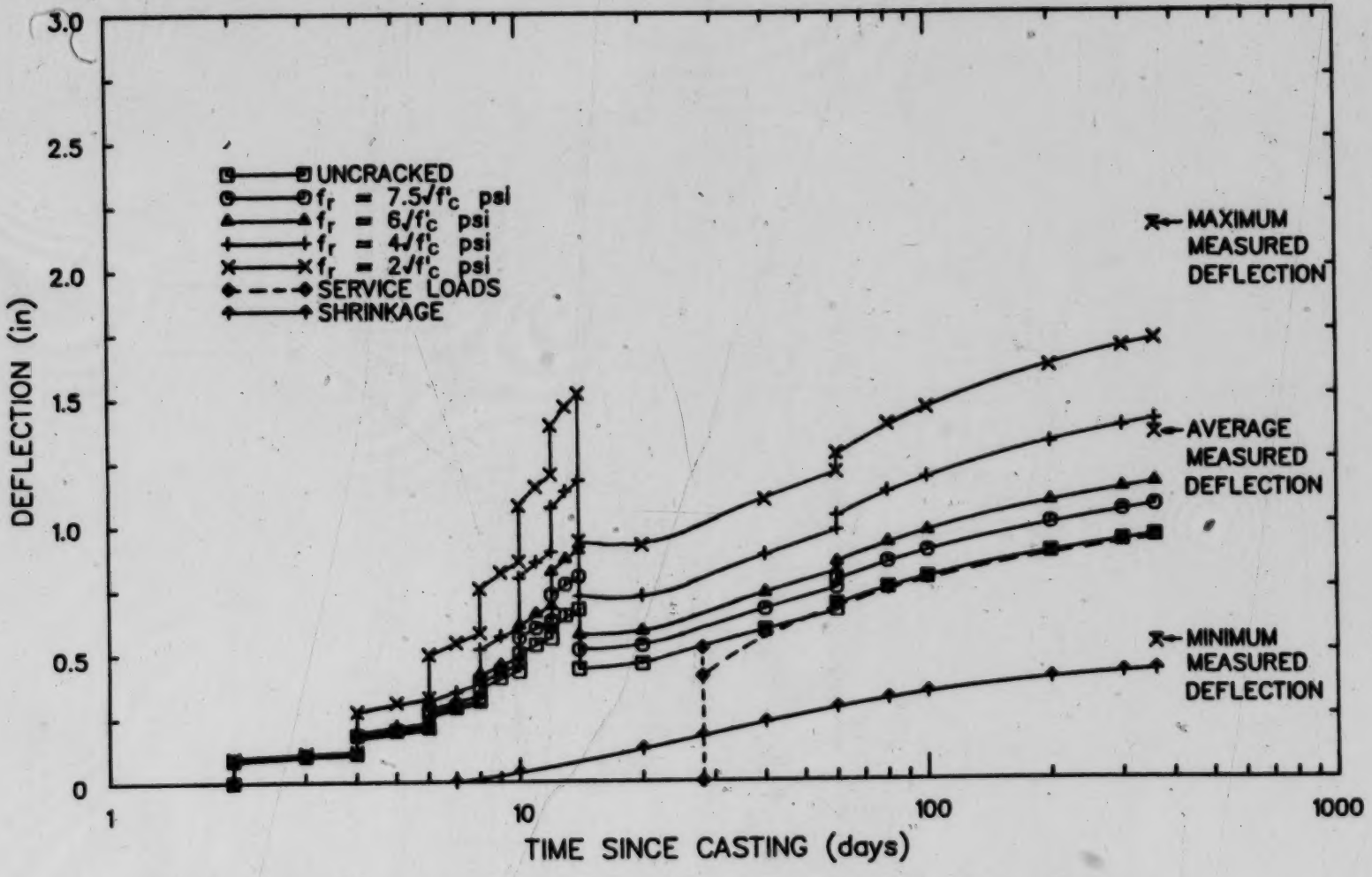

Figure 4.8 Sbarounis' Flat Plate - Long-Time Deflections
(Full Creep Recovery)

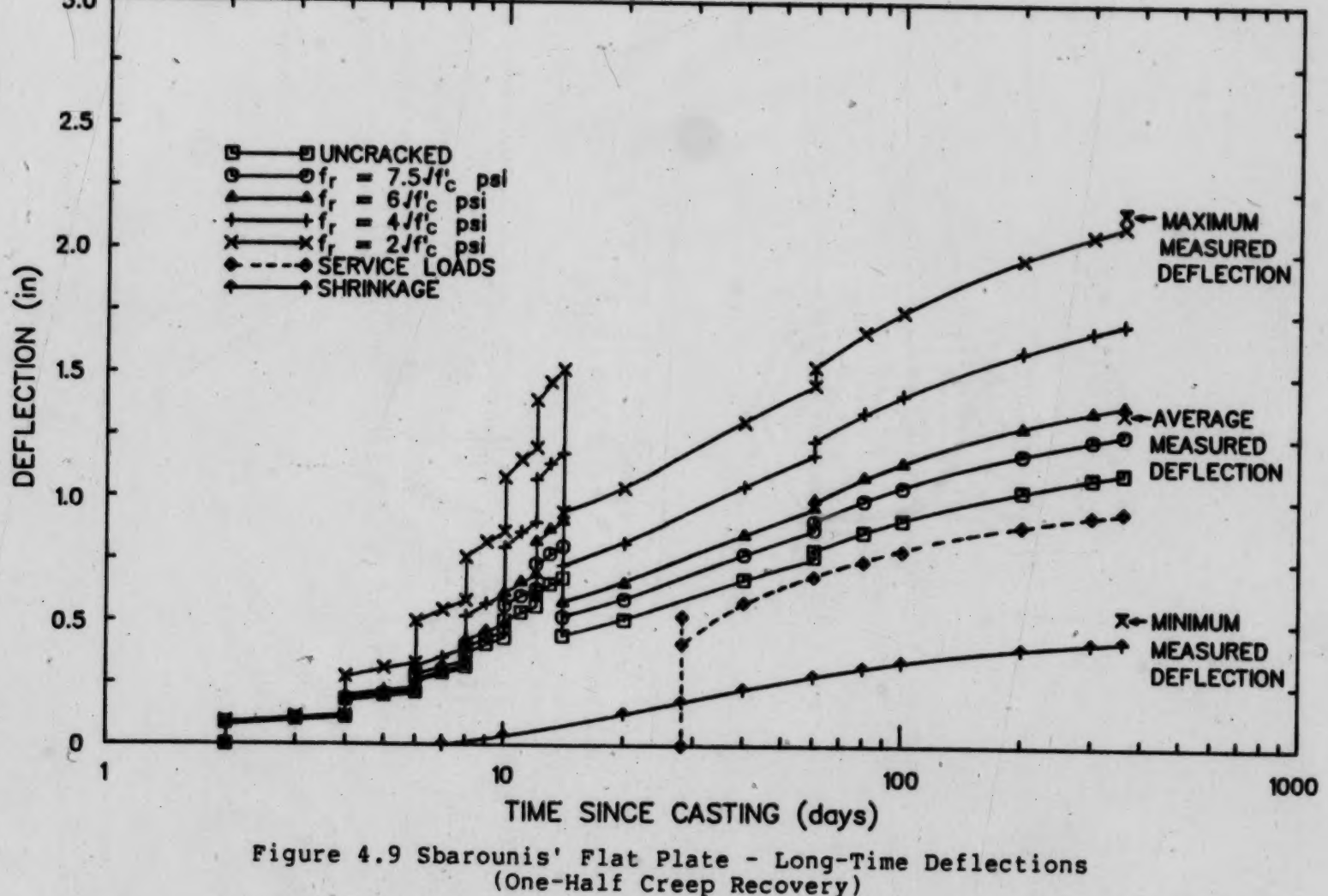

Figure 4.9 Sbarounis' Flat Plate - Long-Time Deflections
(One-Half Creep Recovery)

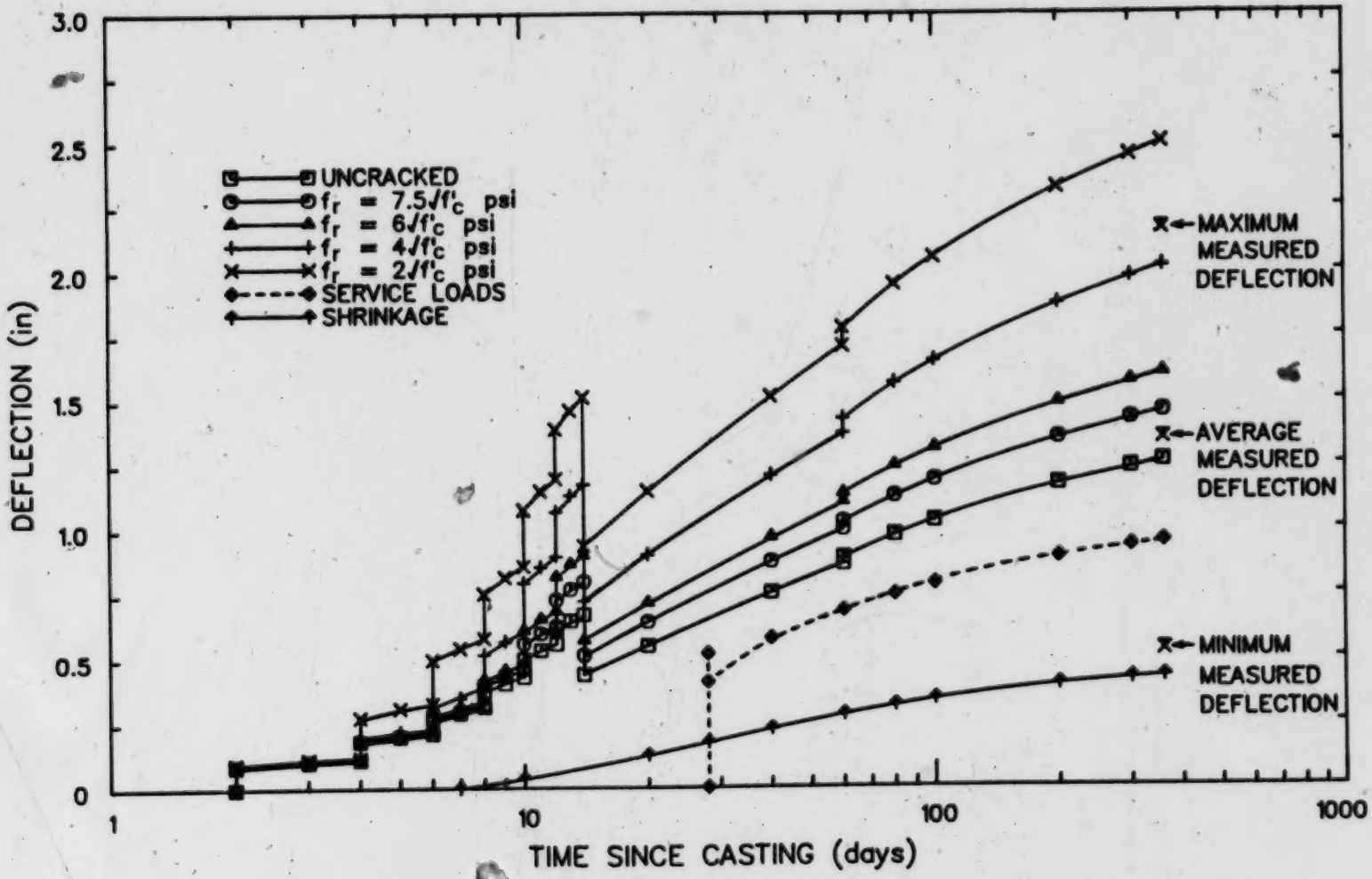

Figure 4.10 Sbarounis' Flat Plate - Long-Time Deflections
(Zero Creep Recovery)

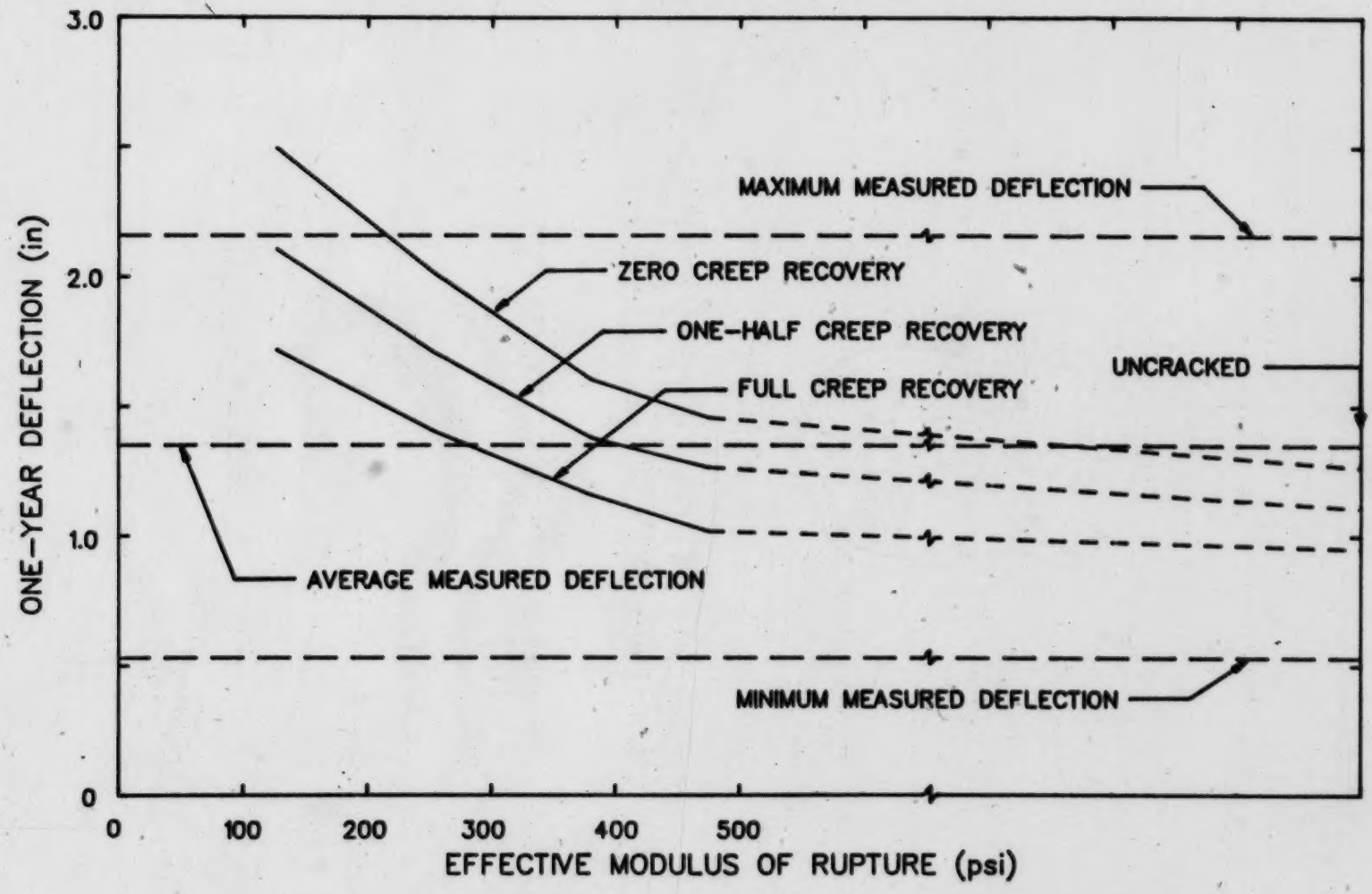

Figure 4.11 Sbarounis' Flat Plate - Comparison of One-Year Deflections

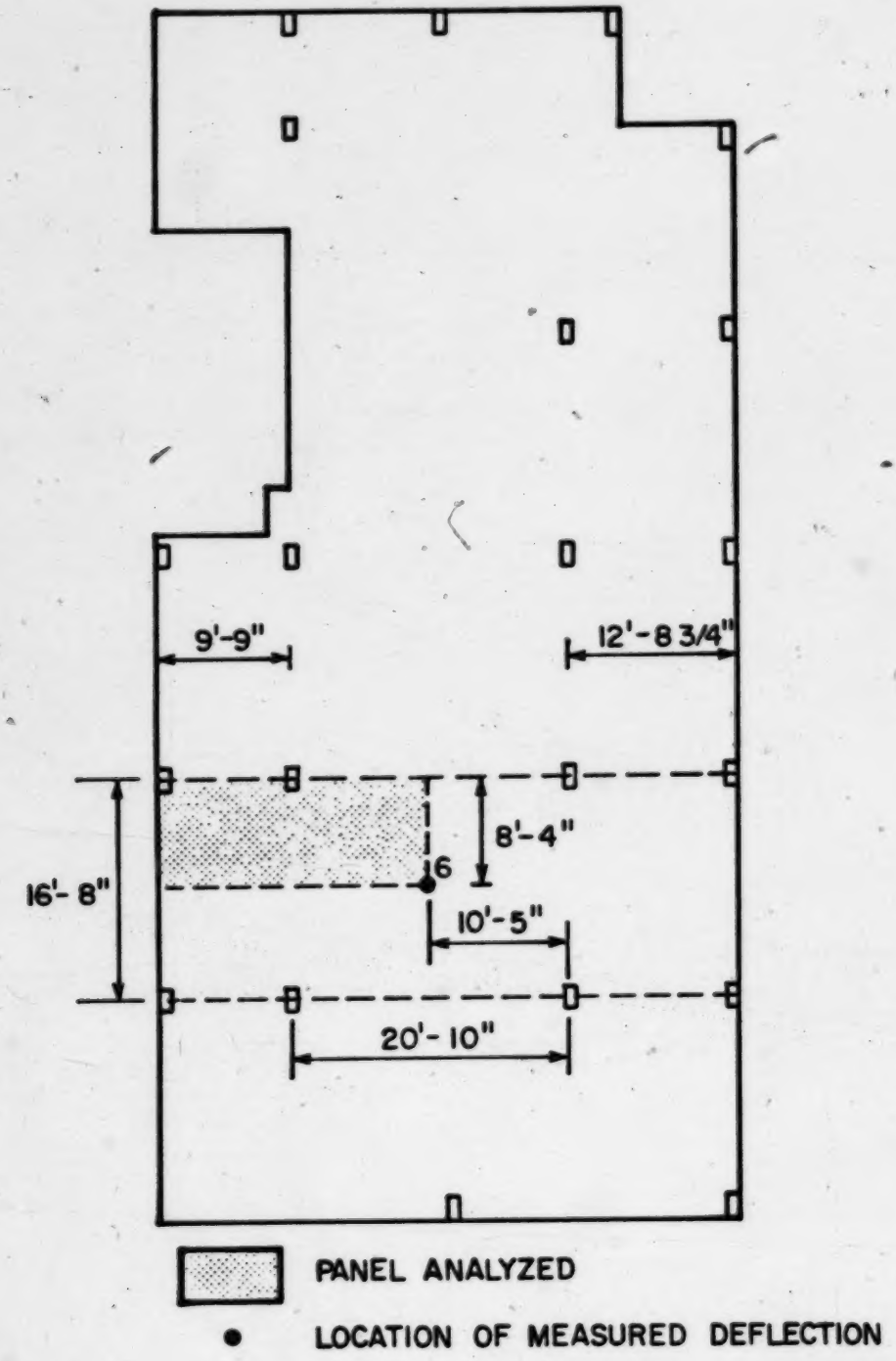

Figure 4.12 Taylor's Flat Plate

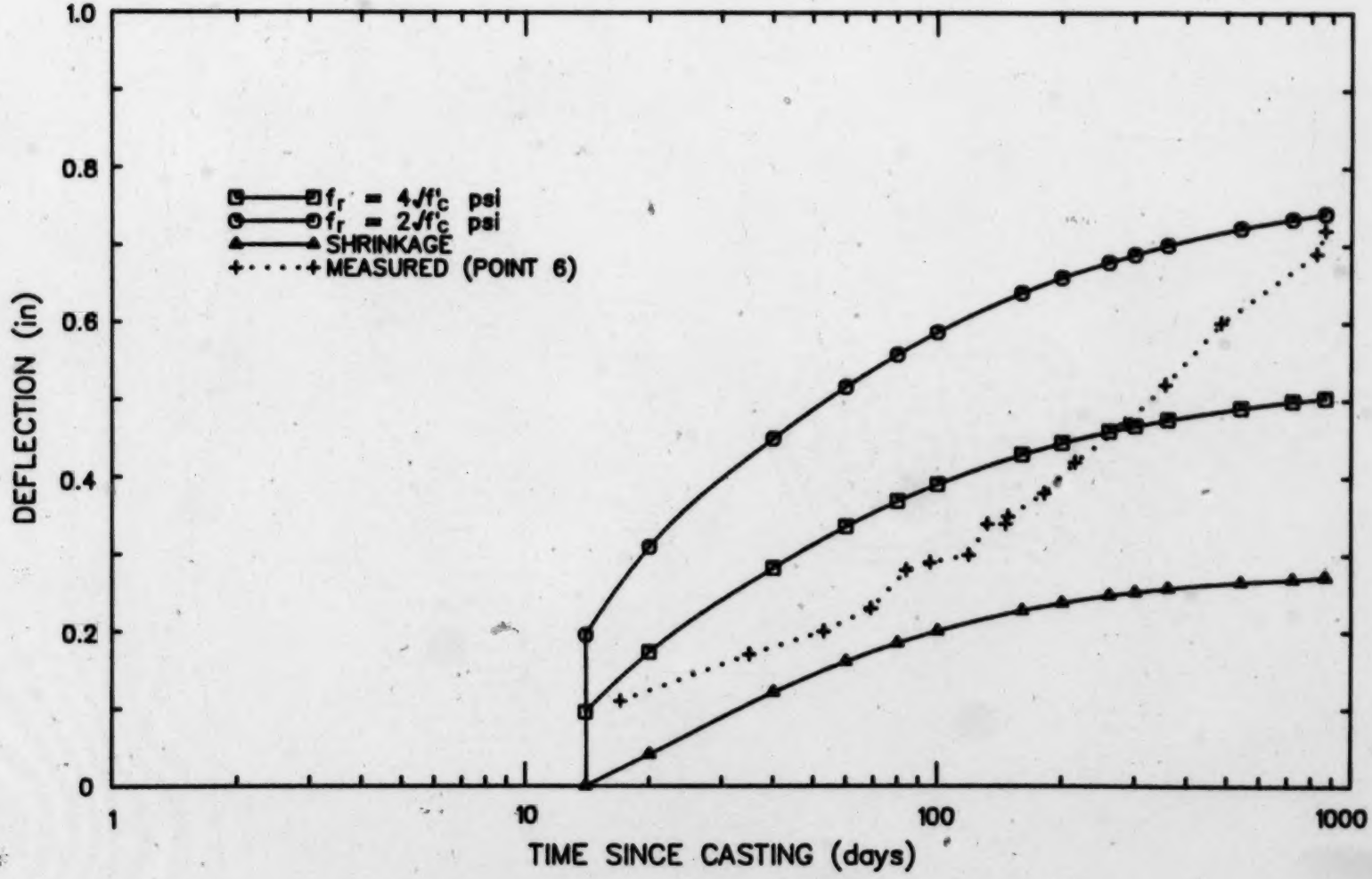

Figure 4.13 Taylor's Flat Plate - Long-Time Deflections

5. PARAMETER STUDY

5.1 Outline of Study

The accurate assessment of two-way slab deflections is dependent on an understanding of the factors involved. For most slabs, the main parameters affecting deflections can be grouped into the following categories:

i) material properties

ii) slab geometery

iii) loads

iv) construction procedures

Using finite element analysis, the sensitivity of the proposed deflection calculation model to these factors is determined. Emphasis for the parameter study is the effect on long-time slab deflection due to construction loads, however some areas apply to slab deflections in general.

5.1.1 Slab Details

Analyses were conducted for a typical square interior panel of a flat plate system. An interior panel may be defined as one with an infinite number of adjacent spans in both directions, all under the same uniform load. Due to symmetry, a quarter panel section with zero edge rotations may be used in the analysis. Boundary conditions are those previously illustrated in Figure 3.8. Three slabs of different thickness were designed using the Direct Design Method of CSA A23.3 M77 (1). Minimum thickness requirements

were satisfied in one case, and thicknesses above and below this value were also considered to give a range of span-to-depth ratios. Table 5.1 shows the specific thicknesses considered.

In all cases, column grids in each direction were spaced at 6 m, with 500 by 500 mm columns. Loads, other than self weight, used for the slab design included a superimposed dead load of 1.75 kPa (finishes, partitions, and mechanical allowance), and a live load of 2.4 kPa. The design concrete strength was taken as 30 MPa and a steel yield stress of 400 MPa was used.

For all designs, required steel areas were not matched with available reinforcing bar sizes. Instead, computed steel areas per unit length were specified in the model. Calculated effective steel depths assumed 20 mm clear cover to all bars, with 10M bars used in the middle strip and 15M bars used in the column strip. Figure 5.1 shows the reinforcement plan used. Each quarter of an interior panel is divided into four quadrants, separated by the middle and column strip boundaries. Reinforcement areas for each quadrant for all slabs designed are given in Table 5.1.

5.2 Parameters Considered

According to the general categories specified in Section 5.1, the following parameters were considered for the study:

i) modulus of rupture

ii) degree of creep recovery during unloading

iii) span-to-depth ratios

iv) number of shored levels

v) number of reshored levels

vi) construction cycle times

vii) effective depth to top reinforcement

In total twenty-seven series of analyses were done using the three slab designs and various load histories to determine the sensitivity of the model to each parameter. Table 5.2 contains a summary of all analyses.

Construction load histories were altered by varying the number of shored and reshored levels in the supporting assembly. A summary of the load sequences considered for the 165 mm slab is given in Table 5.3. The load ratios are multiplied by the slab self weight (3.88 kPa), and increased by 10 percent allowing for form, shore, and reshore weights, to obtain actual load levels. A construction live load of 2.4 kPa was applied to each supporting assembly at the maximum load level, according to Equation 3-9. In each case, a superimposed dead load of 1.75 kPa was added to the slab sixty days after casting to obtain the sustained load for long-time deflection calculations. Ultimate long-time deflections were assumed to occur approximately three years (1080 days) after casting.

5.2.1 Modulus of Rupture

Section 3.1.1 previously outlined the general effect of rupture modulus on slab deflections. The value of the cracking moment is a direct function of the assumed tensile capacity of the concrete. Since most slab systems offer some degree of restraint against shrinkage, the tensile strength may be reduced and cause the modulus of rupture to be less than the accepted value of $0.60\sqrt{f'_c}$ MPa. As a result of restraint against shrinkage, increased cracking will create additional loss of slab stiffness.

Deflection calculations were made for the series LH100 slab having a thickness of 165 mm, assuming three shored levels and a construction cycle time of seven days. Effective modulus of rupture values ranged from an uncracked condition to a reduced value of $0.16\sqrt{f'_c}$ MPa. Figure 5.2 shows the great range in ultimate deflections for the values considered.

There is little difference between deflections calculated assuming a value $0.60\sqrt{f'_c}$ MPa and the uncracked condition, indicating the present provisions are not adequate in modelling the cracking that often occurs in slabs. Deflections increase significantly as the modulus of rupture is reduced to $0.32\sqrt{f'_c}$ MPa and below.

For these analyses, the effective modulus value was assumed constant over the entire slab panel. However greater restraint stresses would be expected near columns and around the boundaries of a given panel compared with those at

midpanel. Therefore, it may be desirable to specify a distribution of effective rupture modulus values across a panel in relation to the expected degree of restraint. This was not considered here.

The distribution of cracking predicted by the model at the maximum load level is shown in Figures 5.3 and 5.4 for $0.60\sqrt{f'_c}$ and $0.32\sqrt{f'_c}$ MPa respectively. The degree of cracking for each element used in the finite element analysis is indicated by the ratio of effective inertia to gross inertia (α value), averaged for both directions. With $0.60\sqrt{f'_c}$ MPa cracking in the half-column strip occurs mainly around the columns, and the half-middle strip remains virtually uncracked. As expected, cracking is more severe using $0.32\sqrt{f'_c}$ MPa. In this case, stiffness of the half-middle strip is also reduced.

The amount of cracking calculated for each element is based on the average moment at the centre of the element. For elements adjacent to columns, cracking may in fact be more severe than indicated, as peak negative moments higher than the average element moment will occur at the column face.

Ultimate deflections considering the sustained load applied at twenty-eight days after casting are shown as single points on Figure 5.2 for $0.60\sqrt{f'_c}$ and $0.32\sqrt{f'_c}$ MPa. The large difference with deflections considering construction loading at $0.32\sqrt{f'_c}$ MPa indicates the significant influence early age cracking due to lower

rupture modulus and increased loads can have on ultimate calculated deflections.

Results from the foregoing analysis confirm that ultimate deflections are dependent on the assumed effective modulus of rupture. A modulus value of $0.60\sqrt{f'_c}$ MPa predicts a conservative degree of cracking throughout the slab. An effective rupture modulus of $0.32\sqrt{f'_c}$ MPa better predicts cracking for panels restrained against shrinkage and results in significantly larger deflections. Values below this may apply to localized areas of high restraint only.

5.2.2 Degree of Creep Recovery

Use of the principle of superposition overestimates the recovery of creep strain during unloading. In Section 3.4.2 it was concluded, on the basis of available data, that recovery of the time-dependent creep strain realistically ranges from one-half to the full value predicted by superposition.

The sensitivity of final long-time deflection to the degree of recovery assumed is dependent on the severity of unloading and age at unloading. With greater unloading and earlier unloading age, the time-dependent portion of the elastic-plus-creep strain curve (Figure 3.11) will be larger. This results in increased long-time deflection when a smaller degree of recovery is assumed.

Long-time midpanel panel deflections calculated for slab series LH100 assuming full, one-half, and zero creep

recovery are shown in Figure 5.5. Both a standard modulus of rupture value, $0.60\sqrt{f'_c}$ MPa, and a reduced value, $0.32\sqrt{f'_c}$ MPa were assumed. Comparing full and zero creep recovery, ultimate deflections increased by 33 percent for the former modulus value and 44 percent for the latter. An assumption of zero creep recovery is not reasonable but serves to illustrate the limits of the superposition method using variable creep recovery.

Comparison of values assuming full creep recovery and $0.60\sqrt{f'_c}$ MPa with one-half creep recovery and $0.32\sqrt{f'_c}$ MPa shows a doubling of ultimate deflection. The combination of effective rupture modulus and degree of creep recovery may produce a significant range of calculated deflections. Subsequent analyses will consider this range for modulus of rupture and degree of creep recovery in calculating deflections.

5.2.3 Span-to-Depth Ratio

Flat plate design results in a relatively narrow range of span-to-depth (L/h) ratios. For economical reasons it is desirable to use the minimum slab thickness while maintaining strength and serviceabilty requirements. Scanlon (43) noted the L/h ratio affects the influence of cracking on slab deflections. For a given load, the ratio of moment in the slab to cracking moment increases with increasing L/h ratio.

In this study, a constant centre-to-centre span of 6 m was used. Varying slab thicknesses of 165 (Code minimum), 155 and, 180 mm gave L/h ratios of 36.4 (series LH100), 38.7 (series LH200), and 33.3 (series LH300). Figure 5.6 shows the ultimate midpanel deflections for all cases.

For the small range of slab thicknesses considered, ultimate deflections varied significantly. Reducing the rupture modulus value from $0.60\sqrt{f'_c}$ to $0.32\sqrt{f'_c}$ MPa gave a greater increase in ultimate deflection between the extreme L/h ratios. The difference between full and one-half creep recovery is more pronounced with the lower modulus of rupture value.

These analyses indicate using the Code minimum slab thickness may, in extreme cases, still result in large deflections due to construction loading and the effects of restraint against shrinkage. Specifying a slab thickness below the Code minimum can give significantly larger deflections than those obtained using the minimum thickness, or one slightly above. The sensitivity of the model-to L/h ratio is more apparent with a reduced modulus of rupture. This also illustrates the increased influence of cracking on slab stiffness with larger L/h ratios.

5.2.4 Number of Shored Levels

The number of shored levels in the supporting assembly affects deflection in two ways. With a small number of shores, the maximum construction load for a given slab will

occur at an earlier time after casting. In addition, the value of the maximum construction load will be slightly larger with a decreasing number of shored levels, as fewer slabs are available to support the construction live load.

Supporting assemblies consisting of two through five shored levels were considered as shown in Table 5.2. Slab thickness and construction cycle time remained constant at 165 mm and seven days respectively. Resulting midpanel deflections are shown in Figure 5.7.

For a modulus of rupture value $0.60\sqrt{f'_c}$ MPa, there is little increase in ultimate deflection with a reduction in the shored levels of the supporting assembly. In this case, little cracking occurs, and the earlier loading age for two shored levels causes an 18 percent increase over the deflection for five shored levels assuming one-half creep recovery. With $0.32\sqrt{f'_c}$ MPa, a greater degree of cracking at early age causes an increase in deflection of 37 percent for one-half creep recovery.

In all cases, there appears to be little reduction in ultimate deflections when more than five levels of shores are used. With a larger number of shores, the load is introduced to the slab in smaller increments. The maximum construction load does not occur until the slab has gained sufficient strength to effectively resist progressive cracking. A critical condition occurs when a reduction from four to two levels of shores takes place.

5.2.5 Number of Reshored Levels

The levels in the supporting assembly may be altered by adding reshores. The concept of reshoring was discussed in Section 2.2. With the addition of reshores, the age at which maximum loading occurs for a slab is not altered from the shored case, but the value of the maximum load is reduced. Table 5.4 gives the maximum converged load ratios (excluding construction live load effects) for several different support assemblies. It is apparent that with an increasing number of shored levels, the addition of reshores has less effect on the maximum construction load level.

To study the effect of reshores on deflections calculated by the model, support assemblies of 2+0 (two shored levels, zero reshored levels), 2+3, 2+5 and 5+0 were considered. The slab depth and cycle time were constant at 165 mm and seven days respectively. Calculated deflections are shown in Table 5.5 for modulus of rupture values $0.60\sqrt{f'_c}$ and $0.32\sqrt{f'_c}$ MPa, and one-half creep recovery.

The addition of reshores to increase the number of levels in the supporting assembly can have a significant effect on deflections. Comparing the cases of 2+0 and 2+5, the maximum construction load is reduced from 9.86 kPa to 6.87 kPa, and ultimate deflections are decreased by 40 percent for $0.32\sqrt{f'_c}$ MPa. Use of reshores instead of shores to increase the size of the supporting assembly also eliminates the need for additional sets of forms.

The effect of substituting shored levels with reshored levels in the supporting assembly is evident comparing the cases 2+3 and 5+0. Although the maximum load level is reduced using the reshores, ultimate deflections only decrease slightly. This is due to the reduced maximum loading age for the case of 2+3 (fourteen days) compared with 5+0 (thirty-five days) for a seven-day construction cycle.

5.2.6 Construction Cycle Time

The rate of construction directly affects the age at which a slab in the supporting assembly is required to carry load. For a particular supporting assembly, as the cycle time between casting of additional floors is decreased, slabs are subjected to the same loading history at earlier ages. Stiffness of the slab will be reduced by a decrease in concrete strength gain and resulting increase in extent of cracking.

Construction cycle times of two (series SR300), four (series SR100), and seven days (series SL300) were considered for a 165 mm slab thickness using four levels of shoring. Corresponding ages at time of maximum loading were eight, sixteen, and twenty-eight days for the respective cycle times. The loading sequence is given in Figure 5.2. Figure 5.8 shows ultimate midpanel deflections.

Assuming a modulus of rupture $0.60\sqrt{f'_c}$ MPa, there is virtually no increase in deflection going from a seven-day

cycle to a four-day cycle, and a minimal increase when the cycle time is reduced to two days. The effect of construction cycle time is more apparent using a reduced rupture modulus value, $0.32\sqrt{f'_c}$ MPa. Cycle times of four and seven days again result in close ultimate deflections. There is a marked increase in deflection when the cycle time is reduced to two days. In both cases, casting slabs at a rate slower than one per week offers little advantage in reducing deflections.

Using a relatively short cycle time of two days will cause increased deflections. In order to maintain such a rapid schedule and control deflections, it may be necessary to alter the support assembly with additional shores and/or reshores. Sections 5.2.4 and 5.2.5 have indicated more effective results when additional reshores are added to the assembly.

A comparison between rates of construction for different supporting assemblies is also shown on Figure 5.8. Deflections based on four shored levels and a four-day cycle time are compared with those from two shored levels and a seven-day cycle time. The load history for each case from Figure 5.2 is shown separately in Figure 5.9. These two cases represent approximately equal load duration.

For both modulus of rupture values, deflections for two shored levels and a seven-day cycle time are greater than those for four shored levels and a four-day cycle. This is largely due to the slightly greater maximum construction

load for the former case. When the maximum construction load for two shored levels is reduced to the same level as for four shored levels (9.18 kPa), deflections do not differ a great deal for $0.60\sqrt{f'_c}$ MPa, but are still greater for $0.32\sqrt{f'_c}$ MPa. The single load increments associated with the two shored levels caused more cracking compared to the two equivalent load increments with four shored levels. This effect is more pronounced with a lower modulus of rupture value.

5.2.7 Effective Depth to Top Reinforcement

Reinforcement that is not placed at the specified design depth may lead to increased long-time deflections. Variations in effective depth can occur due to steel misplacement, sagging of bars between supporting chairs, or as a result of concrete placement. An important aspect of the problem, with regard to flat plate construction, is the reduction in effective depth for top reinforcement at columns during placement of concrete (44). Reduction in effective depth not only affects strength, but also results in decreased stiffness over the support and increased potential for cracking. A substantial reduction may lead to some loss of continuity at the column.

Mirza and MacGregor (45) have compiled data on the in-situ effective depth for top reinforcement in slabs. They recommend a mean reduction in effective depth of 20 mm for a nominal range of depths between 100 and 200 mm.

For this study, analyses considered the effective depth for all top reinforcement in the slab series LH100 reduced by 25 mm and 50 mm. Figure 5.10 shows the ultimate deflections calculated by the model.

Moments and deflections calculated in the model apply only to elastic conditions. For each reduced effective depth investigated, moments in some regions of the slab, at the maximum construction load level, exceeded the yield moment of the reinforced section. Figure 5.11 shows the yielded regions of the quarter panel for effective depths of top reinforcement reduced by 25 mm and 50 mm, and assuming a modulus of rupture $0.32\sqrt{f'_c}$ MPa.

Upon reaching the yield moment of an element, the present analysis for moments and deflections does not apply. Redistribution of excess moment from the yielded elements to adjacent areas would increase cracking in these areas and result in further loss of stiffness. With yielding of the reinforcement, a plastic hinge will form at the section. Such hinges located at columns and along panel boundaries result in a significant increase in ultimate deflection.

Referring to Figure 5.10, calculated deflections for the reduced effective depths are less than those expected due to plastic hinge formation. The moderate increase in deflection with a 50 mm reduction in effective depth is misleading. Actual deflections probably deviate much more sharply as suggested by the dotted lines. Calculation of these deflections is beyond the scope of the present model.

5.3 Summary

Parameters related to the proposed model were identified. Analyses for typical interior panels indicated deflections calculated by the model sensitive to construction loads, effective modulus of rupture, degree of creep recovery, span-to-depth ratio, and addition of reshores to the supporting assembly. Parameters of less importance included number of shored levels in the supporting assembly and construction cycle time.

Table 5.1 Slab Designs for Parameter Study

SLAB	h (mm)	L/h	QUADRANT	REINFORCEMENT AREAS (mm^2/mm) EFFECTIVE DEPTHS (mm) (IN BRACKETS)			
				TOP X-DIRECTION	TOP Y-DIRECTION	BOTTOM X-DIRECTION	BOTTOM Y-DIRECTION
1	165	36.4	1	0.3100 (130)	0.2970[1] (140)	0.2970[1] (130)	0.4003 (140)
			2	0.9663 (122.5)	0.9663 (137.5)	0.2970[1] (130)	0.2970[1] (140)
			3	0.2970[1] (130)	0.3100 (140)	0.4003 (130)	0.2970[1] (140)
			4	-	-	0.2970 (130)	0.2970 (140)
2	155	38.7	1	0.3243 (120)	0.2793[1] (130)	0.2793[1] (120)	0.4193 (130)
			2	1.0163 (112.5)	1.0163 (127.5)	0.2793[1] (120)	0.2793[1] (130)
			3	0.2793[1] (120)	0.3243 (130)	0.4193 (120)	0.2793[1] (130)
			4	-	-	0.2793 (120)	0.2793 (130)
3	180	33.3	1	0.3240 (145)	0.3240[1] (155)	0.3240[1] (145)	0.3757 (155)
			2	0.9033 (137.5)	0.9033 (152.5)	0.3240[1] (145)	0.3240[1] (155)
			3	0.3240[1] (145)	0.3240 (155)	0.3757 (145)	0.3240[1] (155)
			4	-	-	0.3240 (145)	0.3240 (155)

[1] MINIMUM REINFORCEMENT REQUIREMENT

Table 5.2 Parameter Study Summary

PARAMETER	SLAB SERIES	VARIABLES		CONSTANTS
		$f_r = c\sqrt{f'_c}$ (MPa)		
MODULUS OF RUPTURE	LH000	UNCRACKED		L=6000, h=165mm (3+0) T = 7 DAYS $\epsilon_{shu} = 780 \times 10^{-6}$ $C_u = 2.35$
	LH100	0.60		
	LH160	0.48		
	LH140	0.32		
	LH120	0.16		
		CREEP RECOVERY	$f_r = c\sqrt{f'_c}$ (MPa)	
DEGREE OF CREEP RECOVERY	LH100	FULL	0.60	L=6000, h=165mm (3+0) T = 7 DAYS $\epsilon_{shu} = 780 \times 10^{-6}$ $C_u = 2.35$
	LH100	HALF	0.60	
	LH100	ZERO	0.60	
	LH160	FULL	0.32	
	LH160	HALF	0.32	
	LH160	ZERO	0.32	
		h (mm) L/h	$f_r = c\sqrt{f'_c}$ (MPa)	
SPAN-TO-DEPTH RATIO	LH100	165 36.4	0.60	L=6000 mm (3+0) T = 7 DAYS $\epsilon_{shu} = 780 \times 10^{-6}$ $C_u = 2.35$
	LH200	155 38.7	0.60	
	LH300	180 33.3	0.60	
	LH140	165 36.4	0.32	
	LH240	155 38.7	0.32	
	LH340	180 33.3	0.32	
		SUPPORT ASSEMBLY	$f_r = c\sqrt{f'_c}$ (MPa)	
NUMBER OF SHORED LEVELS	LH100	3+0	0.60	L=6000, h=165mm T = 7 DAYS $\epsilon_{shu} = 780 \times 10^{-6}$ $C_u = 2.35$
	SL200	2+0	0.60	
	SL300	4+0	0.60	
	SL400	5+0	0.60	
	LH140	3+0	0.32	
	SL240	2+0	0.32	
	SL340	4+0	0.32	
	SL440	5+0	0.32	

Table 5.2 Parameter Study Summary (continued)

PARAMETER	SLAB SERIES	VARIABLES		CONSTANTS
		SUPPORT ASSEMBLY	$f_r = c\sqrt{f'_c}$ (MPa)	
NUMBER OF RESHORED LEVELS	SL200	2+0	0.60	L=6000, h=165mm T = 7 DAYS $\epsilon_{shu} = 780 \times 10^{-6}$ $C_u = 2.35$
	RE100	2+3	0.60	
	RE200	2+5	0.60	
	SL240	2+0	0.32	
	RE140	2+3	0.32	
	RE240	2+5	0.32	
		T (DAYS)	$f_r = c\sqrt{f'_c}$ (MPa)	
CONSTRUCTION CYCLE TIME	SL300	7	0.60	L=6000, h=165mm (4+0) $\epsilon_{shu} = 780 \times 10^{-6}$ $C_u = 2.35$
	SR100	4	0.60	
	SR300	2	0.60	
	SL340	7	0.32	
	SR140	4	0.32	
	SR340	2	0.32	
		SUPPORT ASSEMBLY	T (DAYS) f_r	
DURATION OF LOAD	SL200	2+0	7 0.60	L=6000, h=165mm $\epsilon_{shu} = 780 \times 10^{-6}$ $C_u = 2.35$
	SR100	4+0	4 0.60	
	SL240	2+0	7 0.32	
	SR140	4+0	4 0.32	
		d (mm)	$f_r = c\sqrt{f'_c}$ (MPa)	
EFFECTIVE DEPTH TO TOP REINFORCEMENT	LH100	d	0.60	L=6000, h=165mm (3+0) T = 7 DAYS $\epsilon_{shu} = 780 \times 10^{-6}$ $C_u = 2.35$
	SD100	d-25	0.60	
	SD200	d-50	0.60	
	LH140	d	0.32	
	SD140	d-25	0.32	
	SD240	d-50	0.32	

Table 5.3 Construction Load Histories for 165 mm Slab

	LOAD RATIOS (AND LOADS BELOW kPa) AT TIME SINCE CASTING (DAYS)											
7-DAY CYCLE	5	7	12	14	19	21	26	28	33	35	40	60
4-DAY CYCLE	2	4	8	10	12	14	14	16	18	20	22	60
2-DAY CYCLE	1	2	3	4	5	6	7	8	9	10	11	60
SUPPORT ASSEMBLY												
2+0	0.50 2.14	1.00 4.27	1.50 6.41	2.31[1] 9.86	0.91 3.88							1.32 5.63
3+0	0.33 1.41	0.67 2.86	1.00 4.23	1.33 5.68	1.67 7.13	2.21[1] 9.39	0.91 3.88					1.32 5.63
4+0	0.25 1.07	0.50 2.14	0.75 3.20	1.00 4.27	1.25 5.34	1.50 6.41	1.75 7.47	2.15[1] 9.18	0.91 3.88			1.32 5.63
5+0	0.20 0.85	0.40 1.71	0.60 2.56	0.80 3.42	1.00 4.27	1.20 5.12	1.40 1.71	1.60 2.56	1.80 3.42	2.12[1] 4.27	0.91 5.12	1.32 5.63
2+3	0.60 2.56	0.80 3.42	1.40 5.98	1.72[1] 7.34	0.91 3.88							1.32 5.63
2+5	0.62 2.65	0.76 3.25	1.38 5.89	1.61[1] 6.87	0.91 3.88							1.32 5.63

[1] INCLUDES CONSTRUCTION LIVE LOAD

Table 5.4 Construction Load Ratios for Various Supporting Assemblies

NUMBER OF SHORES	MAX. CONVERGED CONSTRUCTION LOAD RATIOS[1]						AGE AT MAXIMUM LOADING[2]
	NUMBER OF RESHORES						
	0	1	2	3	4	5	
1	2.00	1.50	1.33	1.25	1.20	1.17	T DAYS
2	2.00	1.77	1.67	1.60	1.55	1.52	2T
3	2.00	1.87	1.83	1.77	1.72	1.70	3T

[1] NOT INCLUDING CONSTRUCTION LIVE LOAD
[2] FOR T-DAY CONSTRUCTION CYCLE

Table 5.5 Effect of Reshored Levels on Ultimate Deflections

SUPPORT ASSEMBLY	w_{max}[1] (kPa)	DEFLECTIONS - $f_r = 0.60\sqrt{f'_c}$ ($0.32\sqrt{f'_c}$) MPa	
		ONE-YEAR (mm)	ULTIMATE (mm)
2+0	9.86	20.7 (38.2)	22.3 (41.4)
2+3	7.34	16.8 (24.8)	18.1 (26.8)
2+5	6.87	16.2 (23.2)	17.7 (25.0)
5+0	9.05	17.5 (27.9)	18.9 (30.2)

[1] INCLUDING 2.4 kPa CONSTRUCTION LIVE LOAD
[2] ONE-HALF CREEP RECOVERY

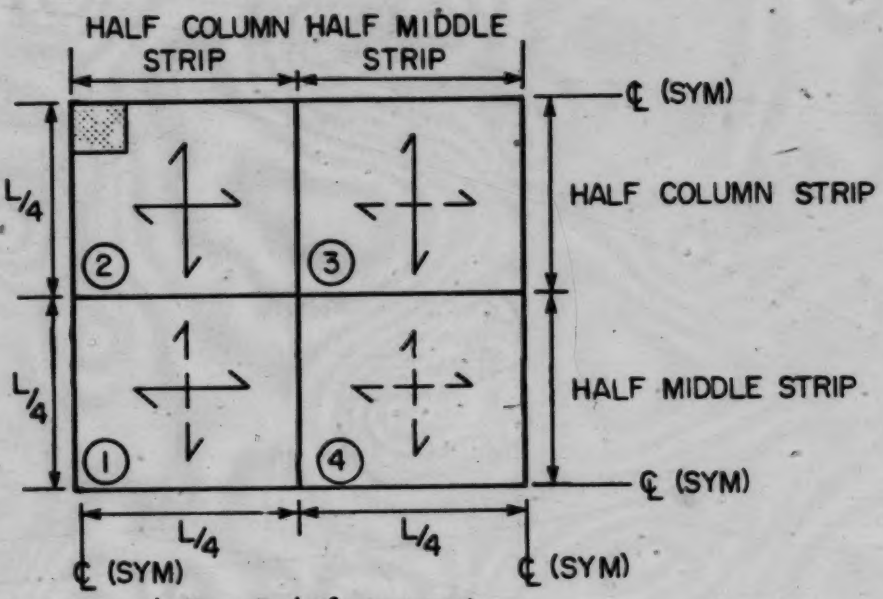

a) Top Reinforcement

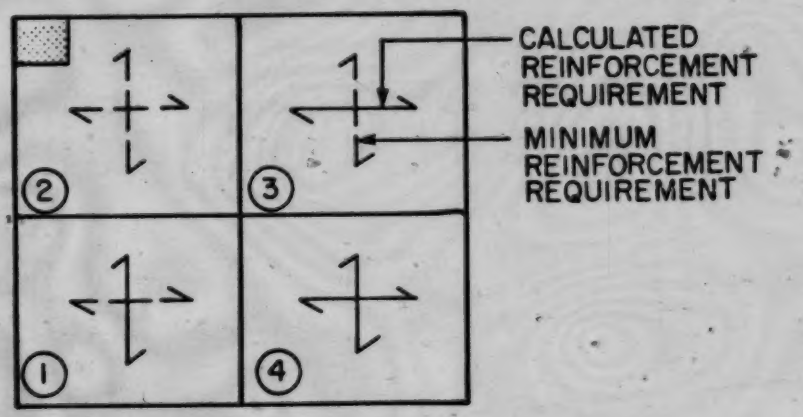

b) Bottom Reinforcement

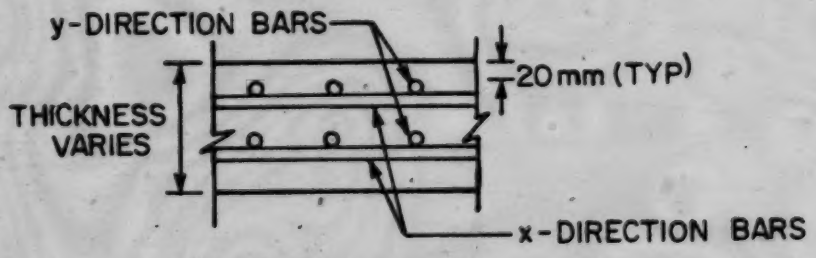

c) Reinforcement Arrangement

Figure 5.1 Parameter Study - Plan of Reinforcement

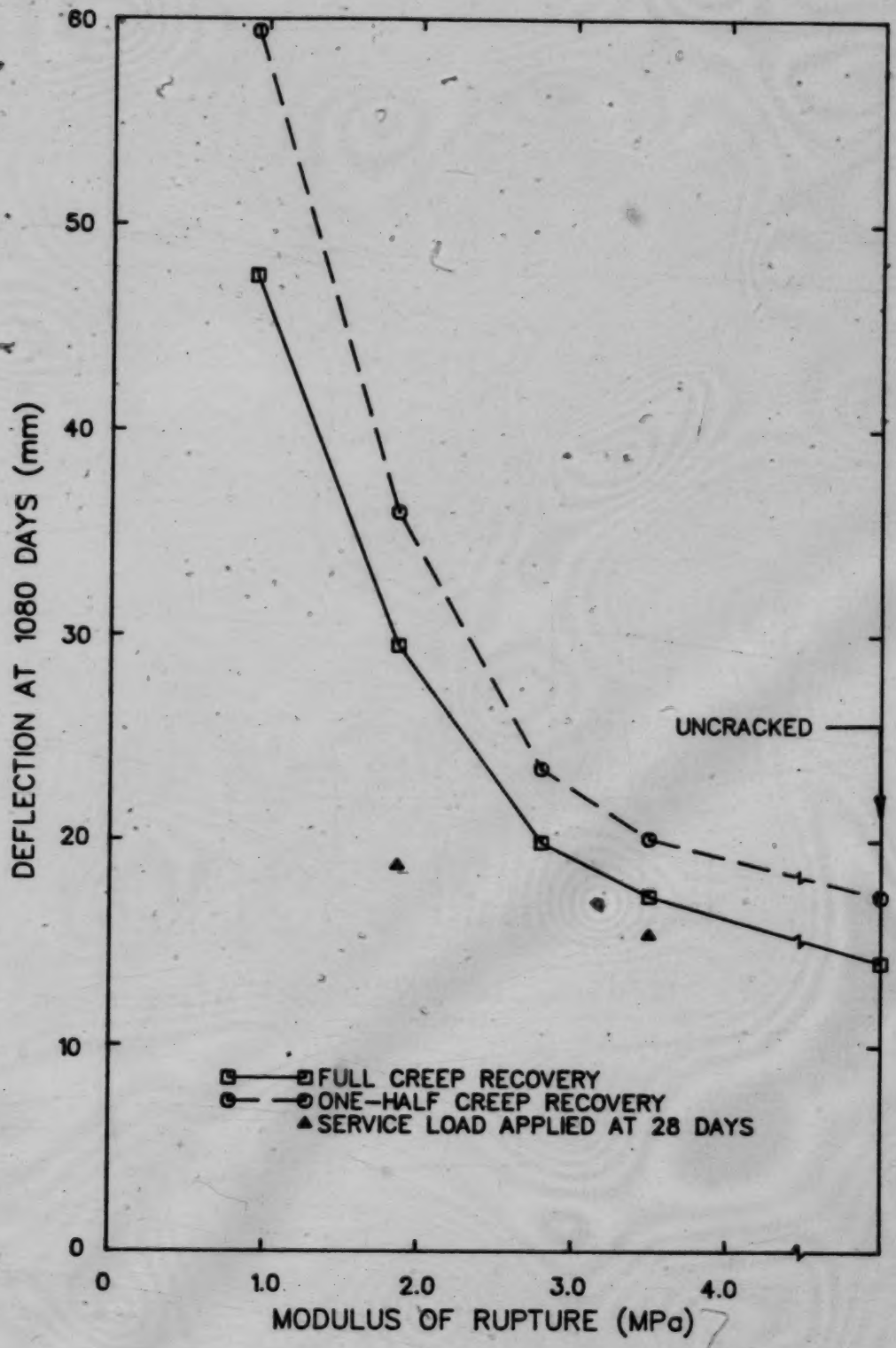

Figure 5.2 Parameter Study - Modulus of Rupture

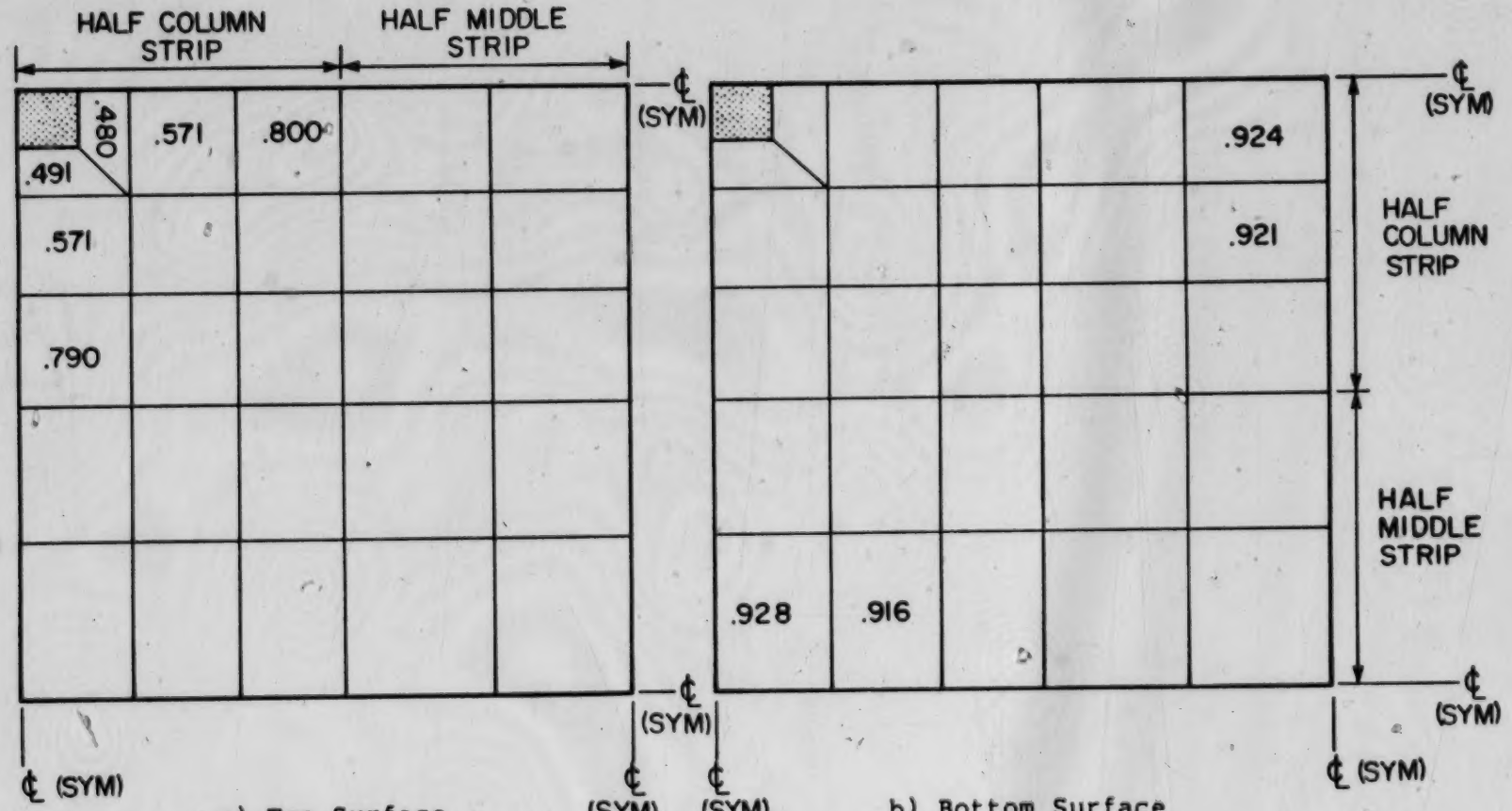

Figure 5.3 Parameter Study - Cracking Distribution
($f_r = 0.60\sqrt{f'_c}$ MPa)

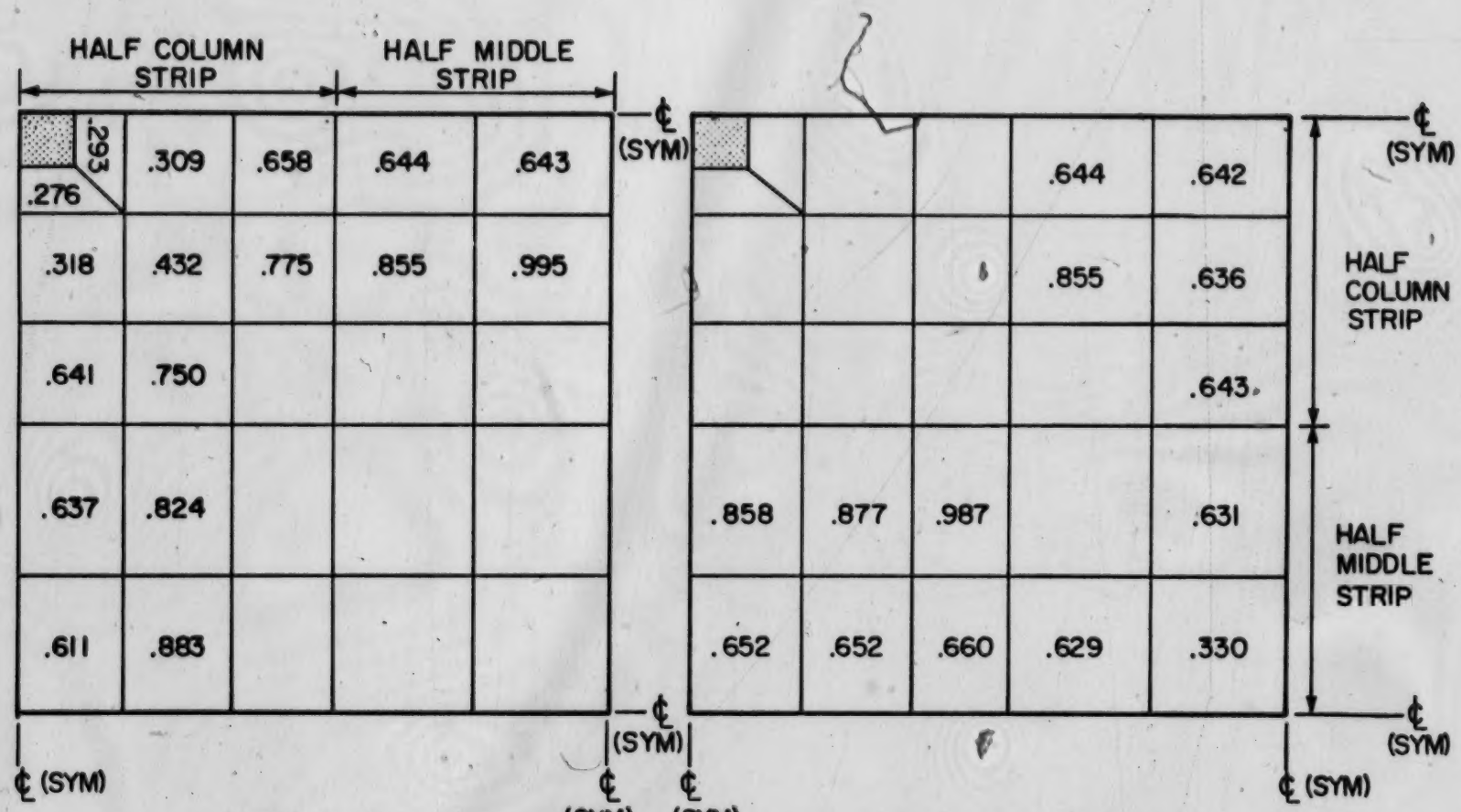

Figure 5.4 Parameter Study - Cracking Distribution
($f_r = 0.32\sqrt{f'_c}$ MPa)

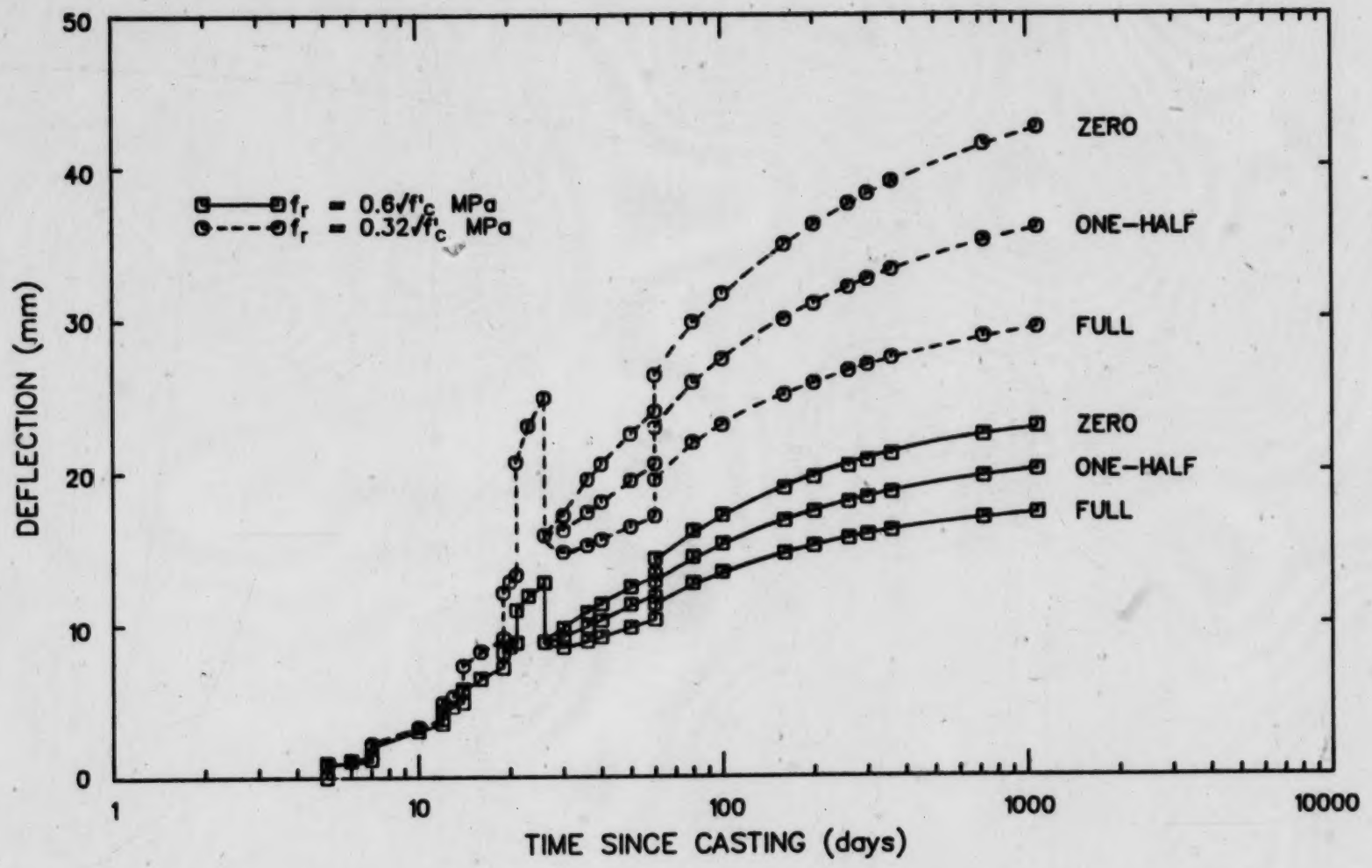

Figure 5.5 Parameter Study - Degree of Creep Recovery

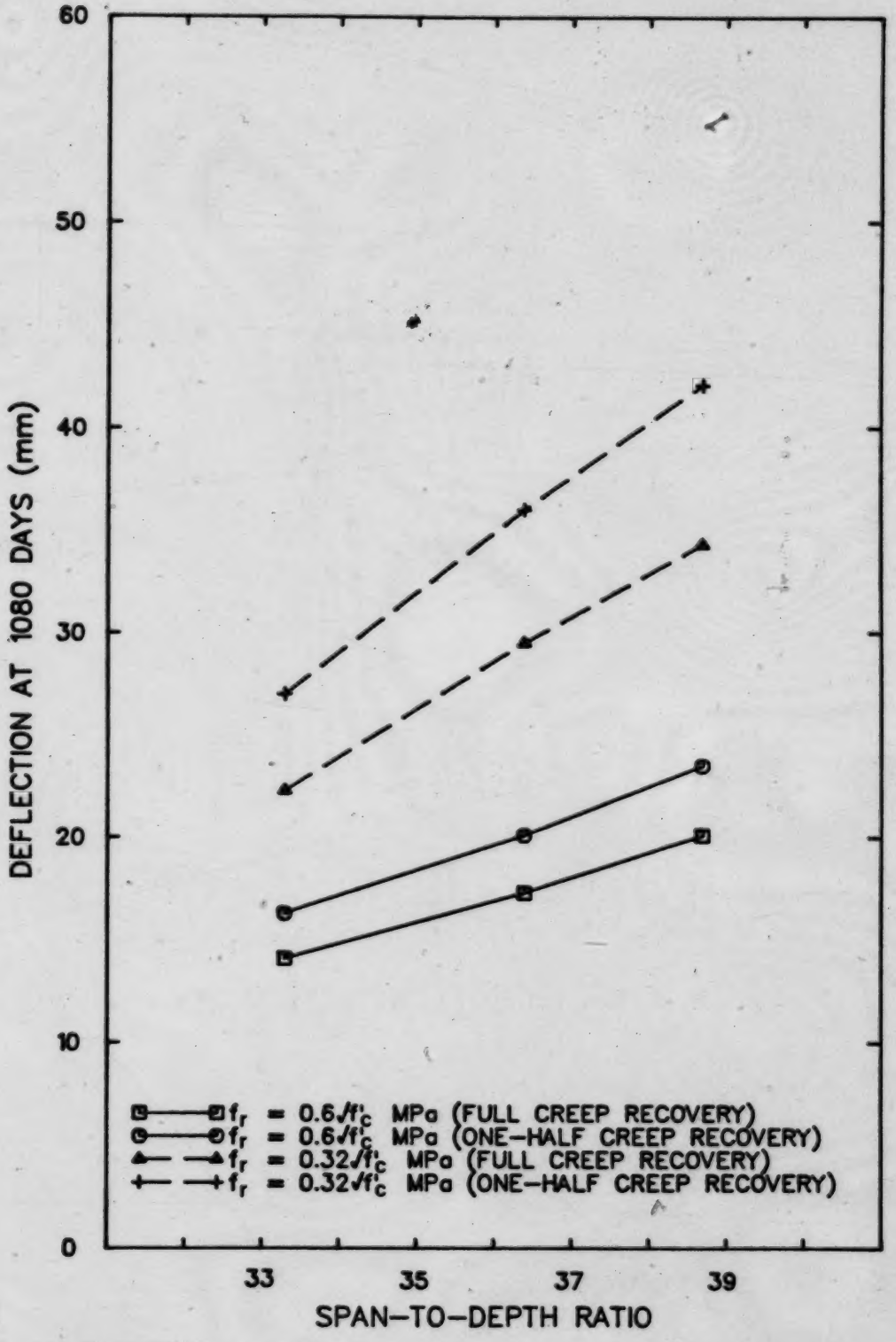

Figure 5.6 Parameter Study - Span-to-Depth-Ratio

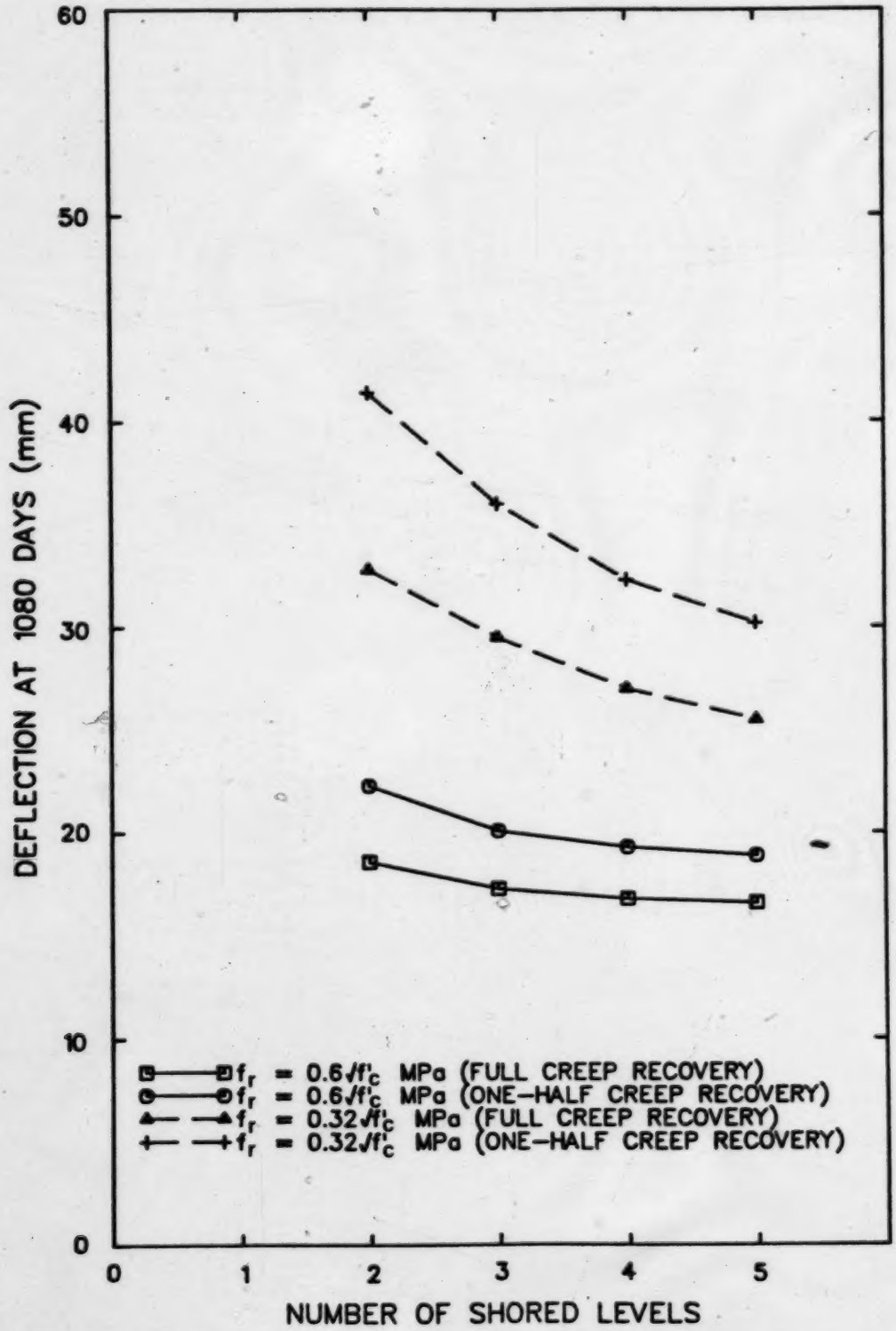

Figure 5.7 Parameter Study - Number of Shored Levels

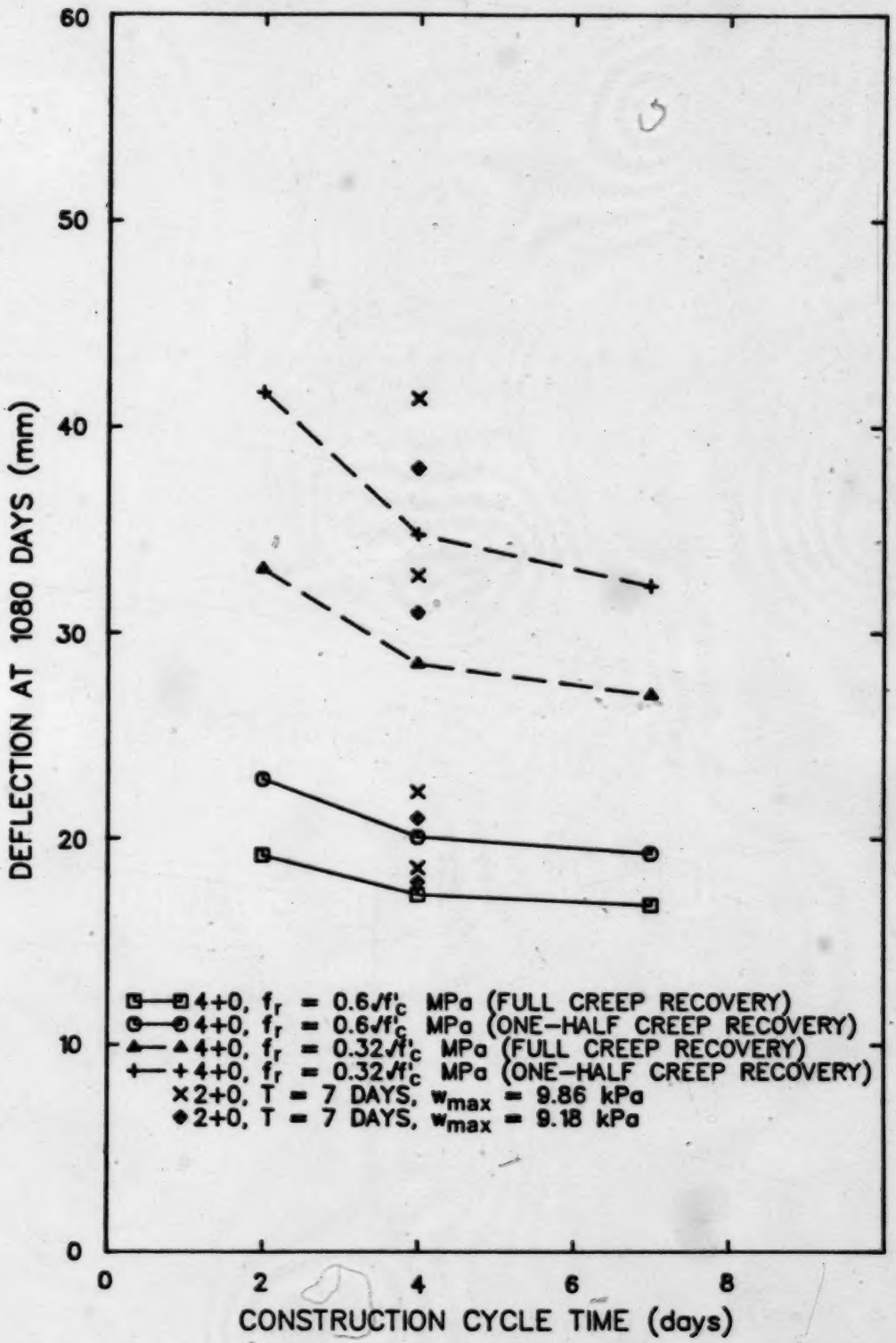

Figure 5.8 Parameter Study - Construction Cycle Time

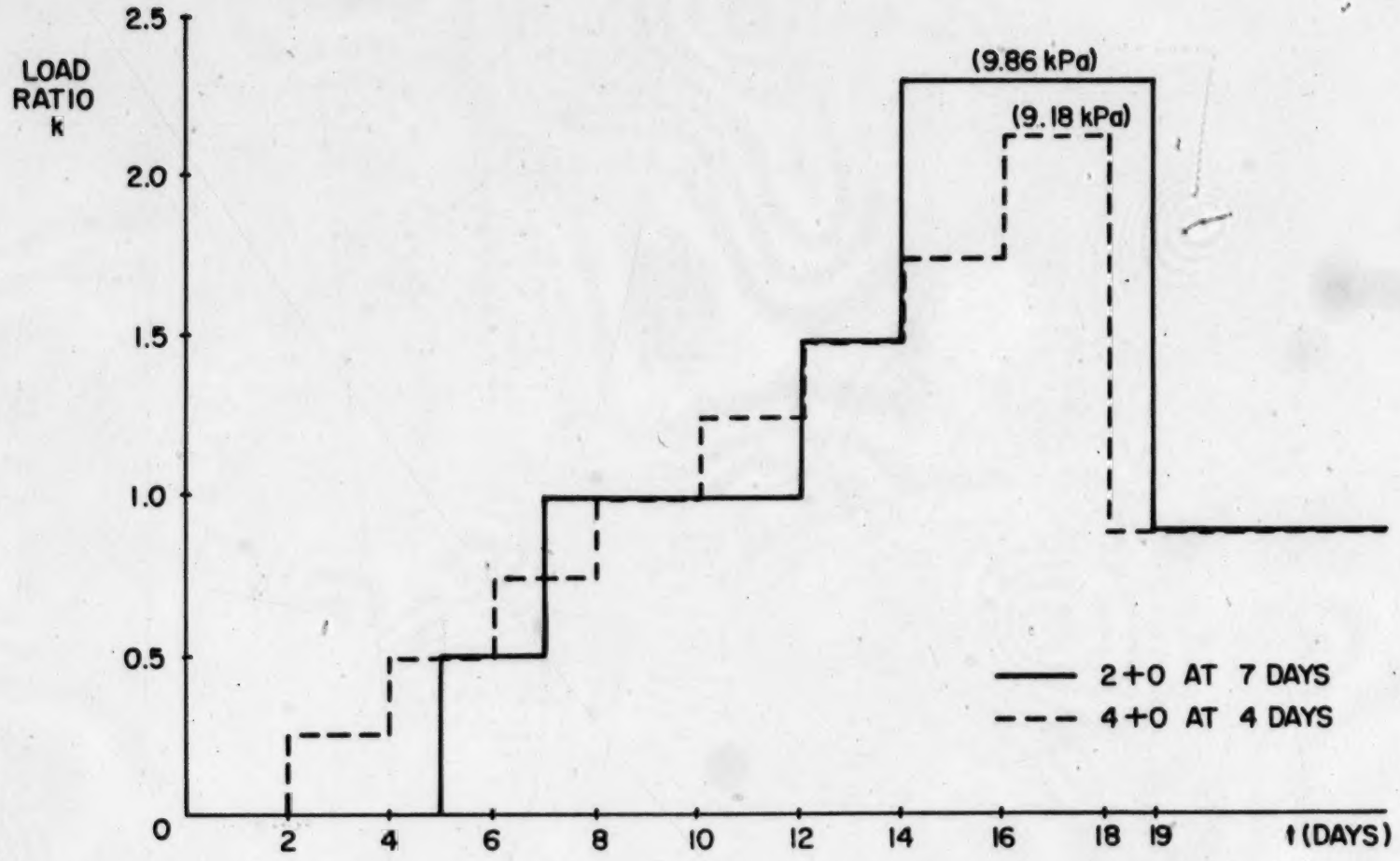

Figure 5.9 Parameter Study - Load Sequences for Construction Cycle Time Comparison

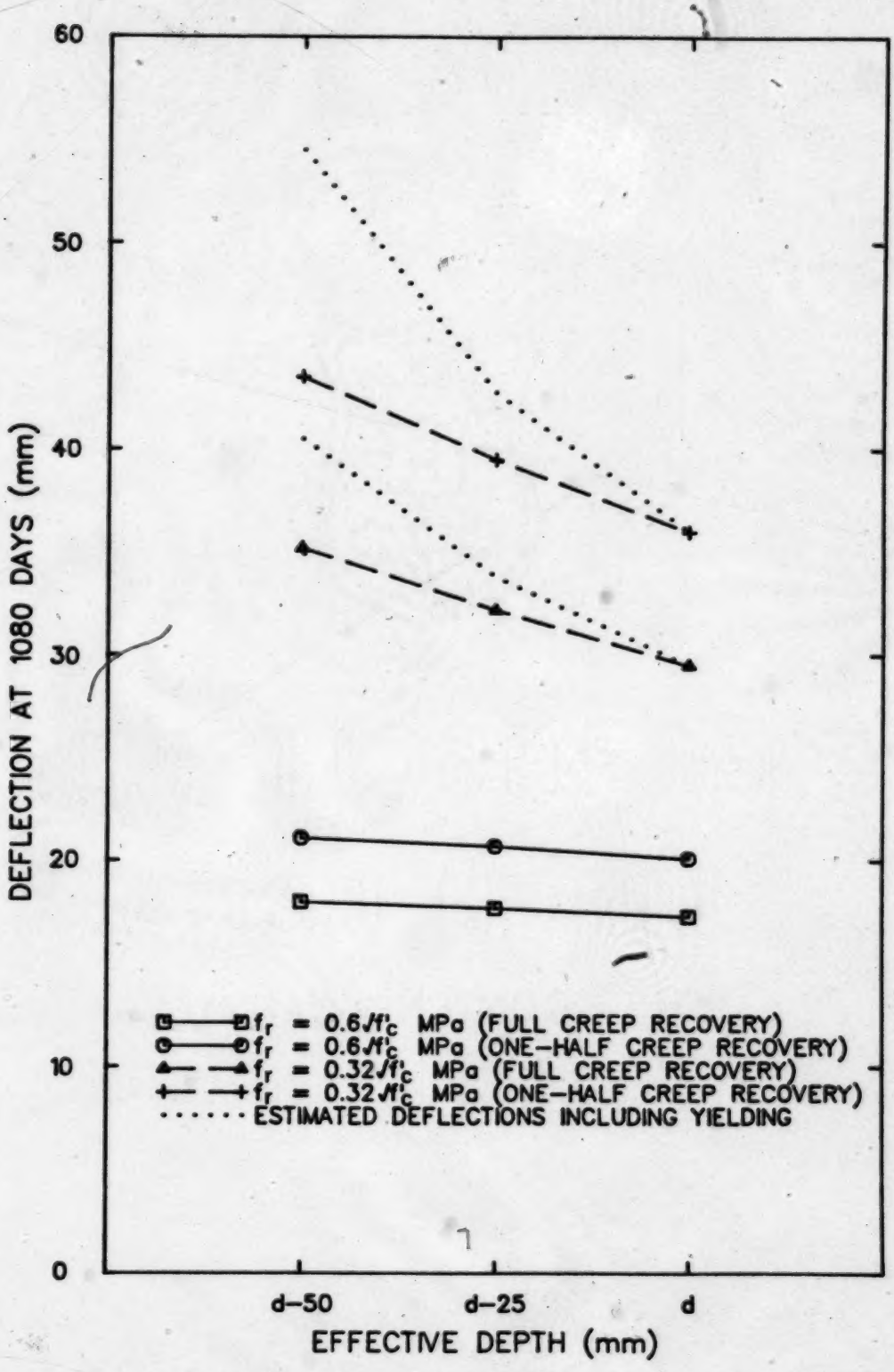

Figure 5.10 Parameter Study - Effective Depth to Top Reinforcement

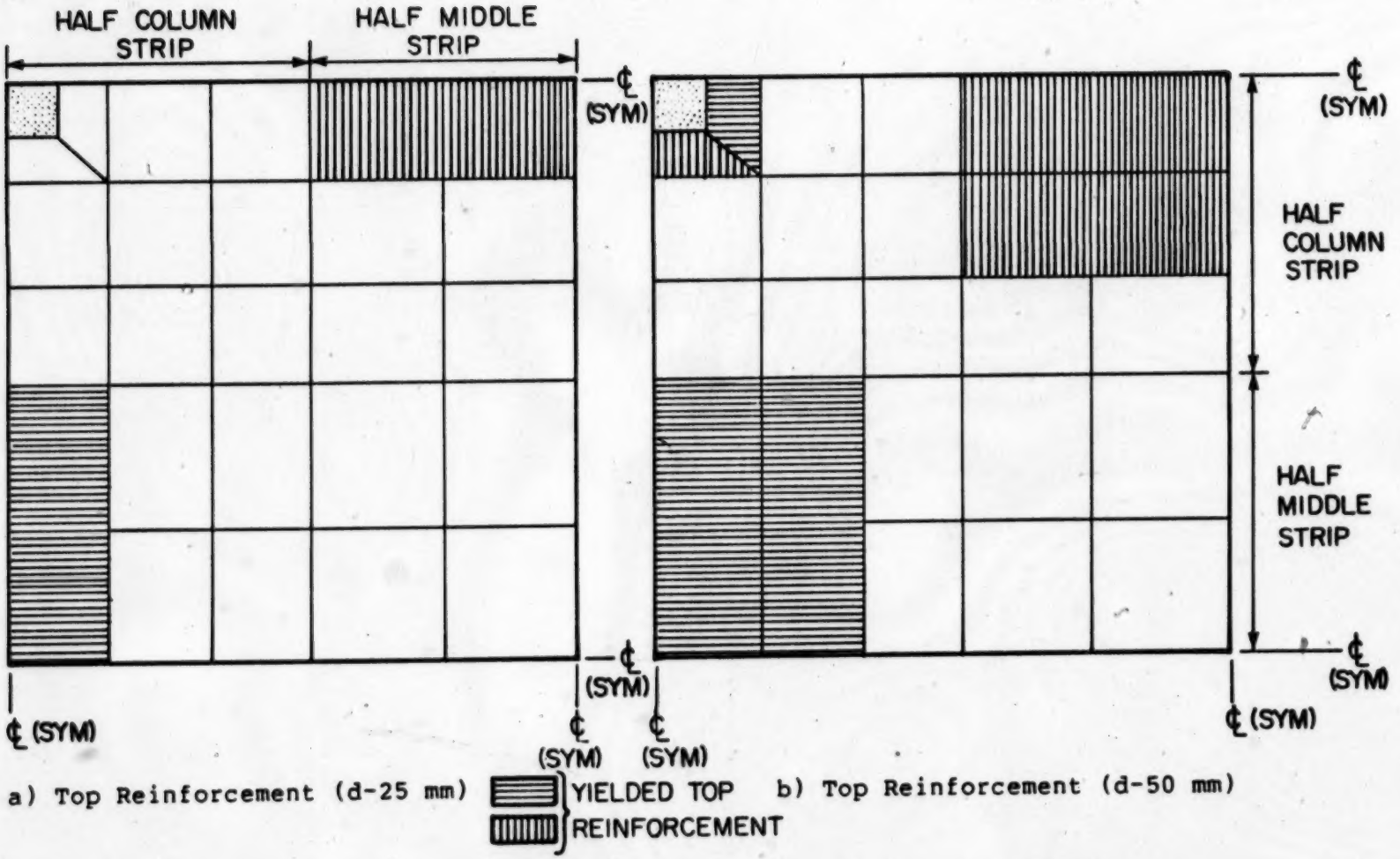

Figure 5.11 Parameter Study - Yield Locations With Reduced Effective Depth to Top Reinforcement

6. SIMPLIFIED METHOD FOR DEFLECTION CALCULATIONS UNDER CONSTRUCTION LOADS

6.1 Introduction

In Chapter 3, a model was developed to calculate deflections for a slab subjected to a construction load history. This model explicitly calculates time-dependent deflections for the entire loading sequence. For most applications, the ultimate deflection is important in determining whether serviceability requirements are met. In addition, consideration should be given to the portion of long-time deflection occurring after the installation of finishes and partitions. Practical calculation of ultimate deflection requires a less rigorous method incorporating some aspects contained in the model.

This chapter develops a procedure based on the current Code multiplier method of calculating additional long-time deflection. Immediate deflections are based on early age loading and corresponding loss of stiffness. Long-time multipliers account for the combined effects of creep and shrinkage. The simplified method can be used to estimate a range of expected deflection.

6.2 Calculation of Maximum Construction Load

The magnitude of the maximum construction load depends on the number of levels in the supporting assembly. Table 5.4 previously outlined the maximum converged construction

load ratios for several different assemblies. These values assume constant flexural stiffness for all levels in the assembly, and rigid shores and reshores. If the supporting assembly to be used during construction is known, the appropriate load ratio can be selected. Alternatively, a ratio of two is recommended for most applications. The actual maximum dead load intensity is obtained by multiplying this ratio by the slab self weight. To account for form, shore, and reshore weights, the slab self weight is increased by 10 percent (21,26). The maximum converged construction dead load is given by:

$$w_{dmax} = 1.1\ k_{max} w_s \qquad (6\text{-}1)$$

where: w_{dmax} = maximum converged construction dead load (kPa)

k_{max} = maximum converged construction dead load ratio

w_s = slab self weight (kPa)

The minimum recommended construction live load is 2.4 kPa (27). A greater value can be specified depending on the type of construction procedure used. The construction live load carried by a slab in the supporting assembly based on the minimum load value is:

$$w_\ell = 2.4/N \qquad (6\text{-}2)$$

where: w_ℓ = construction live load (kPa)

N = number of levels in the supporting assembly

The total maximum construction load on a slab is then given by:

$$w_{max} = w_{dmax} + w_\ell \qquad (6\text{-}3)$$

where: w_{max} = maximum construction load (kPa)

6.3 Calculation of Immediate Deflection

Calculation of deflection using the proposed model was by the superposition of time-dependent effects at each stage of the construction load sequence. This method gave a stepped approximation along the moment-curvature diagram, including the effects of cracking up to each load stage (Figure 3.6). Alternatively, the maximum load level may be reached in a smaller number of increments. The limiting case is to apply the maximum construction load as a single increment at the time this load is reached in the complete load history. This approximation allows for a reduction in slab stiffness due to early age loading without calculating incremental deflections for the entire load history.

An equivalent frame procedure can be used to obtain the deflection due to the maxiumum construction load applied as a single increment. Properties of the concrete at the age corresponding to the maximum loading are obtained from the expressions previously discussed in Section 3.1.1. In calculating cracking moments, consideration should be given to the degree of restraint expected for the slab. For interior panels and other panels where restraint stresses due to shrinkage will be present, a reduced effective modulus of rupture value $0.32\sqrt{f'_c}$ MPa, is recommended. For panels relatively free of restraint stresses, the full $0.60\sqrt{f'_c}$ MPa value for modulus of rupture can be used. This value of modulus of rupture will result in comparatively little cracking in most cases. A range of deflection can be obtained by calculating deflections based on both modulus values.

Alternatively, deflections may be calculated using a general purpose finite element program, as outlined by Scanlon and Murray (10). Modification of element stiffnesses, previously discussed in Section 3.3.1, is necessary to account for cracking. Moments and deflections are initially calculated for the uncracked slab. These moments are used to calculate the degree of cracking, α_x and α_y, and reduced element properties. Stiffness coefficients are recalculated based on the new set of element properties. A subsequent finite element analysis using the reduced stiffness coefficients gives moments and deflections for the

cracked slab. Additional analyses can be made, depending on the degree of accuracy required. This procedure was incorporated into the proposed model as an iterative cracking routine.

6.4 Calculation of Long-Time Deflection

6.4.1 Immediate Deflection due to Sustained Loads

Present Code procedure calculates additional long-time deflection by application of a multiplier to the immediate deflection due to sustained loads. The amount of long-time creep deflection is dependent on the sustained load level. Deflections calculated in Section 6.2 for a single load increment were based on the maximum construction load level. This deflection must be reduced to the sustained load level.

Application of the construction load sequence results in gradual loss of slab stiffness with increasing load. After the maximum load level is reached, unloading of the slab will correspond with the reduced stiffness at that level. Figure 6.1 shows the load-deflection diagrams of four representative slab series from the parameter study. The deflections plotted are the total immediate deflections, Δ_o, corresponding to each load stage. In each case, after the maximum load level was reached, deflections due to unloading follow a secant toward the origin. For the sustained load level, the deflection can be scaled linearly from the maximum deflection value. The deflection due to sustained

loads required for application of a multiplier is expressed as:

$$\Delta_{s\ell} = \Delta_{max}(w_{s\ell}/w_{max}) \qquad (6\text{-}4)$$

where: $\Delta_{s\ell}$ = immediate deflection due to sustained loads accounting for the effects of construction loading at early age (mm)

Δ_{max} = immediate deflection due to the maximum construction load applied as a single increment (mm)

$w_{s\ell}$ = sustained load level (kPa)

This linear reduction in the deflection, Δ_{max}, is dependent on the construction load history, including nature of supporting assembly, and construction cycle time. A similar procedure has been previously suggested by Sbarounis (36).

6.4.2 Derivation of Long-Time Multipliers

6.4.2.1 Basis for Multipliers

Long-time multipliers were calculated for the slabs analyzed in the parameter study of Chapter 5. These analyses represent a range of slab geometries, support assemblies, and construction load sequences. As in the parameter study, the following conditions apply to the derivation of the multipliers:

i) standard ACI Committee 209 expressions for time-dependent concrete properties (Section 3.1)

ii) ultimate creep coefficient of 2.35

iii) ultimate shrinkage strain of 780 x 10^{-6} mm/mm

iv) stepped construction load sequence

v) superimposed dead load of 1.75 kPa applied at sixty days after casting of the slab to obtain the total sustained load

Multipliers were not calculated for analyses considering a reduced depth to top reinforcement (series SD). This was due to the partial yielding of this reinforcement, as discussed in Section 5.2.7.

6.4.2.2 One-Year and Ultimate Multipliers

For each slab series, the maximum construction load was applied as a single increment corresponding to the age at maximum loading for the entire construction load sequence. The scaled immediate deflection due to sustained loads, $\Delta_{s\ell}$, was expressed as a multiple of the total long-time deflection, Δ_t, calculated for the full construction load sequence. Figure 6.2 illustrates the general procedure used to calculate the multipliers.

Total average multipliers and range of multipliers for rupture modulus values $0.60\sqrt{f'_c}$ and $0.32\sqrt{f'_c}$ MPa, and full and one-half creep recovery are shown in Table 6.1. Values for all multipliers are given in Appendix G. Ultimate multipliers refer to conditions at 1080 days, or approximately three years after casting.

Assuming a modulus of rupture value $0.60\sqrt{f'_c}$ MPa, ultimate multipliers range from 4.05 to 4.67 for full and one-half creep recovery respectively. These represent increases of 35 and 56 percent over the current accepted Code multiplier of three. With a rupture modulus $0.32\sqrt{f'_c}$ MPa, the total multipliers range from 2.68 to 3.24. In this case however, the immediate deflection due to sustained loads will be greater than that assuming $0.60\sqrt{f'_c}$ MPa.

Values given in brackets in Table 6.1 indicate the percentage of the total ultimate multiplier for each component. For a rupture modulus $0.60\sqrt{f'_c}$ MPa, immediate-plus-creep deflection represents 60 percent of total deflection, and shrinkage 40 percent. Assuming a modulus $0.32\sqrt{f'_c}$ MPa, the breakdown is approximately 75 percent immediate-plus-creep, and 25 percent shrinkage. With a lower modulus value, loss of slab stiffness is greatly increased and incremental deflections between load steps are larger. Creep deflection is dependent on the initial incremental deflection and should increase proportionately with decreasing modulus of rupture. The amount of shrinkage deflection is independent of loading and slab stiffness.

Additional multipliers were calculated correlating the immediate deflection due to sustained load based on a modulus of rupture value $0.60\sqrt{f'_c}$ MPa, with ultimate deflections calculated for the entire construction load sequence based on a modulus of rupture value $0.32\sqrt{f'_c}$ MPa. For full or one-half creep recovery, the respective total

ultimate multipliers were 6.50 and 7.84. The magnitude of these multipliers indicates the increase in deflection when calculation of immediate deflection ignores the effect of restraint stresses.

6.4.3 Recommended Multipliers

Based on the proposed deflection calculation model and subsequent parameter study, a set of recommended long-time deflection multipliers is given in Table 6.2. These multipliers are based on the conditions outlined in Section 6.4.2.1, and represent average values for several analyses. The multipliers apply to deflection calculations for slabs of multistory structures supported by a series of shores and/or reshores, and subjected to early age loading.

The set of multipliers given in Table 6.2 represent a basis for a likely range of calculated slab deflections. From these, the following design multipliers are recommended to give a representative value of long-time deflection:

i) multistory slabs, significant restraint

- use $f_r = 0.32\sqrt{f'_c}$ MPa ($4\sqrt{f'_c}$ psi) to obtain $\Delta_{s\ell}$

$$\Delta_t = \lambda_t \Delta_{s\ell} \quad , \lambda_t = 3.25$$

ii) multistory slabs, no significant restraint

- use $f_r = 0.60\sqrt{f'_c}$ MPa ($7.5\sqrt{f'_c}$ psi) to obtain $\Delta_{s\ell}$

$$\Delta_t = \lambda_t \Delta_{s\ell} \quad , \lambda_t = 4.75$$

Note that in each case, one-half creep recovery is assumed.

Recommended multipliers from this study are compared with those given by CSA A23.3 M77 (1), Sbarounis (36), and Branson (18) in Table 6.3. The latter multipliers are all based on a value of $0.60\sqrt{f'_c}$ MPa for the modulus of rupture. Multipliers from both CSA A23.3 M77 and Branson assume 28-day concrete properties and are a direct extension of those derived for one-way action. Branson recommended increased creep and shrinkage multiplier components due to the two-way nature of the deformation and the fact that slabs are usually thinner than beams. The multipliers recommended by Sbarounis account for early age construction loading. In all cases, the multipliers pertain to the immediate deflection due to the sustained load.

For creep and shrinkage characteristics greatly different from the assumed standard ACI Committee 209 values (ultimate creep coefficient = 2.35; ultimate shrinkage strain = 780×10^{-6} mm/mm), the recommended design multipliers can be adjusted, as suggested by Sbarounis (36). A general expression for the revised total multiplier considering non-standard creep and shrinkage properties is:

$$\lambda'_t = 1 + \lambda_c(C_u/2.35) + \lambda_{sh}(\varepsilon_{shu}/780 \times 10^{-6}) \qquad (6\text{-}5)$$

where: λ'_t = revised total multiplier

λ_c = creep component multiplier

λ_{sh} = shrinkage component multiplier

6.5 Simplified Deflection Calculation Examples

The simplified method for calculation of long-time deflection under construction loads is illustrated considering the documented slabs presented in Chapter 4. For each of the three slabs, additional finite element analyses calculated the immediate deflection due to sustained loads, $\Delta_{s\ell}$, applying the maximum construction load as a single increment. The results are shown in Table 6.4.

For Sbarounis' Flat Plate, there is good agreement between calculated and measured one-year deflections. Although use of the multipliers does not predict the full range of measured deflection, calculated deflections are close to the average measured deflection. Only when extreme values for modulus of rupture ($0.16\sqrt{f'_c}$ MPa) and degree of creep recovery (zero) were assumed, did calculated deflections by the model match the range measured. These extreme values were not considered for derivation of the multipliers.

In the case of Heiman's Flat Plate, both calculated one-year and ultimate deflections were close to those measured, when a modulus of rupture $4\sqrt{f'_c}$ psi ($0.32\sqrt{f'_c}$ MPa) was assumed. The use of multipliers based on the standard $7.5\sqrt{f'_c}$ psi ($0.60\sqrt{f'_c}$ MPa) modulus value did not predict the full ultimate deflection, as noted in Section 4.2.4.

Deflections were underestimated at both one-year and ultimate for Taylor's Flat Plate. From the complete analysis of Section 4.4 using the proposed model, it was found that

an effective rupture modulus of $2\sqrt{f'_c}$ psi ($0.16\sqrt{f'_c}$ MPa) was required to predict the actual measured deflection. In addition, the recommended multipliers apply to slabs subjected to a stepped construction load sequence. The loading for this slab consisted of a single sustained increment. Although it represents early age loading, it does not completely fulfill the conditions assumed in deriving the multipliers.

The last column in Table 6.4 gives ultimate deflections for each slab calculated according to present Code procedures. The sustained load was applied to the slab assuming 28-day concrete properties and modulus of rupture $7.5\sqrt{f'_c}$ psi. A total multiplier of three was used. In each case, the Code deflections are well below those measured. Better estimates are obtained taking into account early age construction loading.

6.6 Summary

A simplified method for calculation of flat plate deflections under construction loads was given. Immediate deflections were calculated based on the maximum construction load and corresponding slab age at maximum loading. A revised set of multipliers was used to calculate long-time deflection. Comparison of measured deflections and those calculated using the simplified method for the documented slabs of Chapter 4 were satisfactory.

Table 6.1 Average Total One-Year and Ultimate Multipliers

CASE	ONE-YEAR MULTIPLIERS			ULTIMATE MULTIPLIERS		
	λ_{ic}	λ_{sh}	λ_t	λ_{ic}	λ_{sh}	λ_t
i) $f_r = 0.60\sqrt{f'_c}$ MPa						
- FULL CREEP RECOVERY	2.09	1.63	3.69	2.31 (57)	1.74 (43)	4.05
- RANGE	1.61-2.16	1.33-1.88	3.00-4.01	2.19-2.70	1.42-2.00	3.61-4.30
- ONE-HALF CREEP RECOVERY	2.59	1.63	4.22	2.93 (63)	1.74 (37)	4.67
- RANGE	1.91-2.80	1.33-1.88	3.30-4.59	2.69-3.15	1.42-2.00	4.31-4.95
ii) $f_r = 0.32\sqrt{f'_c}$ MPa						
- FULL CREEP RECOVERY	1.81	0.70	2.51	1.94 (72)	0.74 (28)	2.68
- RANGE	1.68-1.91	0.54-0.86	2.34-2.62	1.81-2.05	0.57-0.92	2.51-2.81
- ONE-HALF CREEP RECOVERY	2.30	0.70	3.00	2.50 (77)	0.74 (23)	3.24
- RANGE	1.97-2.51	0.54-0.86	2.83-3.14	2.13-2.73	0.57-0.92	3.05-3.40

Table 6.2 Recommended One-Year and Ultimate Multipliers

CASE	ONE-YEAR MULTIPLIERS			ULTIMATE MULTIPLIERS		
	λ_{ic}	λ_{sh}	λ_t	λ_{ic}	λ_{sh}	λ_t
i) $f_r = 0.60\sqrt{f'_c}$ MPa						
- FULL CREEP RECOVERY	2.05	1.65	3.70	2.25	1.75	4.00
- ONE-HALF CREEP RECOVERY	2.60	1.65	4.25	3.00	1.75	4.75
ii) $f_r = 0.32\sqrt{f'_c}$ MPa						
- FULL CREEP RECOVERY	1.80	0.70	2.50	2.00	0.75	2.75
- ONE-HALF CREEP RECOVERY	2.30	0.70	3.00	2.50	0.75	3.25

Table 6.3 Comparison of Recommended Design Multipliers

SOURCE	RECOMMENDED DESIGN MULTIPLIERS			
	IMMEDIATE	CREEP λ_c	SHRINKAGE λ_{sh}	TOTAL λ_t
PRESENT STUDY				
- $f_r = 0.60\sqrt{f'_c}$	1.0	2.0	1.75	4.75
- $f_r = 0.32\sqrt{f'_c}$	1.0	2.5	0.75	3.25
CSA A23.3 M77	1.0	TOTAL = 2.0		3.0
SBAROUNIS	1.0	2.8	1.2	5.0
BRANSON	1.0	2.0	1.0	4.0

Table 6.4 Multiplier Examples

SLAB	w_{max} (psf)	t_{max} (day)	$w_{s\ell}$ (psf)	$\Delta_{s\ell_1}$ (in)	$\Delta_{s\ell_2}$ (in)	ONE-YEAR DEFLECTIONS (in)			ULTIMATE DEFLECTIONS (in)			
						Δ_1	Δ_2	Δ_3	Δ_1	Δ_2	Δ_3	Δ_4
i) SBAROUNIS' FLAT PLATE												
- FULL CREEP RECOVERY	157	12	87	0.28	0.46	1.04	1.15	0.53-1.63 (1.25 AVG)	-	-	-	0.63
- HALF CREEP RECOVERY	157	12	87	0.28	0.46	1.19	1.38		-	-		
ii) HEIMAN'S FLAT PLATE												
- FULL CREEP RECOVERY	170	14	115	0.15	0.25	0.56	0.63	0.67	0.60	0.69	0.85	0.37
- HALF CREEP RECOVERY	170	14	115	0.15	0.25	0.64	0.75		0.71	0.81		
iii) TAYLOR'S FLAT PLATE	104	14	104	-	0.10	-	0.25	0.52	-	0.28	0.72	0.25

$\Delta_{s\ell 1}$, Δ_1 - $f_r = 0.60\sqrt{f'_c}$ MPa
$\Delta_{s\ell 2}$, Δ_2 - $f_r = 0.32\sqrt{f'_c}$ MPa
Δ_3 - MEASURED
Δ_4 - CALCULATED BY CODE ($\lambda_t = 3$)

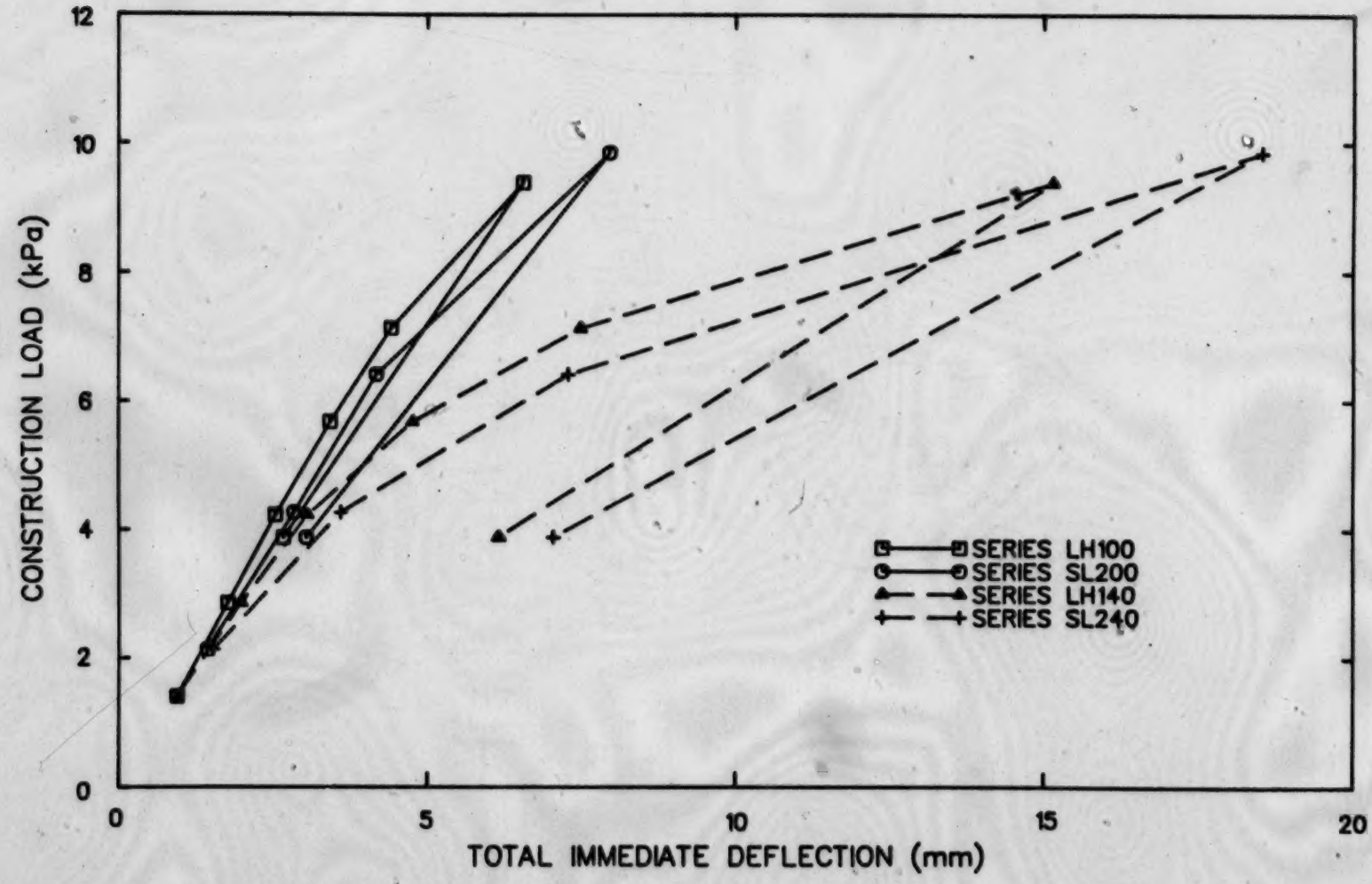

Figure 6.1 Load-Deflection Curves Showing Secant Unloading

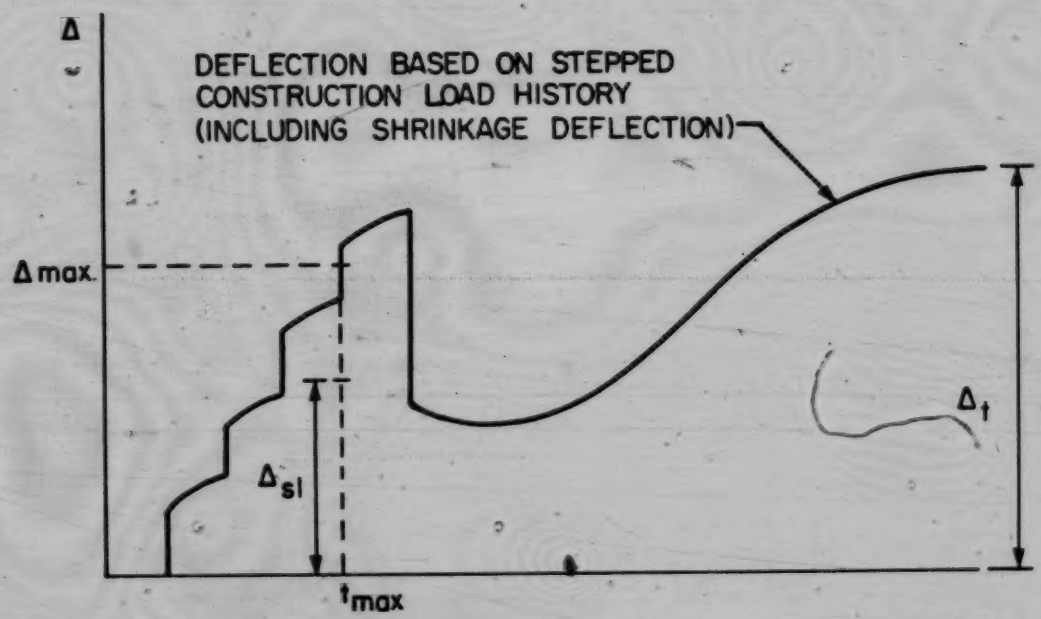

Figure 6.2 Calculation of Total Multiplier

7. SUMMARY, CONCLUSIONS, RECOMMENDATIONS

7.1 Summary

A procedure to calculate flat plate deflections under construction loads was developed. Deflections were calculated using an elastic finite element program. Modifications were made to the program to allow an iterative solution accounting for the effects of cracking.

Early age concrete properties used in the model are based on standard ACI Committee 209 expressions. A reduced effective modulus of rupture, below the Code standard value $0.60\sqrt{f'_c}$ MPa, was used to account for restrained shrinkage in the slab. Stepped construction load histories were calculated from a given supporting assembly of forms, shores, and/or reshores.

At each stage in the construction load history, an incremental immediate deflection corresponding to the previous stage was calculated using finite element analysis. Individual long-time creep deflection curves, based on the incremental deflection at each load stage, were combined using the principle of superposition. Shrinkage deflections were calculated separately and added to obtain total ultimate deflections.

Verification of the model included comparison of calculated deflections with those measured for three previously documented flat plates. A parameter study for the model considered factors including various span-to-depth

ratios, construction load histories, and construction cycle times.

From the results of the parameter study, a revised set of total multipliers was derived for use in a simplified deflection calculation method. With this method, immediate deflections are calculated using the maximum construction load and corresponding age at maximum loading, including the effects of cracking. The multipliers are applied to the immediate deflection, scaled to the sustained load level. These revised multipliers account for construction loading at early age, resulting in greater deflections than those calculated by present Code procedures and ignoring construction loads.

7.2 Conclusions

Several important points regarding the study may be noted:

1. Accurate estimation of two-way slab deflections is difficult. Several methods exist for calculation of these deflections, but few consider the effects of construction loading at early age.
2. Current Code procedures base serviceability requirements for two-way slab deflections on service load conditions. Additional long-time multipliers, developed from tests on one-way beams, may not adequately predict deflections associated with slabs.
3. The construction of multistory flat plate structures

using a series of forms, shores, and/or reshores will result in a stepped loading sequence for a typical slab. Depending on the support assembly used, maximum construction load levels are approximately two times the slab-plus-formwork weight, and may exceed the total service load level. This maximum construction load often occurs at early age before the slab has attained the specified design strength.

4. In addition to slab self weight plus form, shore, and reshore weights, a minimum construction live load of 2.4 kPa should be included in the calculation of construction loads.
5. Loss of stiffness due to cracking greatly affects two-way slab deflections. In addition to moments exceeding the cracking moments, significant cracking may occur due to restrained shrinkage. To account for this behaviour, the Code modulus of rupture value, $0.60\sqrt{f'_c}$ MPa, should be reduced to a lower effective value for slabs restrained against shrinkage. It appears a value of approximately $0.32\sqrt{f'_c}$ MPa ($4\sqrt{f'_c}$ psi) is reasonable.
6. A procedure to calculate long-time flat plate deflections under construction loading resulted in satisfactory predictions of previously documented slab deflections. The model included the effects of:
    i) early age concrete properties
    ii) construction loading

iii) restrained shrinkage

iv) additional long-time creep and shrinkage deflections

v) variable degree of creep recovery

The parameter study associated with the proposed deflection calculation model resulted in the following conclusions:

1. In most cases, creep and shrinkage are major components of ultimate long-time deflections of two-way slabs.
2. The assumed modulus of rupture has a significant effect on calculated deflections. Using the Code value of $0.60\sqrt{f'_c}$ MPa, very little cracking was predicted. Greater loss of slab in both middle and column strips occurred when the modulus of rupture was reduced to $0.32\sqrt{f'_c}$ MPa. For areas of high restraint, (ie. at columns), an even lower effective modulus may be required.
3. If significant unloading occurs during the construction load sequence (ie. from the maximum load level to the slab self weight), the degree of creep recovery assumed in the superposition of individual creep deflection curves can affect total long-time deflection. It appears a value between one-half and full recovery of that normally predicted by superposition is reasonable.

4. For a relatively narrow range of span-to-depth ratios (33.3 to 38.7), calculated ultimate deflections varied considerably, depending on the degree of restraint assumed. Even by specifying the Code minimum thickness, deflections may be significant due to construction loads and loss of stiffness from restrained shrinkage.
5. Increasing the number of levels in the supporting assembly is an effective method to control deflections. With more than five levels of shores, little reduction in deflection is evident. Addition of reshores to the supporting assembly reduces the maximum construction load level and ultimate deflections. Substitution of shores with reshores does not greatly affect ultimate deflections.
6. A reduction in construction cycle time from a new slab cast every seven days to one cast every four days did not alter deflections appreciably. Further reduction to a two-day cycle showed increased deflections.
7. When the effective depth to the top steel was reduced, yielding was detected in this reinforcement. Since the analytical model does not include the effects of steel yielding, actual deflections significantly greater than those predicted by the model would be expected.

7.3 Recommendations

The following simplified procedure is recommended to account for early age construction loading when calculating long-time deflection:

i) multistory slabs, significant restraint

- use $f_r = 0.32\sqrt{f'_c}$ MPa ($4\sqrt{f'_c}$ psi) to calculate the immediate deflection due to the sustained load, $\Delta_{s\ell}$

  $\Delta_t = \lambda_t \Delta_{s\ell}$, $\lambda_t = 3.25$

ii) multistory slabs, no significant restraint

- use $f_r = 0.60\sqrt{f'_c}$ MPa ($7.5\sqrt{f'_c}$ psi) to calculate the immediate deflection due to the sustained load, $\Delta_{s\ell}$

  $\Delta_t = \lambda_t \Delta_{s\ell}$, $\lambda_t = 4.75$

Deflection should be calculated for the maximum construction load level and corresponding time of maximum loading, and scaled to the sustained load level. A general purpose finite element program and the procedure of Section 6.3 is recommended for calculation of deflections. Alternatively, an equivalent frame procedure and correct modulus of rupture value may be used.

Future research into the calculation of deflections for two-way slabs under construction loads may be related to the following areas:

1. An investigation using the proposed procedure to estimate deflections for:

i) edge, corner, and cantilever panels of flat plate systems

ii) slab systems without beams

iii) slab systems with beams

2. Further study regarding the effect of reduced modulus of rupture values on deflections. A distribution of effective values reflecting the degree of restraint for different locations in the panel could be assumed, instead of a constant modulus value for the entire slab.
3. Modification of the linear elastic model to account for yielding of reinforcement due to misplacement during construction.
4. Statistical study of variability of slab deflections.

REFERENCES

1. CSA-CAN3-A23.3-M77, "Code for the Design of Concrete Structures for Buildings." Canadian Standards Association, Rexdale, Ontario, 1977, 131 pp.

2. ACI COMMITTEE 318, "Building Code Requirements for Reinforced Concrete (ACI 318-83)." American Concrete Institute, Detroit, 1983, 111 pp.

3. TAYLOR, P. J., and HEIMAN, J. L., "Long-Time Deflection of Reinforced Concrete Flat Slabs and Plates." Proceedings, ACI Journal, Vol. 74, No. 11, November 1977, pp. 556-561.

4. TIMOSHENKO, S., and WOINOWSKY-KRIEGER, S., "Theory of Plates and Shells." McGraw-Hill Book Company, New York, 1959, 580 pp.

5. PEABODY, D., "Continuous Frame Analysis of Flat Slabs." Journal of Boston Society of Civil Engineers, Vol. 35, No. 1, January 1948.

6. VANDERBILT, M. D., SOZEN, M. A., and SIESS, C. P., "Deflections of Multiple-Panel Reinforced Concrete Floor Slabs." Proceedings, ASCE, Vol. 91, No. ST4 Part 1,

August 1965, pp. 77-101.

7. NILSON, ARTHUR H., and WALTERS, DONALD B. JR., "Deflection of Two-Way Floor Systems by the Equivalent Frame Method." Proceedings, ACI Journal, Vol. 72, No. 5, May 1975, pp. 210-218.

8. KRIPANARAYAN, K. M., and BRANSON, D. E., "Short-Time Deflections of Flat Plates, Flat Slabs, and Two-Way Slabs." Proceedings, ACI Journal, Vol. 73, No. 12, December 1976, pp. 686-690.

9. RANGAN, B. VIJAYA, "Prediction of Long-Term Deflections of Flat Plates and Slabs." Proceedings, ACI Journal, Vol. 73, No. 4, April 1976, pp. 223-226.

10. SCANLON, A., and MURRAY, D. W., "Practical Calculation of Two-Way Slab Deflections." Concrete International, November 1982, pp. 43-50.

11. ACI COMMITTEE 435, SUBCOMMITTEE 5, "State-of-the-Art Report: Deflection of Two-Way Reinforced Concrete Floor Systems." Deflections of Concrete Structures, SP-43, American Concrete Institute, Detroit, 1982, pp. 53-88.

12. JOFRIET, JAN C., "Short-Term Deflections of Concrete Flat Plates." Proceedings, ASCE, Vol. 99, No. ST1,

January 1973, pp. 167-182.

13. JOFRIET, JAN C., and McNEICE, GREGORY, M., "Finite Element Analysis of Reinforced Concrete Slabs." Proceedings, ASCE, Vol. 97, No. ST3, March 1971, pp. 785-806.

14. SCANLON, A., "Time-Dependent Deflections of Reinforced Concrete Slabs." Structural Engineering Report No. 38, Department of Civil Engineering, University of Alberta, December 1971, 174 pp.

15. WASHA, G. W., and FLUCK, P. G., "The Effect of Compressive Reinforcement on the Plastic Flow of Reinforced Concrete Beams." Proceedings, ACI Journal, Vol. 49, No. 8, October 1952, pp. 89-108.

16. WASHA, G. W., and FLUCK, P. G., "Plastic Flow (Creep) of Reinforced Concrete Continuous Beams." Proceedings, ACI Journal, Vol. 52, No. 5, January 1956, pp. 549-561.

17. YU, WEI-WEN, and WINTER, GEORGE, "Instantaneous and Long-Term Deflections of Reinforced Concrete Beams Under Working Loads." Proceedings, ACI Journal, Vol. 57, No. 1, July 1960, pp. 29-50.

18. BRANSON, D. E., "Deformation of Concrete Structures."

McGraw-Hill Book Company, New York, 1977, 546 pp.

19. ACI COMMITTEE 209, "Prediction of Creep, Shrinkage, and Temperature Effects in Concrete Structures." Designing for Creep and Shrinkage in Concrete Structures, SP-76, American Concrete Institute, Detroit, 1982, pp. 193-300.

20. NIELSEN, KNUD E. C., "Loads on Reinforced Concrete Floor Slabs and Their Deformations During Construction." Proceedings No. 15, Swedish Cement and Concrete Research Institute, Royal Institute of Technology, Stockholm, 1952, 113 pp.

21. GRUNDY, PAUL, and KABAILA, A., "Construction Loads on Slabs with Shored Formwork in Multistory Buildings." Proceedings, ACI Journal, Vol. 60, No. 12, December 1963, pp. 1729-1738.

22. SBAROUNIS, JOHN A., "Multistory Flat Plate Buildings - Construction Loads and Immediate Deflections." Concrete International, Vol. 6, No. 2, February 1984, pp. 70-77.

23. BLAKEY, F. A., and BERESFORD, F. D., "Stripping of Formwork for Concrete in Buildings in Relation to Structural Design." Civil Engineering Transactions, The Institution of Engineers, Australia, Vol. CE7, No. 2, October 1965, pp. 92-96.

24. TAYLOR, P. J., "Effects of Formwork Stripping Time on Deflections of Flat Slabs and Plates." Australian Civil Engineering and Construction (Melbourne), Vol. 8, No. 2, February 1967, pp. 31-35.

25. AGARWAL, R. K., and GARDNER, NOEL, J., "Form and Shore Requirements for Multistory Flat Slab Type Buildings." Proceedings, ACI Journal, Vol. 71, No. 11, November 1974, pp. 559-569.

26. LASISI, MOHAMMED Y., and NG, SIMON F., "Construction Loads Imposed on High-Rise Floor Slabs." Concrete International ,Vol. 1, No. 2, February 1979, pp. 24-29.

27. HURD, M. K., "Formwork for Concrete." SP-4, 4th Edition, American Concrete Institute, Detroit, 1981, 464 pp.

28. BRANSON, D. E., "Instantaneous and Time-Dependent Deflections of Simple and Continuous Reinforced Concrete Beams." HPR Publication 7, Part 1, Alabama Highway Department, Bureau of Public Roads, August 1963, pp. 1-78.

29. HEIMAN, J. L., "A Comparison of Measured and Calculated Deflections of Flexural Members in Four Reinforced Concrete Buildings." Deflections of Concrete Structures,

SP-43, American Concrete Institute, Detroit, 1974, pp. 515-545.

30. TAYLOR, P. J., "Long-Term Deflection Calculation Methods for Flat Plates." Constructional Review (Sydney), Vol. 43, No. 2, May 1970, pp. 68-74.

31. HEIMAN, J. L., and TAYLOR, P. J., Long-Term Deflections of a Reinforced Concrete Flat Plate." Architectural Science Review (Sydney), Vol. 15, No. 2, July 1972, pp. 25-29.

32. BLAKEY, F. A., "Deformations of an Experimental Lightweight Flat Plate Structure." Civil Engineering Transactions, The Institution of Engineers, Australia, Vol. CE3, No. 1, March 1961, pp. 18-24.

33. BLAKEY, F. A., "Australian Experiments with Flat Plates." Proceedings, ACI Journal, Vol. 60, No. 4, April 1963, pp. 515-525.

34. JENKINS, B. R., "Tests on a Flat Plate Floor." Civil Engineering Transactions, The Institution of Engineers, Australia, Vol. CE16, No.2, 1974, pp. 164-167.

35. SBAROUNIS, JOHN A., "Multistory Flat Plates - Measured and Computed One-Year Deflections." Submitted to ACI for

Publication, MS #5490, 1983.

36. SBAROUNIS, JOHN A., "Multistory Flat Plate Buildings - Effect of Construction Loads on Long-Term Deflections." Concrete International, Vol. 6, No. 4, April 1984, pp. 62-70.

37. NEVILLE, A. M., DILGER, W. H., and BROOKS, J. J., "Creep of Plain and Structural Concrete." Construction Press, London, 1983, 361 pp.

38. BATHE, K. J., WILSON, E. L., and PETERSON, F. E., "SAPIV - A Structural Analysis Program for Static and Dynamic Response of Linear Systems." Department of Civil Engineering, University of California, Berkeley, 1974, 59 pp.

39. McHENRY, DOUGLAS, "A New Aspect of Creep in Concrete and its Application to Design." Proceedings, ASTM, Vol. 43, 1943, pp. 1069-1084.

40. BAZANT, Z. P., and WITTMANN, F. H. (Editors), "Creep and Shrinkage in Concrete Structures." John Wiley and Sons, New York, 1982, 363 pp.

41. CEB-FIP, "Structural Effects of Time-Dependent Behaviour of Concrete - CEB Design Manual." Bulletin D'Information

No. 136, Comite Euro-International du Beton, July 1980, 268 pp.

42. TAYLOR, P. J., "Initial and Long-Term Deflections of a Reinforced Concrete Flat Plate Structure." Paper No. 2794, Conference on the Deformation of Concrete and Concrete Structures, The Institution of Engineers, Australia, Brisbane, September 1969, pp. 16-22.

43. SCANLON, ANDREW, "A Parameter Study of Factors Affecting Time-Dependent Slab Deflections." Designing for Creep and Shrinkage in Concrete Structures, SP-76, American Concrete Institute, Detroit, 1982, pp. 53-88.

44. GHOSH, S. K., "Deflections of Two-Way Reinforced Concrete Slab Systems." Proceedings, International Conference on Forming Economical Concrete Buildings, Portland Cement Association, Skokie, 1982, pp. 29.1-29.21.

45. MIRZA, S. A., and MacGREGOR, J. G., "A Statistical Study of Variables Affecting the Strength of Reinforced Normal Weight Concrete Members." Structural Engineering Report No. 58, Department of Civil Engineering, University of Alberta, December 1976, 133 pp.

APPENDIX A

CALCULATION OF CONSTRUCTION LOAD RATIOS AND LOADS

Calculation of construction load ratios and loads is illustrated by considering two supporting assemblies:

i) three levels of shores (3+0)

ii) two levels of shores and one level of reshores (2+1)

As outlined in Section 3.2, the construction load sequence is generated by assuming the following operations comprise a complete construction cycle:

i) Operation 1 - erect shores and forms on new top level and cast slab.

ii) Operation 2 - strip shores and forms at the lowest level and move them to the new top floor level,

or when reshores are used,

Operation 2 - remove the lowest level of reshores, strip the lowest level of shores and forms, and immediately reshore this slab.

The load ratio histories for each supporting assembly are calculated in Figures A.1 and A.2, and are summarized in Figures A.3 and A.4. These ratios are calculated based on the assumptions of Grundy and Kabaila (21) given in Section 2.2 , considering all slabs in the supporting assembly to have the same flexural stiffness.

For the case of 3+0 (Figure A.1), the slabs in the supporting assembly carry no load until the assembly leaves the ground. With the casting of a new slab, an additional load ratio of 1.0 is distributed equally to the three slabs

in the supporting assembly. Shores transfer the load not carried by the slabs above to the slabs below. When the shore is removed from the lowest level in the supporting assembly, the load carried by this shore is distributed equally to the slabs above.

The case of 2+1 (Figure A.2) is similar to that described above. When a shored level is replaced by reshores, the reshores are assumed to transfer zero load and the load that was originally carried by the shore is distributed equally to the slabs above.

In each case, the slabs at level three (for 3+0) and level two (for 2+1) reach higher maximum load ratios than the remaining slabs (shown by the dashed lines in Figures A.3 and A.4). For this study, only the converged load history was considered.

To obtain load histories, consider a normal weight slab of thickness 165 mm, having a self weight of 3.88 kPa. Construction loads at each stage are calculated using Equation 3-8. The maximum construction load (including live load) is calculated using Equation 3-9. The resulting converged construction load histories are given in Figures A.5 and A.6.

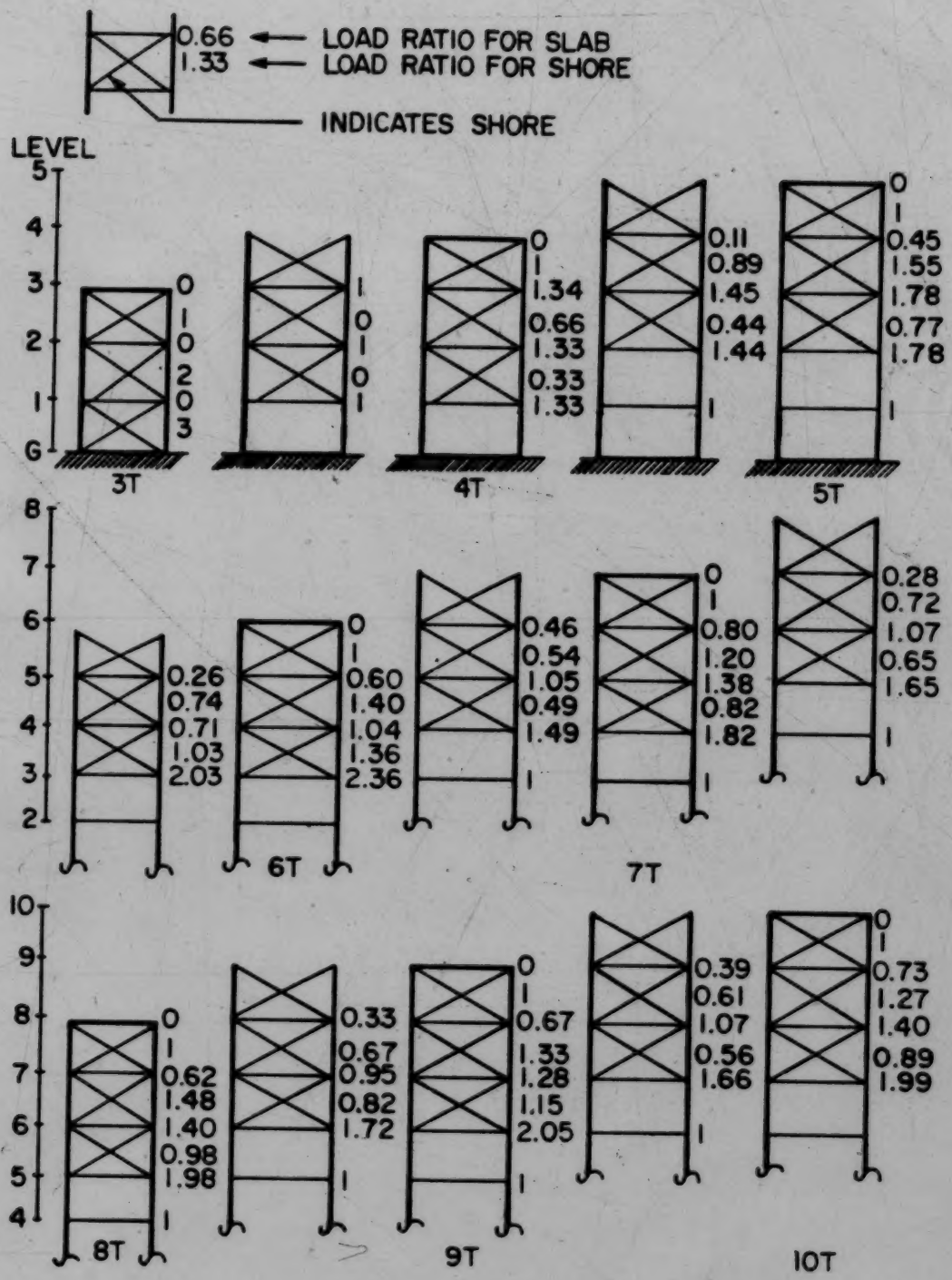

Figure A.1 Calculation of Load Ratios (3+0)

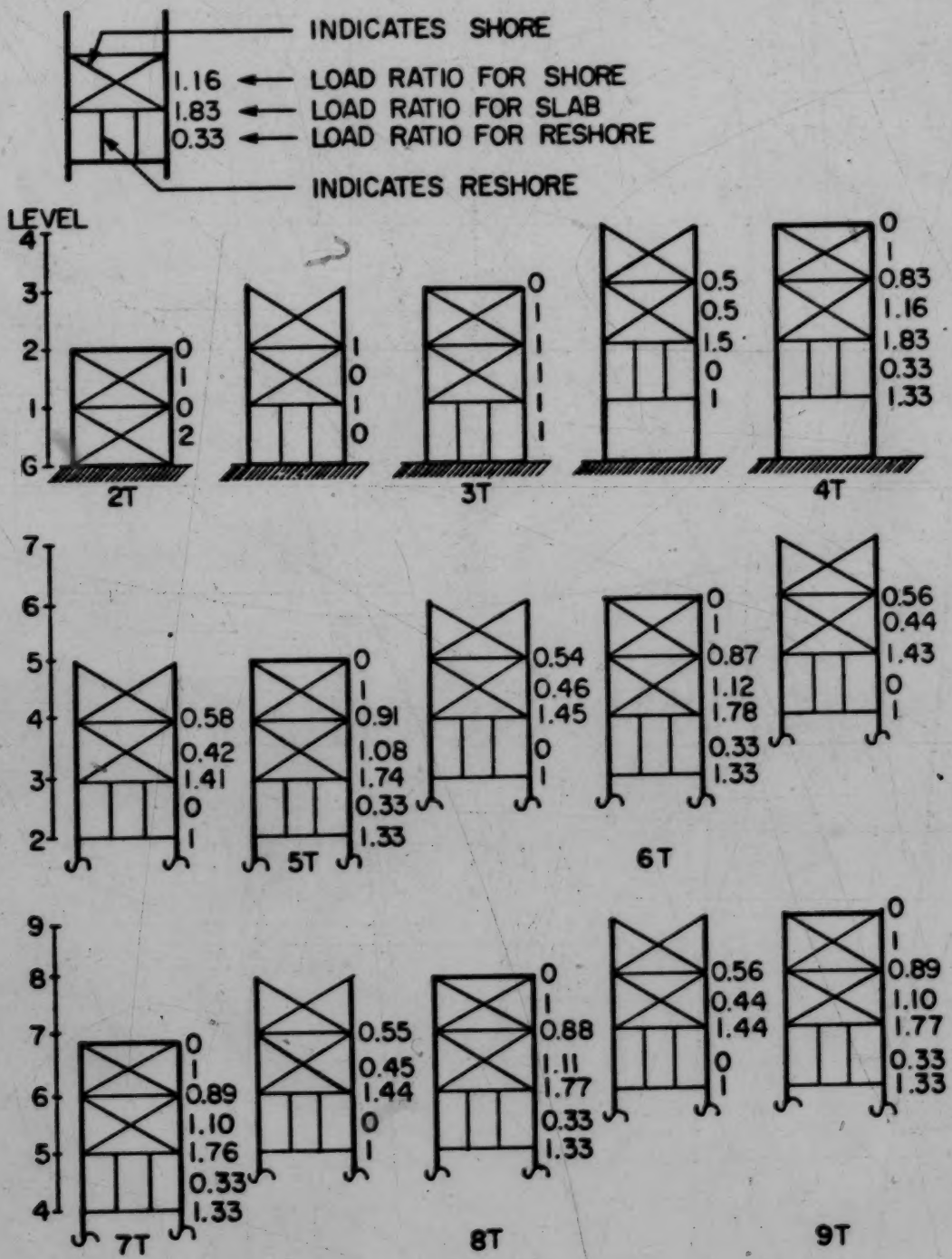

Figure A.2 Calculation of Load Ratios (2+1)

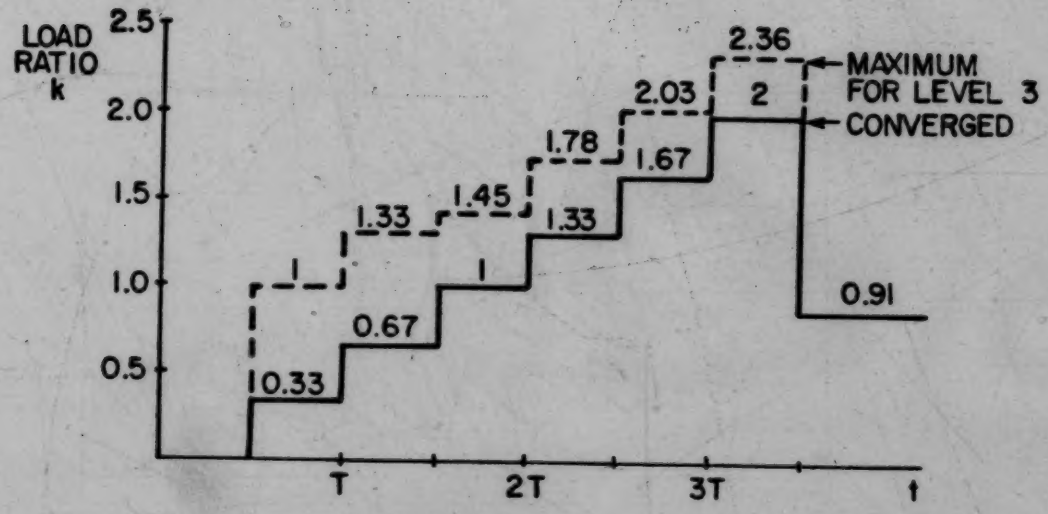

Figure A.3 Load Ratio History (3+0)

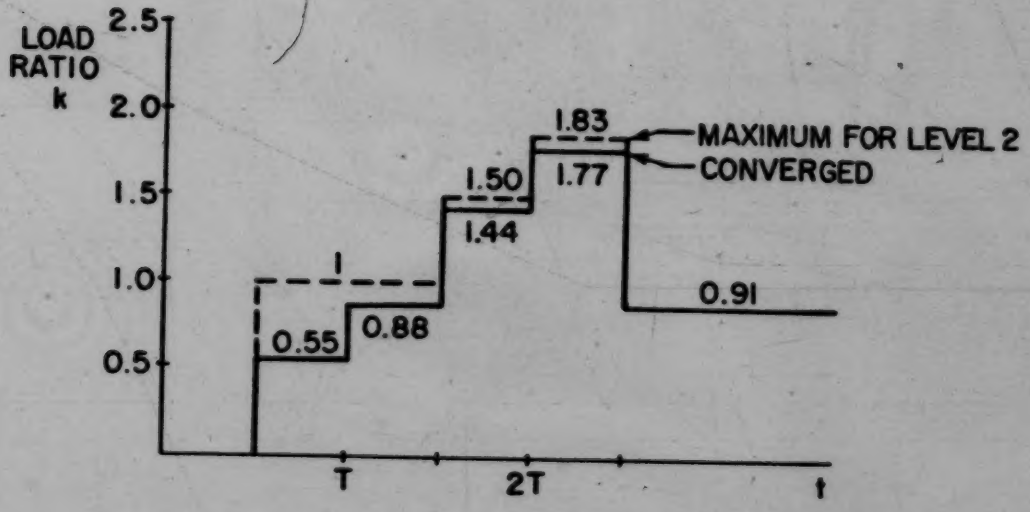

Figure A.4 Load Ratio History (2+1)

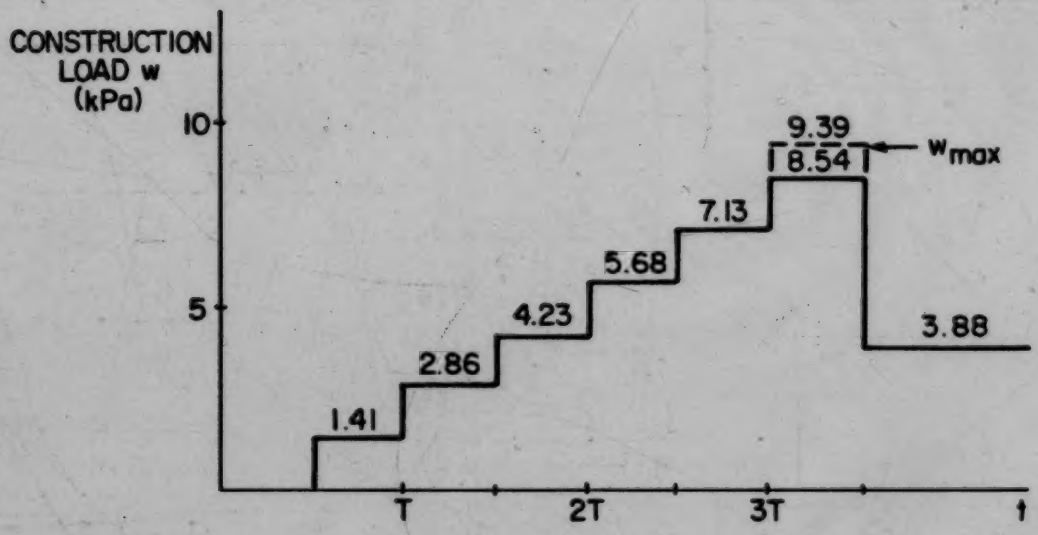

Figure A.5 Construction Load History (3+0)

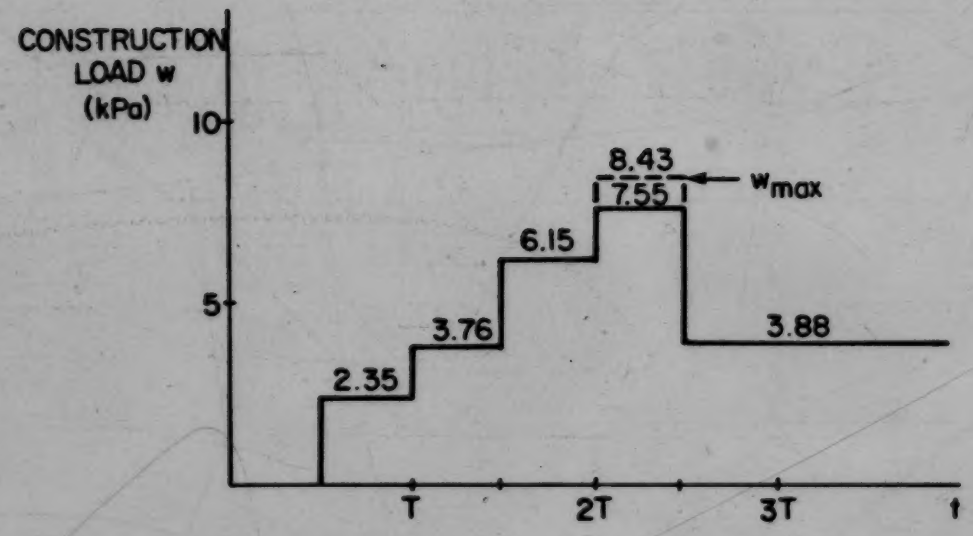

Figure A.6 Construction Load History (2+1)

APPENDIX B

PROGRAM LISTING AND DATA FOR ITERATIVE CRACKING ROUTINE

To illustrate the data required for the iterative cracking routine, consider slab series LH100 of the parameter study. Details of the slab are summarized as follows:

i) panel size = 6000 by 6000 mm

ii) columns = 500 by 500 mm

iii) slab thickness = 165 mm

iv) concrete - f'_c = 30 MPa

- $f_r = 0.60\sqrt{f'_c}$ MPa

v) reinforcement - areas given in Table 5.1

- plan shown in Figure 5.1

vi) supporting assembly - three levels of shores (3+0)

vii) construction loads - given in Table 5.3

viii) construction cycle time = 7 days

Figure B.1 shows the finite element grid used for the analysis of a typical interior quarter panel for this slab.

The form of the input data for the iterative cracking routine (ITER8) is as follows:

```
NEDP,NPRT,
1,THE(1),FRE(1),EC(1),VC(1),RME(1),BX(1),BY(1),
TSAX(1),DTSX(1),TSAY(1),DTSY(1),BSAX(1),DBSX(1),
        BSAY(1),DBSY(1),
.
.
.
NEDP,THE(NEDP),FRE(NEDP),EC(NEDP),VC(NEDP),
        RME(NEDP),BX(NEDP),BY(NEDP),
TSAX(NEDP),DTSX(NEDP),TSAY(NEDP),DTSY(NEDP),BSAX(NEDP),
        DBSX(NEDP),BSAY(NEDP),DBSY(NEDP),
NEL,MATT,
.
.
.
NEL,MATT,
```

where: NEDP = number of element types with different properties (thickness, steel areas, effective depths, degree of cracking, etc)

NPRT = control variable for output of element moments and deflections

= 0 - output after each iteration

= 1 - output after final iteration only

NEL = element number

MATT = material type number (there are NEDP material types)

The remaining variables are defined in the program listing.

NOTES:

1. Referring to Figure 5.1, initially there are four element types with different properties (each quadrant has different reinforcement properties - NEDP = 4).
2. Input for NEL and MATT starts with the first element and then must be given for consecutively increasing element numbers. Element numbers ommitted in the sequence are assigned the same material type number as the last element entered, up to but not including the present element number. Input for the last element number must be given.

In addition, the following variables must be added as input data to the normal SAPIV master control card data:

i) column 50 - ITERC - if = 1, initiates modified SAPIV run using ITER8
- if = 0, initiates normal SAPIV run

ii) column 60 - MITER - controls the number of iterations processed (usually a value of 5 or less is adequate)

Input for ITER8 is added to the data file for a normal SAPIV run directly after the Concentrated Load/Mass Data (Part V). Following the ITER8 input data, the usual two blank cards terminate the SAPIV data file.

For the initial load stage of the construction load history (assume three iterations), the SAPIV master control card and ITER8 data the slab is:

```
38,1,1,0,0,0,0,0,0,1,3,


4,1,
1,165.,2.716,21558.,0.15,9.28,0.,0.,
0.3100,130.,0.2970,140.,0.2970,130.,0.4003,140.,
2,165.,2.716,21558.,0.15,9.28,0.,0.,
0.9663,122.5,0.9663,137.5,0.2970,130.,0.2970,140.,
3,165.,2.716,21558.,0.15,9.28,0.,0.,
0.2970,130.,0.3100,140.,0.4003,130.,0.2970,140.,
4,165.,2.716,21558.,0.15,9.28,0.,0.,
0.,130.,0.,140.,0.2970,130.,0.2970,140.,
1,1,
3,2,
7,1,
9,2,
12,1,
14,2,
17,4,
19,3,
22,4,
24,3,
26,3,
```

0
0

Any cracking that occurs will be indicated by AX (=1-BX) and/or AY (=1-BY) values less than one output for an element. For subsequent runs in the same load history, this precracking in the slab must be accounted for by:

i) Creating additional material types with stiffness coefficients calculated based on the reduced element properties (Section 3.3) for each cracked element. Assign these new material types to the respective elements in the main SAPIV data section.

ii) Create additional element types with different properties for each cracked element in the ITER8 data, including the revised BX and/or BY values. Assign these new element types to the respective elements in the ITER8 data section.

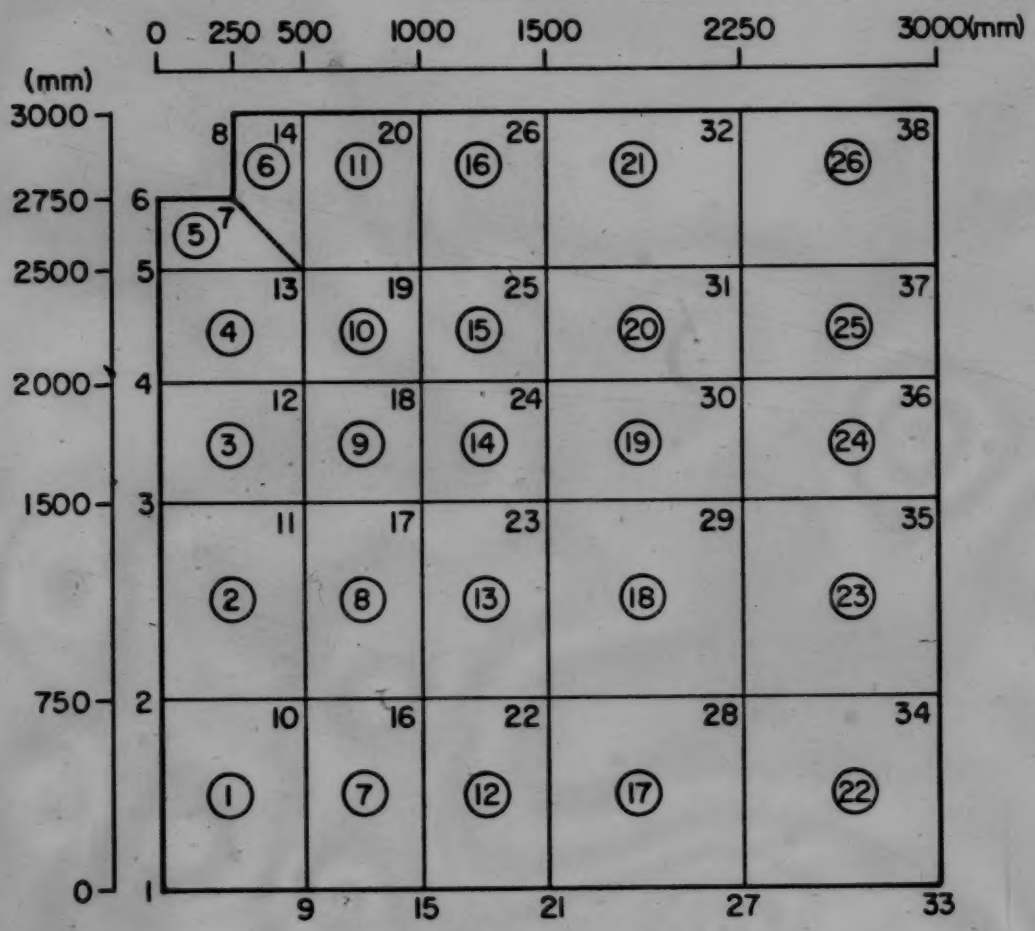

Figure B.1 Finite Element Grid for Slab Series LH100

```
      SUBROUTINE ITER8 (THE,FRE,EC,VC,RME,TSAX,DTSX,TSAY,
     1                  DTSY,BSAX,DBSX,BSAY,DBSY,MPRO,AXP,
     1                  AYP,BX,BY,NUMEL)
C
C     This subroutine calculates reduced element
C     stiffness properties for shell and plate elements
C     to account for cracking.  The moments calculated
C     by a regular SAPIV run are compared to calculated
C     cracking moments and if they exceed those values
C     new stiffness coefficients are evaluated accordingly.
C     The variables which are read, passed, or used in this
C     subroutine include:
C
C           MITER......Maximum number of iterations to be
C                      executed
C           ITER.......Current number of iterations executed
C           THE........Overall depth of element
C           EC.........Initial modulus of elasticity of
C                      concrete element
C           *****CHANGE 07/83 (c.g.)
C           EX.........Actual modulus of elasticity of
C                     concrete element in the X-direction
C           EY.........Actual modulus of elasticity of
C                      concrete element in the Y-direction
C           *****END CHANGE
C           VC.........Initial Poisson's ratio of concrete
C           *****Change 07/83 (c.g.)
C           VX.........Actual Poisson's ratio of concrete
C                      in the X-direction
C           VY.........Actual Poisson's ratio of concrete
C                      in the Y-direction
C           *****End Change
C           RME........Modular ratio of concrete (=Es/Ec)
C           TSAX.......Top steel area in the X-direction
C           TSAY.......Top steel area in the Y-direction
C           BSAX.......Bottom steel area in the X-direction
C           BSAY.......Bottom steel area in the Y-direction
C           DTSX.......Distance to top steel area in the
C                      X-direction
C                      (ie: distance from compression face
C                           to centroid of steel area)
C           DTSY.......Distance to top steel area in the
C                      Y-direction
C           DBSX.......Distance to bottom steel area in the
C                      X-direction
C           DBSY.......Distance to bottom steel area in the
C                      Y-direction
C           NUMEL......Total number of elements in the
C                      structure
C           NEDP.......Number of elements with different
C                      properties (ie: steel areas, depths,
C                                  depth of element, etc.)
C           MPRO(JJ)...An array containing integer values
```

```
C                   identifying the material properties
C                   of each element
C           GMI.....Gross moment of inertia of element
C           FRE.....Modulus of rupture for the concrete
C           CRM.....Cracking moment for element
C           XMOM....Moment calculated in the X-direction
C           YMOM....Moment calculated in the Y-direction
C           SAX.....Steel area in the X-direction
C           SAY.....Steel area in the Y-direction
C           DSX.....Distance to steel centroid in
C                   X-direction
C           DSY.....Distance to steel centroid in
C                   Y-direction
C           VAL.....Calculation variable
C           VAL1....Calculation variable
C           VARX....Calculation variable
C           VARY....Calculation variable
C           CRIX....Cracked moment of inertia in
C                   X-direction
C           CRIY....Cracked moment of inertia in
C                   Y-direction
C           XIE.....Effective moment of inertia in the
C                   X-direction
C           YIE.....Effective moment of inertia in the
C                   Y-direction
C           AX......Alpha factor in X-direction (Iex/Igx)
C           AY......Alpha factor in Y-direction (Iey/Igy)
C           AXP.....Alpha factor in X-direction from
C                   previous iteration
C           AYP.....Alpha factor in Y-direction from
C                   previous iteration
C           MATT....Material type
C           *****Change 07/83 (c.g.)
C           BX......Proportionality constant relating
C                   actual modulus of elasticity and
C                   Poisson's ratio to their respective
C                   initial values in the X-direction
C                   (ie. AX=(1-BX)                    )
C                   (    ECX=(1-BX)*EC   VCX=(1-BX)*VC )
C           BY......As above in the Y-direction
C           *****End Change
C
C
      IMPLICIT REAL*8 (A-H,O-Z)
C
C     Called by:  Main
C
      COMMON /ITERV/ ITERC,MITER,NEDP,NPRT,ITER,JD,IRSP,MOM
C     *****Change 07/83 (c.g.)
      DIMENSION THE(NEDP),FRE(NEDP),EC(NEDP),VC(NEDP),
     1      RME(NEDP),TSAX(NEDP),DTSX(NEDP),
     2      TSAY(NEDP),DTSY(NEDP),BSAX(NEDP),DBSX(NUMEL),
     3      BSAY(NEDP),DBSY(NEDP),MPRO(NUMEL),AXP(NUMEL),
     4      AYP(NUMEL),BX(NEDP),BY(NEDP)
```

```
C     *****End Change
C
C
      ITER = ITER+1
      WRITE (6,2014) ITER
      NPROP=15
      IF (ITER.GT.1) GO TO 90
      REWIND NPROP
C
C     Read and print material properties for reduced
C     stiffness calculations.
C
      WRITE (6,2004)
      WRITE (6,2005)
      DO 10 N=1,NEDP
C     *****Change 07/83 (c.g.)
      READ (5,1000) K,THE(K),FRE(K),EC(K),VC(K),RME(K),
     1BX(K),BY(K),TSAX(K),DTSX(K),TSAY(K),DTSY(K),
     2BSAX(K),DBSX(K),BSAY(K),DBSY(K)
C
      WRITE (6,2006) K,THE(K),FRE(K),EC(K),VC(K),RME(K),
     1               BX(K),BY(K)
C
C     Write element properties on tape for later recall
C
      WRITE (NPROP) K,THE(K),FRE(K),EC(K),VC(K),RME(K),
     1BX(K),BY(K),TSAX(K),DTSX(K),TSAY(K),DTSY(K),
     2BSAX(K),DBSX(K),BSAY(K),DBSY(K)
C     *****End Change
   10 CONTINUE
      WRITE (6,2021)
      WRITE (6,2007)
      DO 17 K=1,NEDP
      WRITE (6,2008) K,TSAX(K),DTSX(K),TSAY(K),DTSY(K),
     1BSAX(K),DBSX(K),BSAY(K),DBSY(K)
   17 CONTINUE
      GO TO 20
   90 CONTINUE
      REWIND NPROP
      DO 21 J=1,NEDP
C     *****Change 07/83 (c.g.)
      READ (NPROP) K,THE(K),FRE(K),EC(K),VC(K),RME(K),
     1BX(K),BY(K),TSAX(K),DTSX(K),TSAY(K),DTSY(K),
     2BSAX(K),DBSX(K),BSAY(K),DBSY(K)
C     *****End Change
   21 CONTINUE
   20 CONTINUE
C
C     Assign material properties to each element
C
      IF (ITER.NE.1) GO TO 80
      JJ=0
   68 READ (5,1001) NEL,MATT
      JJ=JJ+1
```

```
      IF (NEL-JJ) 600,40,30
   30 NELL=NEL-1
      II=JJ
      DO 50 JJ=II,NELL
      MPRO(JJ)=MEM
   50 CONTINUE
      JJ=NEL
      MPRO(JJ)=MATT
      MEM=MATT
      GO TO 60
   40 MPRO(JJ)=MATT
      MEM=MATT
   60 IF (JJ.EQ.NUMEL) GO TO 70
      GO TO 68
   70 CONTINUE
C
C     Write out material identifications
C
      WRITE (6,2021)
      WRITE (6,2010)
      DO 80 I=1,NUMEL
      WRITE (6,2011) I,MPRO(I)
      WRITE (NPROP) MPRO(I)
   80 CONTINUE
C
C
C
C   Check if calculated moments exceed cracking moment and,
C   if they do, evaluate new element stiffness properties.
C
C   Loop to read in alpha factors from previous iteration
C
      IF (ITER.EQ.1) GO TO 301
      REWIND 16
      DO 301 I=1,NUMEL
      READ (16) AXP(I),AYP(I)
  301 CONTINUE
C
C
      IRSP = 13
      REWIND MOM
      REWIND IRSP
      REWIND 16
      WRITE (6,2021)
      WRITE (6,2012)
      DO 100 I=1,NUMEL
      IF (ITER.EQ.1) GO TO 105
      READ (NPROP) MPRO(I)
  105 MPROP = MPRO(I)
      HE = THE(MPROP)
      FR = FRE(MPROP)
      RM = RME(MPROP)
      GMI = (HE**3)/12.0
      CRM = FR*GMI/(HE/2.0)
```

```
      READ (MOM) XMOM,YMOM
      IF (XMOM) 110,120,130
  110 IF (DABS(XMOM).LE.CRM) GO TO 120
      SAX = BSAX(MPROP)
      DSX = DBSX(MPROP)
      XMOM=DABS(XMOM)
      GO TO 140
  130 IF (XMOM.LE.CRM) GO TO 120
      SAX = TSAX(MPROP)
      DSX = DTSX(MPROP)
  140 CONTINUE
      VAL = 2.0*DSX/(RM*SAX)
      DNAX = RM*SAX*(DSQRT(1.0+VAL)-1.0)
      VAL1 = DSX-DNAX
      CRIX = (DNAX**3/3.0)+(RM*SAX*VAL1**2)
      VARX = (CRM/XMOM)**3
      XIE = VARX*GMI+((1.0-VARX)*CRIX)
      IF (XIE.GT.GMI) XIE=GMI
      GO TO 200
  120 CONTINUE
      XIE = GMI
C     OPT1 = 1
C
C
  200 IF (YMOM) 210,220,230
  210 IF (DABS(YMOM).LE.CRM) GO TO 220
      SAY = BSAY(MPROP)
      DSY = DBSY(MPROP)
      YMOM=DABS(YMOM)
      GO TO 240
  230 IF (YMOM.LE.CRM) GO TO 220
      SAY = TSAY(MPROP)
      DSY = DTSY(MPROP)
  240 CONTINUE
      VAL = 2.0*DSY/(RM*SAY)
      DNAY = RM*SAY*(DSQRT(1.0+VAL)-1.0)
      VAL1 = DSY-DNAY
      CRIY = (DNAY**3/3.0)+(RM*SAY*VAL1**2)
      VARY = (CRM/YMOM)**3
      YIE = VARY*GMI+((1.0-VARY)*CRIY)
      IF (YIE.GT.GMI) YIE=GMI
      GO TO 300
  220 CONTINUE
      YIE = GMI
C     OPT2 = 1
  300 CONTINUE
C
C     Calculate new stiffness coefficients for element
C
C     IF (OPT1.EQ.1.AND.OPT2.EQ.1) GO TO 310
      AX = XIE/GMI
      AY = YIE/GMI
      IF (ITER.EQ.1) GO TO 303
      IF (AX.GT.AXP(I)) AX=AXP(I)
```

```
      IF (AY.GT.AYP(I)) AY=AYP(I)
      GO TO 304
C     *****CHANGE 08/83 (c.g.)
  303 CONTINUE
      IF(AX.GT.(1.-BX(MPROP))) AX=1.-BX(MPROP)
      IF(AY.GT.(1.-BY(MPROP))) AY=1.-BY(MPROP)
C     *****END CHANGE
  304 CONTINUE
      WRITE(16) AX,AY
C     *****Change 07/83 (c.g.)
      EX = AX*EC(MPROP)
      VX = AX*VC(MPROP)
      EY = AY*EC(MPROP)
      VY = AY*VC(MPROP)
C     *****End Change
      CXX = EX/(1.0-VX*VY)
      CXY = VX*EY/(1.0-VX*VY)
      CXS = 0.0
      CYY = EY/(1.0-VX*VY)
      CYS = 0.0
C     *****Change 07/83 (c.g.)
      GXY = (EC(MPROP))/(2.*(1.+VC(MPROP)))
C     *****End Change
C     IPATH = 0
      WRITE (IRSP) CXX,CXY,CXS,CYY,CYS,GXY
      WRITE (6,2013) I,AX,AY,CXX,CXY,CXS,CYY,CYS,GXY
      GO TO 320
C 310 IPATH = 1
C     WRITE (IRSP) IPATH
  320 CONTINUE
  100 CONTINUE
      RETURN
  600 WRITE (6,2002) NEL
      STOP
 2004 FORMAT (//2X,32HELEMENT PROPERTIES FOR REDUCED
     1,21HSTIFFNESS CALCULATIONS,//)
C     *****Change 07/83 (c.g.)
 2005 FORMAT ('MATERIAL',5X,'OVERALL',4X,'MODULUS',4X,
     1     'MODULUS',4X,'POISSON',4X,'MODULAR',8X,'BX',10X,
     2     'BY',/,2X,'TYPE',7X,'ELEMENT',6X,'OF',8X,'OF',8X,
     3     'RATIO',6X,'RATIO',1X,/,11X,'THICKNESS',4X,
     4     'RUPTURE',5X,'ELAST.',/)
 2006 FORMAT (I5,5X,F8.2,4X,F8.3,3X,E10.4,2(2X,F8.3),
     1     2(6X,F7.3))
C     *****End Change
 2007 FORMAT (//28X,'STEEL',15X,'PROPERTIES',//'MATERIAL',
     1     5X,'AREA',5X,'DEPTH',3(6X,'AREA',5X,'DEPTH'),/2X,
     2     'TYPE',6X,'X-DIR',5X,'X-DIR',2(5X,'Y-DIR'),
     3     2(5X,'X-DIR'),2(5X,'Y-DIR'),/12X,'(TOP)',
     4     3(5X,'(TOP)'),4(5X,'(BOT)'),/)
 2008 FORMAT (2X,I5,8F10.4)
 2010 FORMAT ('ELEMENT MATERIAL IDENTIFICATION CHECK',//
     1     3X,'ELEMENT',5X,'MATERIAL',/4X,'NUMBER',6X,
     2     'NUMBER')
```

```
 2011 FORMAT (5X,I5,7X,I5)
 2012 FORMAT (10X,'REDUCED STIFFNESS COEFFICIENTS',//
     1    'ELEM',4X,'AX',5X,'AY',8X,'CXX',8X,'CXY',7X,
     2    'CXS',9X,'CYY',9X,'CYS',9X,'GXY',//)
 2013 FORMAT (I4,2F7.3,6(3X,E9.3))
 2014 FORMAT ('ITERATION NUMBER',I6)
 2021 FORMAT (/)
 1008 FORMAT (2F10.0)
C     *****Change 07/83 (c.g.)
 1000 FORMAT (I4,7F10.0/8F10.0)
C     *****End Change
 1001 FORMAT (2I5)
 2002 FORMAT('ERROR IN ORDERING OF ELEMENTS',I4)
      END
```

APPENDIX C

PROGRAM LISTING AND INPUT DATA
FOR SUPERPOSITION OF CREEP CURVES
AND CALCULATION OF TOTAL LONG-TIME DEFLECTION

The form of the input data for the superposition program is as follows:

```
N,
NTIME(1),UCC(1), ECI(1),CF(1),EDEF(1),XKR(1),
.
.
.
NTIME(N),UCC(N),ECI(N),CF(N),EDEF(N),XKR(N),
XKWC,SPANC,XKWM,SPANM,
THE,RRM,RRC,USS,SF,NCT,CR,NYR,
NN,
NSDAY(1),
.
.
.
NSDAY(NN),
```

See the program listing for the definition of variables.

For the slab considered in Appendix B (LH100), the following additional data are required:

i) creep coefficient:
   - ultimate value $C_u = 2.35$
   - total of correction factors (as given by ACI Committee 209) γ_c = (see below)

ii) shrinkage strain:
   - ultimate value $\epsilon_{shu} = 780 \times 10^{-6}$ mm/mm
   - total of correction factors (as given by ACI Committee 209) $\gamma_{sh} = 0.98$
   - seven-day moist-curing period

iii) assumed degree of creep recovery equal to one-half of the full value predicted by superposition

iv) deflections are required for three years after

casting and specifically at 56, 128, and 510 days after casting

Additional data pertaining to each stage of the construction load sequence is as follows:

DAY	Δ_t (mm)	C_u	γ_c	E_c (MPa)	k_r
5	0.943	2.35	1.02	21558	0.85
7	0.833	2.35	0.99	23226	0.85
12	0.754	2.35	0.92	23456	0.85
14	0.888	2.35	0.91	25984	0.85
19	0.996	2.35	0.87	26890	0.85
21	2.138	2.35	0.86	27148	0.85
26	-3.625	2.35	0.84	27638	0.85
60	1.075	2.35	0.76	27791	0.85

The input data required to evaluate the long-time deflection for this slab is:

```
 8,
 5,2.35,21558.,1.02,0.943,0.85,
 7,2.35,23226.,0.99,0.833,0.85,
12,2.35,23456.,0.92,0.754,0.85,
14,2.35,25984.,0.91,0.888,0.85,
19,2.35,26890.,0.87,0.996,0.85,
21,2.35,27148.,0.86,2.138,0.85,
26,2.35,27638.,0.84,-3.625,0.85,
60,2.35,27791.,0.76,1.075,0.85,
0.0625,5500.,0.0625,5500.,
165.,0.220,0.297,780.E-06,0.98,7,0.5,3,
3,
56,
128,
510,
```

NOTES: 1. Creep curve data must be input according to the construction load sequence.

2. For this interior panel, the column and middle

strips were assumed continuous at both ends resulting in XKWC = XKWM = 0.0625. For one end continuous use XKWC or XKWM = 0.0859.

3. Deflections are calculated according to the following time steps:

   i) between successive load stages

      time step = 1 day

   ii) after last load stage

      time step = 1 day for 10 days, then

      time step = 20 days until 1 year, then

      time step = yearly (every 360 days).

4. Deflections may be evaluated at up to ten additional specified days. If the additional deflection analyses are not required, input NN=0 and do not input any values for NSDAY.

```
C THIS PROGRAM CALCULATES INDIVIDUAL CREEP COMPLIANCE
C CURVES AND CORRESPONDING DEFLECTION CURVES. IT ALSO
C CALCULATES SHRINKAGE WARPING STRAINS AND DEFLECTIONS
C FOR THE GIVEN SLAB. IT THEN SUPERIMPOSES THESE CREEP
C AND SHRINKAGE DEFLECTIONS WITH THE IMMEDIATE ELASTIC
C DEFLECTIONS (FROM SAPIV) TO GIVE THE TOTAL LONG-TIME
C DEFLECTIONS DUE TO A PARTICULAR CONSTRUCTION LOADING
C SEQUENCE.
C
C
C ***************************************************************
C  DEFINITION OF VARIABLES
C
C NTIME  - TIME WHEN CREEP FCN. STARTS SINCE SLAB CAST
C          (DAYS)
C UCC    - ULTIMATE CREEP COEFFICIENT
C ECI    - MODULUS OF ELASTICITY
C CF     - ULTIMATE CREEP COEFFICIENT CORRECTION FACTOR
C EDEF   - ELASTIC DEFLECTION INCREMENT CORRESPONDING TO A
C          GIVEN CREEP FUNCTION
C XKR    - 0.85 FACTOR
C CDEF   - CREEP DEFLECTION
C TCOMP  - TOTAL COMPLIANCE (ELASTIC + CREEP)
C CT     - CREEP COEFFICIENT
C NDAY   - TIME SCALES FOR INDIVIDUAL CREEP FUNCTIONS
C DEF    - IMMEDIATE PLUS CREEP DEFLECTIONS FOR INDIVIDUAL
C          CREEP FUNCTIONS
C NAT    - ACTUAL TIMES SINCE SLAB CAST (DAYS)
C ITER   - FLAG
C ITER1  - FLAG
C ITER2  - FLAG
C TDEF   - IMMEDIATE PLUS CREEP DEFLS. CONSIDERING ALL
C          CREEP FUNCTIONS
C XDEF   - DUMMY DEFLECTION
C NFT    - TIME SCALE FOR INDIVIDUAL CREEP FCN. CALCULATIONS
C COMP   - CREEP COMPLIANCE
C NCOUNT - COUNTER
C INC    - COUNTER
C SDEF   - SHRINKAGE DEFLECTION
C TOTDEF - TOTAL IMMEDIATE + CREEP + SHRINKAGE DEFLECTIONS
C NS     - NUMBER OF TIME STEPS
C J      - CREEP FUNCTION NUMBER
C N      - NUMBER OF CREEP FUNCTIONS
C NRT    - ACTUAL TIME COUNTER (DAYS)
C NVAL   - COUNTER
C XKWC   - DEFL. COEFF. DEPENDING ON END CONDITIONS - LONG
C          COLUMN STRIP
C XKWM   - DEFL. COEFF. DEPENDING ON END CONDITIONS - MIDDLE
C          STRIP
C SPANC  - LONG COL. STRIP SPAN
C SPANM  - MIDDLE STRIP SPAN
C THE    - SLAB THICKNESS
C RRM    - REINFORCEMENT PERCENTAGE IN MIDDLE STRIP
```

```
C RRC     - REINFORCEMENT PERCENTAGE IN COLUMN STRIP
C USS     - ULTIMATE SHRINKAGE STRAIN
C SF      - ULTIMATE SHRINKAGE STRAIN CORRECTION FACTOR
C NCT     - CURING TIME (DAYS)
C SS      - SHRINKAGE STRAIN
C STIME   - TIME SINCE CURING PERIOD ENDED (DAYS)
C CR      - DEGREE OF CREEP RECOVERY (0 < CR < 1)
C NYR     - NUMBER OF YEARS DEFLECTIONS REQUIRED
C NN      - NUMBER OF SPECIFIED DAYS FOR WHICH DEFLECTIONS
C           ARE TO BE EVALUATED AT
C KK      - COUNTER
C NSDAY   - SPECIFIED DAYS FOR WHICH DEFLECTIONS ARE TO BE
C           EVALUATED AT
C NSPEC   - SAME AS NSDAY
C
C ***************************************************************
C
C
      COMMON /A/ NTIME(15),UCC(15),ECI(15),CF(15),EDEF(15),
     1           XKR(15),CDEF(15,99),TCOMP(15,99),CT(15,99),
     1           NDAY(15),DEF(15,99),NAT(99),ITER(15),
     1           TDEF(99),XDEF(99),NFT(15),COMP(15,99),
     1           NCOUNT(15),SDEF(99)
      COMMON /B/ NS,J,N,NRT,NVAL
      COMMON /C/ XKWC,XKWM,SPANC,SPANM,THE,RRM,RRC,USS,SF,
     1           NCT,CR,NYR
      COMMON /D/ NN,KK,NSPEC,NSDAY(10),ITER1,INC
      DIMENSION TOTDEF(99)
      READ (5,100) N
      DO 7 L=1,N
        READ (5,110) NTIME(L),UCC(L),ECI(L),CF(L),EDEF(L)
     1               XKR(L)
    7 CONTINUE
      READ (5,130) XKWC,SPANC,XKWM,SPANM
      READ (5,120) THE,RRM,RRC,USS,SF,NCT,CR,NYR
      READ (5,100) NN
      IF(NN.NE.0) GO TO 50
      ITER1=0
      GO TO 60
   50 CONTINUE
      DO 1 II=1,NN
        READ (5,140) NSDAY(II)
    1 CONTINUE
      KK=1
      INC=0
      NSPEC=NSDAY(KK)
   60 CONTINUE
      NVAL=0
      WRITE (6,200)
C***
C  LOOP TO CONSIDER EACH CREEP FUNCTION
C***
      DO 77 J=1,N
C***
```

```
C  CALCULATE REQUIRED NUMBER OF TIME STEPS:
C        1) BETWEEN SUCCESSIVE CREEP CURVES
C                TIME STEP = 1 DAY
C        2) AFTER LAST CREEP CURVE
C                TIME STEP = 1 DAY FOR 10 DAYS, THEN
C                TIME STEP = 20 DAYS UNTIL 1 YEAR, THEN
C                TIME STEP = YEARLY
C***
      NRT=NTIME(J)
      IF(J.EQ.N.AND.J.EQ.1) GO TO 10
      IF(J.EQ.N) GO TO 10
      IF(J.LE.N-1) NS=NTIME(J+1)-NTIME(J)
      GO TO 70
   10 NS= 10+((360-NTIME(J))/20+1+NYR)
   70 CONTINUE
C***
C  CALL SUPERPOSITION SUBROUTINE
C***
      CALL ADDCRP
   77 CONTINUE
      DO 777 L=1,N
        WRITE (6,210) NTIME(L)
        M=NCOUNT(L)
        WRITE (6,220) ((NDAY(L,K),TCOMP(L,K),DEF(L,K)),
     1                  K=M,NVAL)
  777 CONTINUE
      DO 7777 LL=1,NVAL
        TOTDEF(LL)=TDEF(LL)+SDEF(LL)
 7777 CONTINUE
      WRITE (6,230)
      WRITE (6,240) ((NAT(L),TDEF(L),SDEF(L),TOTDEF(L)),
     1                L=1,NVAL)
  100 FORMAT(I2)
  110 FORMAT(I5,5F10.0)
  120 FORMAT(5F9.0,I3,F4.0,I2)
  130 FORMAT(4F9.0)
  140 FORMAT(I5)
  200 FORMAT('1',T8,'INDIVIDUAL COMPLIANCE AND DEFLECTION'
     1'CURVES',/,T8,43('-'),//)
  210 FORMAT(' ',//,T15,'**CONCRETE LOADED AT ',I3,' DAYS**'
     1,//,T10,'DAY',T20,'COMPLIANCE',T40,'DEFLECTION',/)
  220 FORMAT(' ',T10,I4,T19,E12.5,T40,F7.3)
  230 FORMAT(' ',///,T20,'SUPERIMPOSED DEFLECTIONS',
     1/,T20,24('-'),//,T10,'DAY',T20,'IMMEDIATE',
     1T35,'SHRINKAGE',T50,'TOTAL',/,T20,'PLUS CREEP',/)
  240 FORMAT(' ',T10,I4,T20,F7.3,T35,F7.3,T50,F7.3)
      STOP
      END
C
C
C
      SUBROUTINE ADDCRP
      COMMON /A/ NTIME(15),UCC(15),ECI(15),CF(15),EDEF(15),
     1           XKR(15),CDEF(15,99),TCOMP(15,99),CT(15,99),
```

```
     1            NDAY(15),DEF(15,99),NAT(99),ITER(15),
     1            TDEF(99),XDEF(99),NFT(15),COMP(15,99),
     1            NCOUNT(15),SDEF(99)
      COMMON /B/ NS,J,N,NRT,NVAL
      COMMON /C/ XKWC,XKWM,SPANC,SPANM,THE,RRM,RRC,USS,SF,
     1           NCT,CR,NYR
      COMMON /D/ NN,KK,NSPEC,NSDAY(10),ITER1,INC
      ITER(J)=1
      ITER2=0
C***
C  TIME STEP LOOP
C***
      DO 8 K=1,NS
        NVAL=NVAL+1
C***
C  LOOP TO CONSIDER EACH CREEP FUNCTION
C  AT EACH TIME STEP
C***
        DO 88 JJ=1,J
          IF(ITER(JJ).NE.1) GO TO 5
          NCOUNT(J)=NVAL
C***
C  EVALUATE TOTAL ELASTIC + CREEP COMPLIANCES AND
C  DEFLECTIONS AT START OF A CREEP CURVE (IE. AT FIRST
C  TIME STEP OF CURVE, DEFLECTIONS ARE INITIALLY ZERO
C  THEN INCREASE TO THE ELASTIC VALUE)
C***
          COMP(JJ,NVAL)=0.
          TCOMP(JJ,NVAL)=0.
          CDEF(JJ,NVAL)=0.
          NDAY(JJ,NVAL)=NRT
          DEF(JJ,NVAL)=0.
          IF(J.EQ.1) TDEF(NVAL)=0.
          NAT(NVAL)=NRT
          IF(JJ.EQ.1) SDEF(NVAL)=0.
          NVAL=NVAL+1
          COMP(JJ,NVAL)=1./ECI(JJ)
          TCOMP(JJ,NVAL)=COMP(JJ,NVAL)
          CDEF(JJ,NVAL)=0.
          NDAY(JJ,NVAL)=NRT
          DEF(JJ,NVAL)=EDEF(JJ)
          TDEF(NVAL)=TDEF(NVAL-1)+EDEF(JJ)
          NAT(NVAL)=NRT
          XDEF(NVAL)=TDEF(NVAL)
          IF(JJ.NE.1) GO TO 6
          STIME=NRT-NCT
          IF(STIME.LE.0.) GO TO 9
          GO TO 6
     9    SDEF(NVAL)=0.
     6    CONTINUE
          IF(J.EQ.1) GO TO 45
          MM=J-1
          DO 888 MN=1,MM
            NDAY(MN,NVAL)=NDAY(MN,NVAL-1)
```

```
            TCOMP(MN,NVAL)=TCOMP(MN,NVAL-1)
            DEF(MN,NVAL)=DEF(MN,NVAL-1)
  888       CONTINUE
            SDEF(NVAL)=SDEF(NVAL-1)
            GO TO 55
    5       CONTINUE
C***
C  CALCULATE TOTAL ELASTIC + CREEP COMPLIANCE AND
C  DEFLECTION AT REMAINING TIME STEPS
C***
            NFT(JJ)=NRT-NTIME(JJ)
            COMP(JJ,NVAL)=((NFT(JJ)**0.6)/(10.+NFT(JJ)**0.6))
     1                    *UCC(JJ)*CF(JJ)/ECI(JJ)
            IF(EDEF(JJ).LT.0.) COMP(JJ,NVAL)=CR*COMP(JJ,NVAL)
            TCOMP(JJ,NVAL)=(1./ECI(JJ))+COMP(JJ,NVAL)
            CT(JJ,NVAL)=COMP(JJ,NVAL)*ECI(JJ)
            CDEF(JJ,NVAL)=EDEF(JJ)*CT(JJ,NVAL)*XKR(JJ)
            DEF(JJ,NVAL)=EDEF(JJ)+CDEF(JJ,NVAL)
            NDAY(JJ,NVAL)=NRT
            TDEF(NVAL)=XDEF(NVAL)+DEF(JJ,NVAL)
            XDEF(NVAL)=TDEF(NVAL)
            NAT(NVAL)=NRT
   45       CONTINUE
C***
C  CALCULATE SHRINKAGE DEFLECTIONS
C***
            STIME=NRT-NCT
            IF(STIME.LE.0.) GO TO 99
            SS=0.7*USS*SF/THE*STIME/(35.+STIME)
            SSC=SS*(RRC**(1./3.))
            SSM=SS*(RRM**(1./3.))
            SDEFC=XKWC*SSC*(SPANC**2.)
            SDEFM=XKWM*SSM*(SPANM**2.)
            SDEF(NVAL)=SDEFC+SDEFM
            GO TO 55
   99       SDEF(NVAL)=0.
   55       CONTINUE
   88    CONTINUE
         IF(ITER2.NE.1) GO TO 56
         NRT=NINTER
         ITER2=0
         GO TO 8
   56    CONTINUE
         ITER(J)=2
         NNRT=NRT
C***
C  INCREMENT TIME STEP
C***
         IF(J.EQ.N.AND.J.EQ.1) GO TO 565
         IF(J.EQ.N) GO TO 565
         IF(J.LE.N-1) GO TO 555
  565    IF(NNRT.LT.(NTIME(J)+10)) GO TO 555
         GO TO 545
  555    NRT=NRT+1
```

```
      GO TO 525
  545 IF(NNRT.GE.360) GO TO 535
      NRT=((NRT+20)/20)*20
      GO TO 525
  535 NRT=NRT+360
C***
C  COMMANDS TO EVALUATE DEFLECTIONS AT SPECIFIED DAYS
C***
  525 CONTINUE
      IF(ITER1.EQ.0) GO TO 8
      IF(INC.EQ.NN) GO TO 8
      IF(NRT.EQ.NSPEC) GO TO 515
      IF(NRT.GT.NSPEC) GO TO 505
      GO TO 8
  515 KK=KK+1
      NSPEC=NSDAY(KK)
      INC=INC+1
      GO TO 8
  505 NS=NS+1
      ITER2=1
      NINTER=NRT
      NRT=NSPEC
      KK=KK+1
      NSPEC=NSDAY(KK)
      INC=INC+1
    8 CONTINUE
      RETURN
      END
```

APPENDIX D

ANALYSIS OF HEIMAN'S FLAT PLATE

The plan of the structure is given in Figure 4.1. Basic details of the structure are as follows:

i) interior bay size = 24 ft 9 in by 23 ft 9 in

ii) interior column size = 30 in by 9 in

iii) slab thickness = 9.5 in

iv) design properties - f'_c = 3000 psi

f_y = 60000 psi

v) measured properties - $E_c(28) = 3.2 \times 10^6$ psi

$C(t,t_o)$ = 1.3 at two years

$\epsilon_{sh} = 620 \times 10^{-6}$ in/in at one year

vi) design service loads - slab self weight = 115 psf

live load = 60 psf

v) average measured relative humidity = 65 percent

Reinforcement areas calculated from Reference (29) for an interior panel are given in Figure D.1. A clear cover of 0.75 in was assumed for all bars. The grid used for the finite element analyses of an interior quarter panel is shown in Figure D.2. Boundary conditions assumed were those given in Figure 3.8.

The construction load sequence of Figure 4.3 was used. Corresponding material properties calculated using the ACI Committee 209 expressions at each load stage are given in Table D.1.

For the calculation of long-time deflections, the following values for ultimate creep coefficient and shrinkage strain were derived according to ACI Committee

209:

i) ultimate creep coefficient

$$C_u = 2.35\gamma_c$$

where: γ_c = total of correction factors

- corrections were made for age at loading ($\gamma_{\ell a}$), thickness (γ_h), and relative humidity (γ_λ), resulting in:

DAY	$\gamma_{\ell a}$	γ_h	γ_λ	γ_c	C_u
7	1.0	0.92	0.83	0.76	1.79
14	0.92	0.92	0.83	0.69	1.62
21	0.87	0.92	0.83	0.66	1.56

ii) ultimate shrinkage strain

- to obtain the measured shrinkage strain of 620×10^{-6} in/in at one year, an ultimate value of 680×10^{-6} in/in was used in the ACI Committee 209 expression:

$$\varepsilon_{sh}(t) = \frac{t - t_m}{35 + (t - t_m)} \varepsilon_{shu}$$

$$620 \times 10^{-6} = \frac{365}{35 + 365} \varepsilon_{shu}$$

$\therefore \varepsilon_{shu} = 680 \times 10^{-6}$ in/in

and γ_{sh} = 1.0 (total of correction factors)

Table D.1 Heiman's Flat Plate - Construction Load Stage Data

	TIME SINCE CASTING (DAYS)		
	7	14	21
LOAD (psi)	0.590	1.181	0.799
E_c (psi)	2785152	3115853	3255333
MODULAR RATIO	10.41	9.31	8.91
$f_r = 4\sqrt{f'_c}$ (psi)	195.0	218.2	228.0
$f_r = 6\sqrt{f'_c}$ (psi)	292.5	327.3	342.0
$f_r = 7.5\sqrt{f'_c}$ (psi)	365.6	409.1	427.5
C_u	1.79	1.62	1.56
ϵ_{shu} (x 10^{-6} in/in)	680	680	680

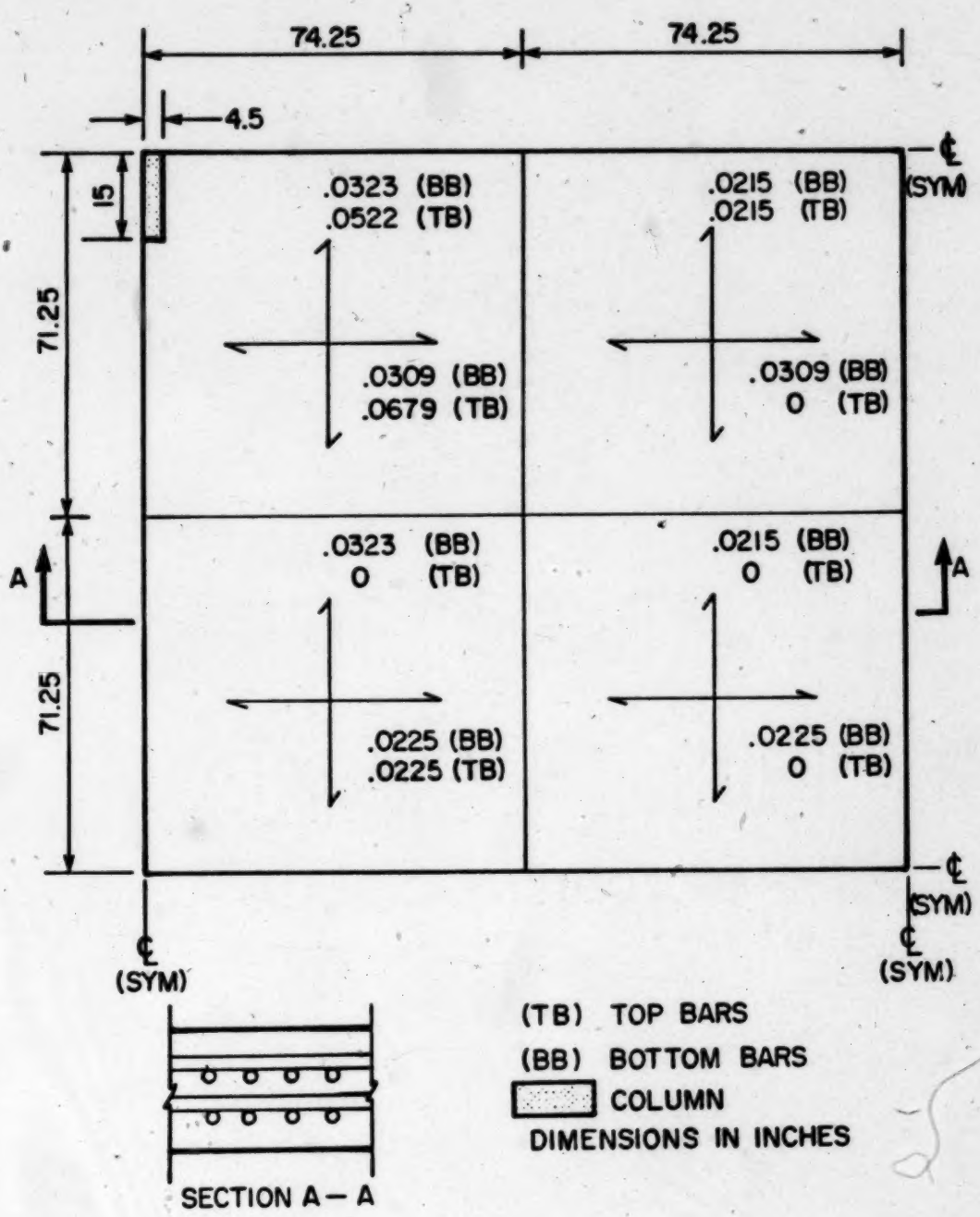

Figure D.1 Heiman's Flat Plate - Reinforcement Areas (in^2/in)

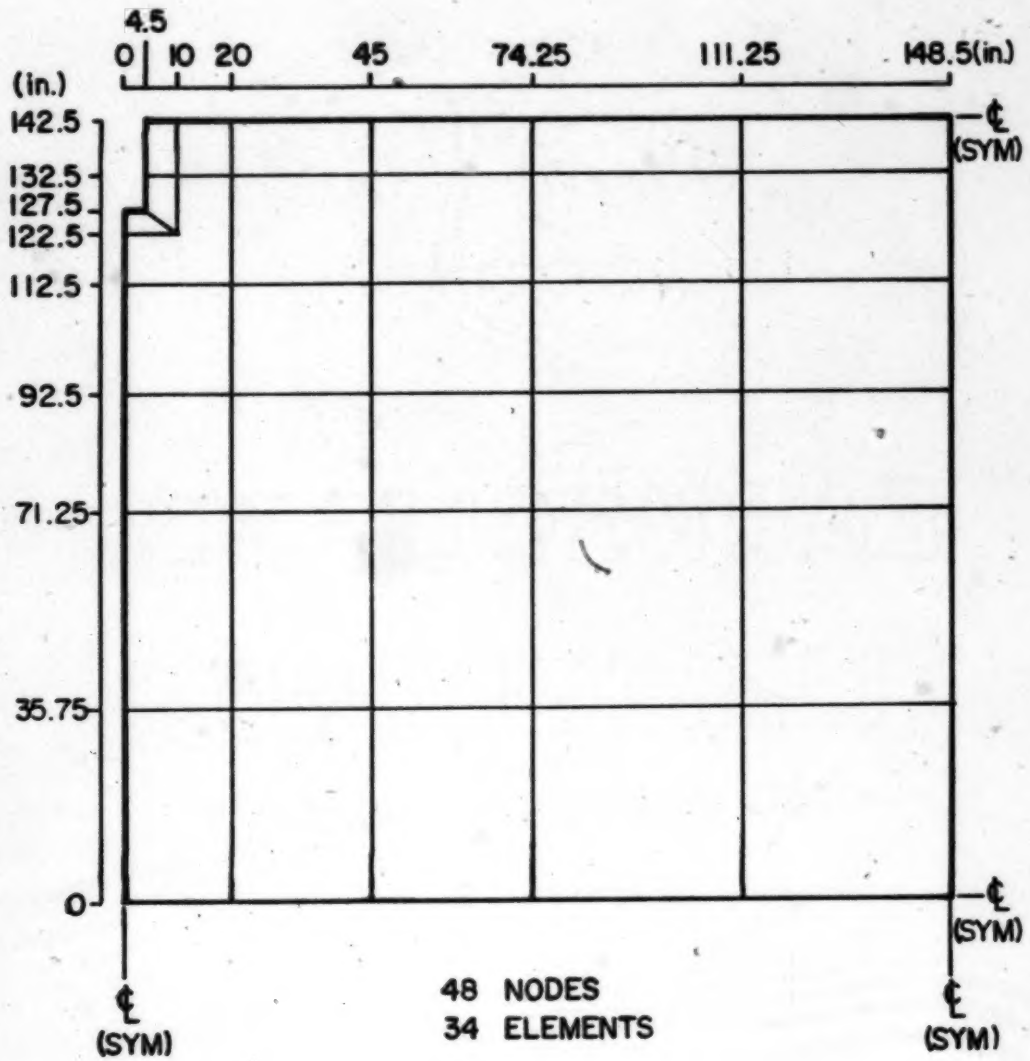

Figure D.2 Heiman's Flat Plate - Finite Element Grid

APPENDIX E

ANALYSIS OF SBAROUNIS' FLAT PLATE

Basic details of the slab system are as follows:

i) centre-to-centre span = 22 ft

ii) clear span = 20.9 ft

iii) slab thickness = 7.25 in

iv) concrete, ~~li~~ghtweight - w_c = 110 lb/ft^3

f'_c = 4000 psi

v) reinforcement - f_y = 60000 psi

at columns, A_s = 5 in^2/strip

all others, A'_s = 1.8 in^2/strip

vi) loads - slab self weight = 67 psf

superimposed dead load at 60 days = 20 psf

construction live load = 50 psf

forms = 15 psf; reshores = 5 psf

maximum construction load, w_{max} = 157 psf

vii) effective supporting assembly = 3 levels of shores

viii) construction schedule - 2 floors/week (taken as 1 floor every 4 days with 2 days between removal of of lowest shore level and casting of top floor)

Calculated reinforcement areas are shown in Figure E.1, assuming a clear cover of 0.75 in and #4 bars (0.5 in diameter). The finite element grid is given in Figure E.2 for an interior quarter panel. As with Heiman's Flat Plate, the assumed boundary conditions are those given in Figure 3.8.

The assumed construction load history is shown in Figure 4.6. This load sequence is based on that generated by the theory of Grundy and Kabaila (21) using three shored levels. The reported maximum construction load of 157 psf was matched with the maximum converged dead load ratio predicted by Grundy and Kabaila (2.00), and the remaining intermediate load levels scaled accordingly. Corresponding material properties calculated using the ACI Committee 209 expressions are given in Table E.1.

For the calculation of long-time deflection, the following values for ultimate shrinkage strain were derived according to ACI Committee 209:

i) ultimate creep coefficient

$$C_u = 2.35\gamma_c$$

where: γ_c = total of correction factors

- corrections were made for age at loading (γ_{la}) and member thickness (γ_h) resulting in:

DAY	γ_{la}	γ_h	γ_c	C_u
2	1.15	0.97	1.12	2.63
4	1.06	0.97	1.02	2.40
6	1.01	0.97	0.98	2.30
8	0.98	0.97	0.95	2.23
10	0.95	0.97	0.92	2.16
12	0.93	0.97	0.90	2.12
14	0.92	0.97	0.88	2.07
28	0.84	0.97	0.81	1.90
60	0.78	0.97	0.75	1.76

ii) ultimate shrinkage strain

- the value 800 x 10^{-6} in/in reported by Sbarounis was used.

- corrections were made for a 7-day moist curing period (γ_{cp}) and member thickness (γ_h) resulting in:

$$\epsilon_{shu} = 800 \times 10^{-6} \gamma_{sh}$$

where: γ_{sh} = total of correction factors

$$= \gamma_{cp}\gamma_h$$

$$= (1.0)(0.95)$$

$$= 0.95$$

$$\therefore \epsilon_{shu} = 800 \times 10^{-6}(0.95)$$

$$= 760 \times 10^{-6} \text{ in/in}$$

Table E.1 Sbarounis' Flat Plate - Construction Load Stage Data

	TIME SINCE CASTING (DAYS)								
	2	4	6	8	10	12	14	28	60
LOAD (psi)	0.15	0.34	0.52	0.70	0.91	1.09	0.47	-	0.60
E_c (psi)	1426299	1770301	1955185	2072364	2153664	2213499	2259428	2407870	2514938
MODULAR RATIO	20.33	16.38	14.83	13.99	13.47	13.10	12.84	12.04	11.53
$f_r = 2\sqrt{f'_c}$ (psi)	68.1	84.5	93.4	99.0	102.8	105.7	107.9	115.4	120.1
$f_r = 4\sqrt{f'_c}$	136.2	169.1	186.7	197.9	205.7	211.4	215.8	230.8	240.2
$f_r = 6\sqrt{f'_c}$	204.3	253.7	280.1	296.5	308.5	317.1	323.7	346.2	360.2
$f_r = 7.5\sqrt{f'_c}$	255.4	317.0	350.1	371.1	385.6	396.4	404.6	432.7	450.3
C_u	2.63	2.40	2.30	2.23	2.16	2.12	2.07	1.90	1.76
ϵ_{shu} ($\times 10^{-6}$ in/in)	760	760	760	760	760	760	760	760	760

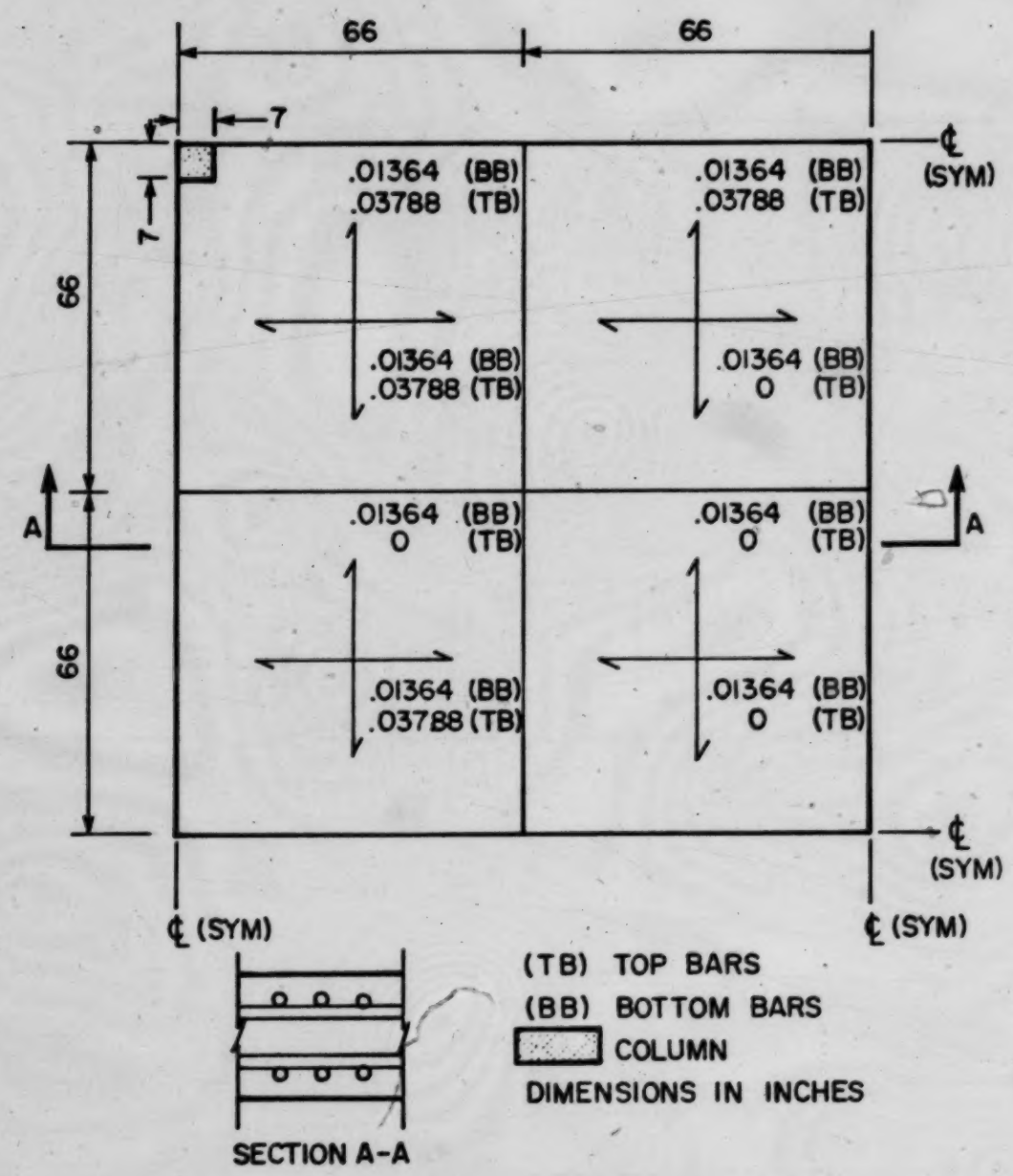

Figure E.1 Sbarounis' Flat Plate - Reinforcement Areas (in^2/in)

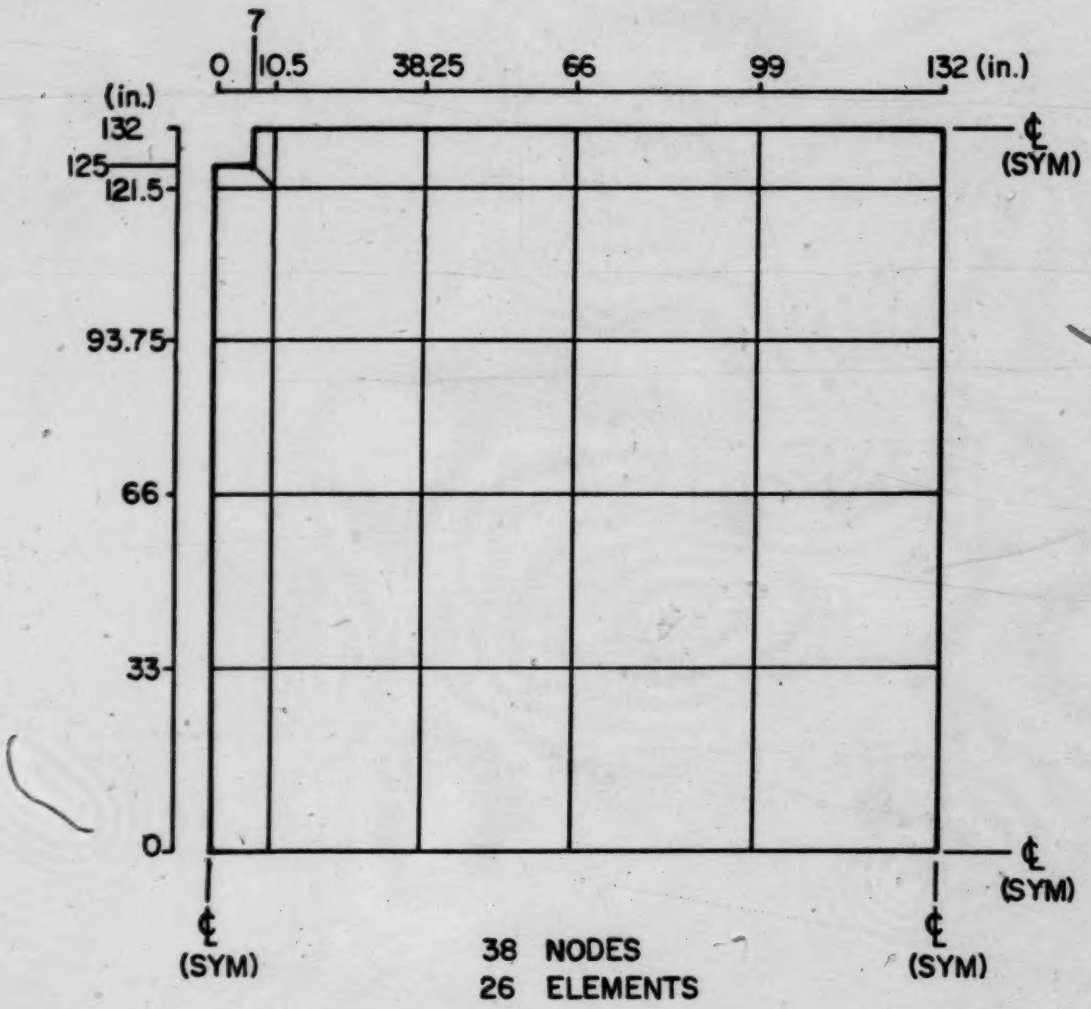

Figure E.2 Sbarounis' Flat Plate - Finite Element Grid

APPENDIX F

ANALYSIS OF TAYLOR'S FLAT PLATE

The layout of the structure and panel analyzed is shown in Figure 4.11. Basic details of the structure are as follows:

i) interior bay size = 20 ft 10 in by 16 ft 8 in

ii) interior column size = 14 in by 14 in

iii) slab thickness = 8 in

iv) concrete, normal weight - w_c = 150 lb/ft^3
f'_c = 3000 psi

v) reinforcement - f_y = 50000 psi

vi) design service loads - slab self weight = 100 psf
finishes = 10 psf
live load = 75 psf

vii) measured properties - E_c = 3.55 x 10^6 psi at 13 days
f_r = 420 psi at 35 days

viii) average measured relative humidity = 50 percent

ix) construction procedures - slab loaded by self weight at 14 days
- building paper applied to slab 1 day after casting and removed 28 days later

Reinforcement areas calculated from Reference (42) for the panel analyzed are given in Figure F.1. A clear cover of 0.75 in was assumed for all bars. The finite element grid used is shown in Figure F.2. Since this slab system could not be modelled as a symmetrical interior panel, the exterior panel and columns where included in the analysis. Edge beams and regions at the columns where modelled using

thickened plate bending elements. Beam elements were used to account for the columns. Boundary conditions for this panel consisted of:

i) zero vertical displacement at the beam-plate element junctions

ii) zero rotations in a direction perpendicular to lines of symmetry

The construction load sequence consisted of a single sustained load of 104 psf applied at 14 days after casting. The following data were used:

i) load = 0.722 psi

ii) E_c = 3550000 psi

iii) modular ratio = 8.17

iv) $f_r = 4\sqrt{f'_c}$ = 218.2 psi

$= 2\sqrt{f'_c}$ = 109.1 psi

For the calculation of long-time deflection, the following values for ultimate creep coefficient and ultimate shrinkage strain were derived according to ACI Committee 209:

i) ultimate creep coefficient

$C_u = 2.35\gamma_c$

where: γ_c = total of correction factors

- corrections were made for age at loading (γ_{la}), member thickness (γ_h), and relative humidity (γ_λ) resulting in:

DAY	γ_{la}	γ_h	γ_λ	γ_c	C_u
14	0.92	0.96	0.94	0.83	1.95

ii) ultimate shrinkage strain

- to obtain a shrinkage strain of 800×10^{-6} in/in at 864 days after casting as assumed by Taylor, an ultimate value of 833×10^{-6} in/in was used in the ACI Committee 209 expression
- a 14-day moist-curing period was assumed corresponding to the time of form removal:

$$\varepsilon_{sh}(t) = \frac{(t - t_m)}{35 + (t - t_m)} \varepsilon_{shu}$$

$$800 \times 10^{-6} = \frac{850}{35 + 850} \varepsilon_{shu}$$

$\therefore \varepsilon_{shu} = 833 \times 10^{-6}$ in/in

and $\gamma_{sh} = 1.0$ (total of correction factors)

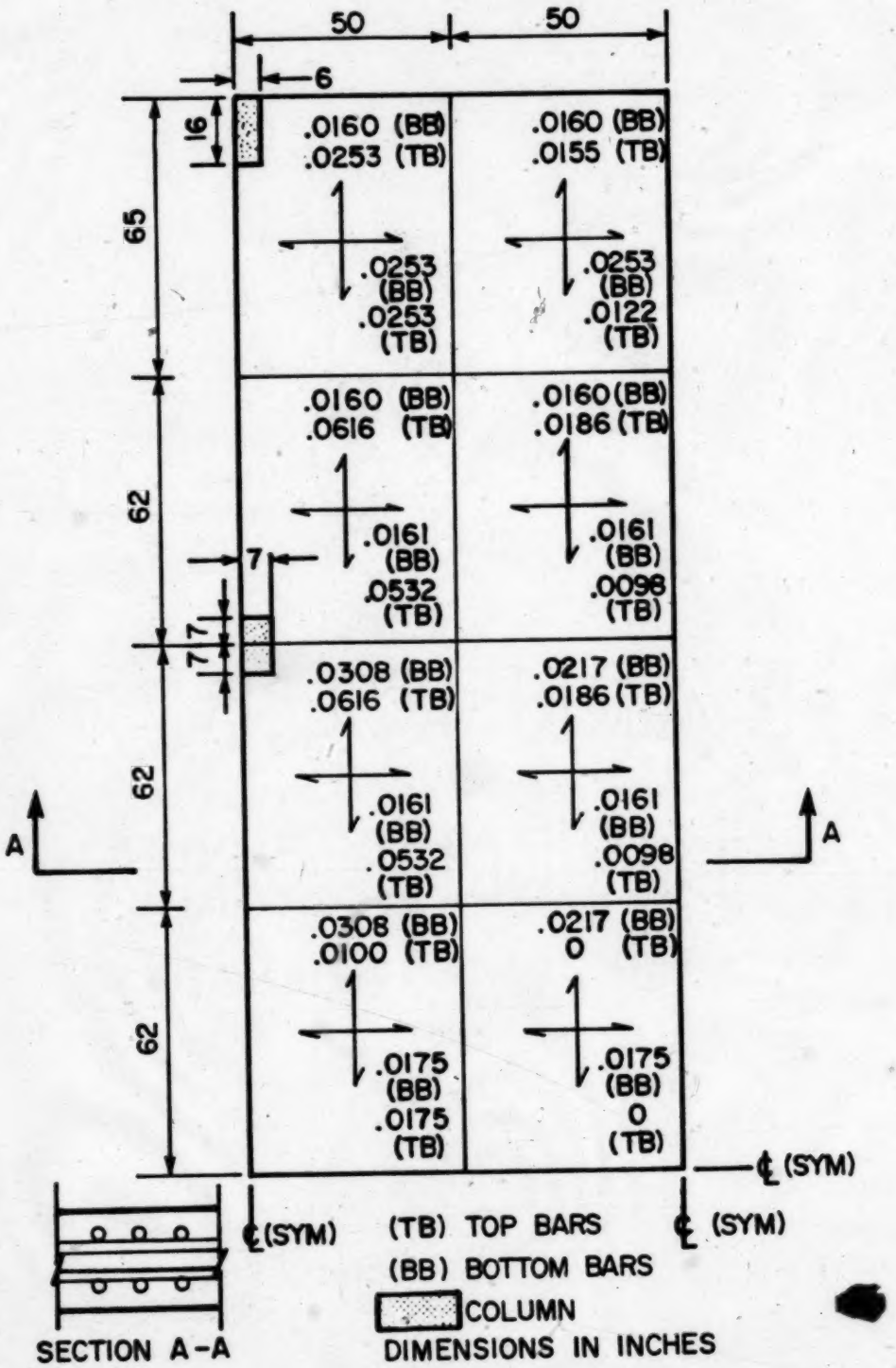

Figure F.1 Taylor's Flat Plate - Reinforcement Areas (in^2/in)

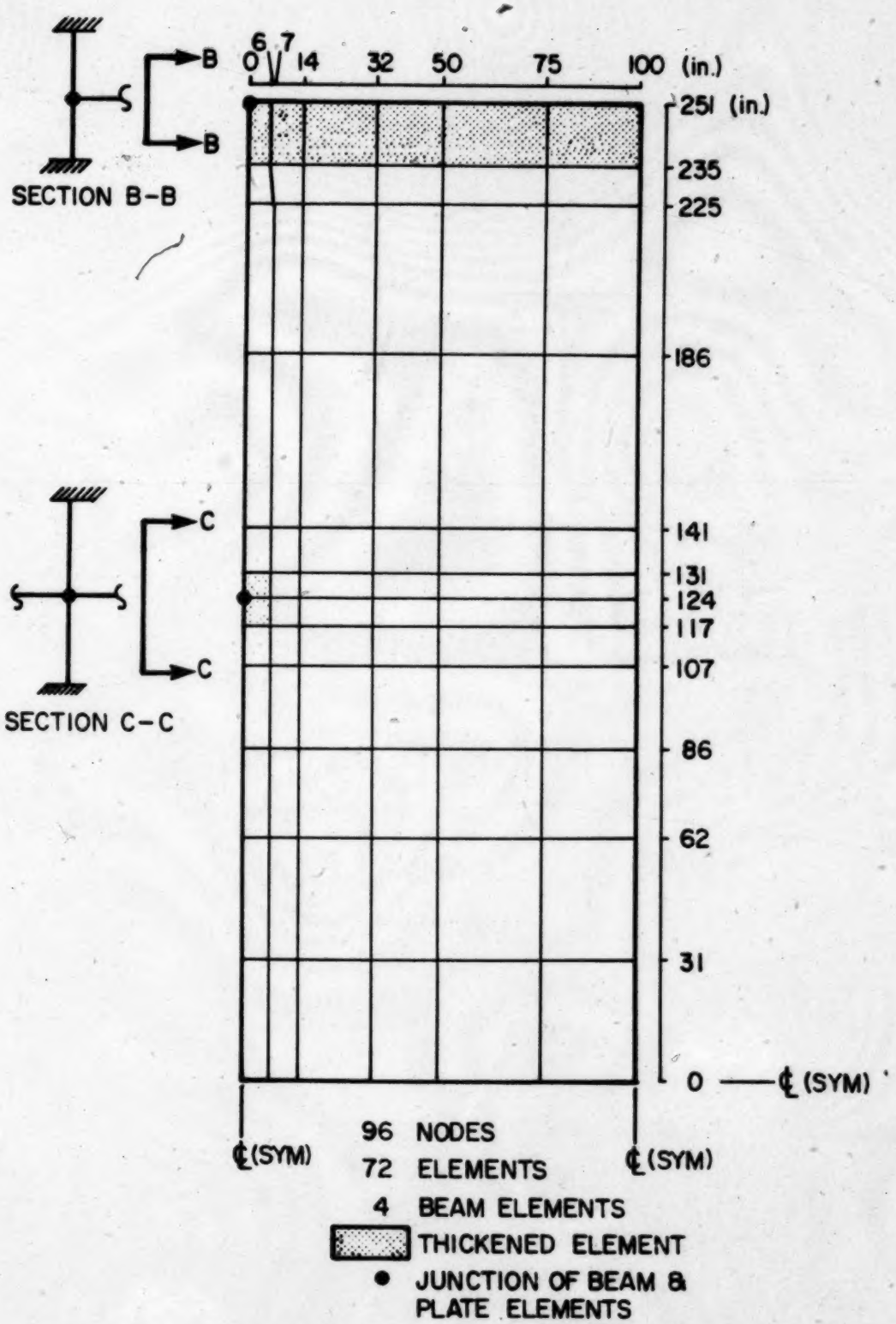

Figure F.2 Taylor's Flat Plate - Finite Element Grid

APPENDIX G

DERIVATION OF LONG-TIME MULTIPLIERS

For each slab series of the parameter study (excluding series SD slabs), additional analyses calculated the immediate deflection, Δ_{max}, due to the maximum construction load applied as a single increment. Application of this load corresponded to the age at maximum loading for the entire construction load sequence. Equation 6-4 was used to obtain the scaled immediate deflection due to the sustained load only, $\Delta_{s\ell}$.

Table G.1 gives values for all calculated multipliers, from which the average values of Table 6.1 were obtained.

Table G.1 One-Year and Ultimate Multipliers

SLAB SERIES	w_{max} (kPa)	t_{max} (days)	$w_{s\ell}$ (kPa)	$\Delta_{s\ell}$ (mm)	Δ_t (mm)	MULTIPLIERS					
						ONE-YEAR			ULTIMATE		
						λ_c	λ_{sh}	λ_t	λ_c	λ_{sh}	λ_t
LH100	9.39	21	5.63	4.26	17.34	1.12	1.67	3.79	1.30	1.77	4.07
					20.15	1.71	1.67	4.38	1.96	1.77	4.73
LH200	8.88	21	5.40	5.23	20.14	1.09	1.51	3.60	1.24	1.61	3.85
					23.54	1.66	1.51	4.17	1.89	1.61	4.50
LH300	10.16	21	5.99	3.29	14.11	1.14	1.87	4.01	1.29	2.00	4.29
					16.29	1.72	1.87	4.59	1.95	2.00	4.95
LH140	9.39	21	5.63	10.70	29.53	0.91	0.66	2.57	1.05	0.71	2.76
					36.06	1.45	0.66	3.11	1.66	0.71	3.37
LH240	8.88	21	5.40	13.19	34.29	0.82	0.60	2.42	0.96	0.64	2.60
					42.08	1.34	0.60	2.94	1.55	0.64	3.19
LH340	10.16	21	5.99	7.96	22.37	0.85	0.77	2.62	0.99	0.82	2.81
					27.06	1.37	0.77	3.14	1.58	0.82	3.40
SL200	9.86	14	5.63	4.85	18.62	1.12	1.46	3.58	1.28	1.56	3.84
					22.36	1.80	1.46	4.26	2.05	1.56	4.61
SL300	9.18	28	5.63	4.03	16.85	1.14	1.76	3.90	1.31	1.87	4.18
					19.34	1.69	1.76	4.45	1.93	1.87	4.80
SL400	9.05	35	5.63	3.90	16.61	1.16	1.82	3.98	1.32	1.94	4.26
					18.92	1.67	1.82	4.49	1.91	1.94	4.85
SL240	9.86	14	5.63	12.40	32.74	0.89	0.57	2.46	1.03	0.61	2.64
					41.42	1.51	0.57	3.08	1.73	0.61	3.34

Table G.1 One-Year and Ultimate Multipliers (continued)

SLAB SERIES	w_{max} (kPa)	t_{max} (days)	$w_{s\ell}$ (kPa)	$\Delta_{s\ell}$ (mm)	Δ_t (mm)	MULTIPLIERS					
						ONE-YEAR			ULTIMATE		
						λ_c	λ_{sh}	λ_t	λ_c	λ_{sh}	λ_t
SL340	9.18	28	5.63	9.87	26.95	0.83	0.72	2.55	0.97	0.76	2.73
					32.37	1.31	0.72	3.03	1.52	0.76	3.28
SL440	9.05	35	5.63	9.45	25.52	0.77	0.75	2.52	0.90	0.80	2.70
					30.24	1.21	0.75	2.96	1.40	0.80	3.20
RE100	7.34	14	5.63	3.90	16.30	0.61	1.39	3.00	1.70	1.48	4.18
					18.06	0.91	1.39	3.00	2.15	1.48	4.63
RE200	6.87	14	5.63	3.77	16.21	1.13	1.88	4.01	1.30	2.00	4.30
					17.68	1.48	1.88	4.36	1.69	2.00	4.69
RE140	7.34	14	5.63	8.34	23.60	0.77	0.84	2.61	0.90	0.90	2.80
					26.81	1.11	0.84	2.95	1.28	0.90	3.18
RE240	6.87	14	5.63	8.20	22.39	0.68	0.86	2.54	0.81	0.92	2.73
					25.01	0.97	0.86	2.83	1.13	0.92	3.05
SR100	9.18	16	5.63	4.38	17.30	1.07	1.62	3.69	1.23	1.72	3.95
					20.10	1.64	1.62	4.26	1.87	1.72	4.59
SR300	9.18	8	5.63	5.31	19.17	1.04	1.33	3.37	1.19	1.42	3.61
					22.89	1.66	1.33	3.99	1.89	1.42	4.31
SR140	9.18	16	5.63	10.92	28.50	0.78	0.65	2.43	0.92	0.69	2.61
					34.83	1.29	0.65	2.94	1.50	0.69	3.19
SR340	9.18	8	5.63	13.15	33.01	0.80	0.54	2.34	0.94	0.57	2.51
					41.69	1.38	0.54	2.92	1.60	0.57	3.17